Western University
Scholarship@Western

Digitized Theses

Digitized Special Collections

2011

DESIGN AND MICROFABRICATION OF EDGE-LIT OPTICAL LIGHT CURTAINS

Rahima Afrose Ronny

Follow this and additional works at: https://ir.lib.uwo.ca/digitizedtheses

Recommended Citation
Ronny, Rahima Afrose, "DESIGN AND MICROFABRICATION OF EDGE-LIT OPTICAL LIGHT CURTAINS" (2011). *Digitized Theses*. 3320.
https://ir.lib.uwo.ca/digitizedtheses/3320

This Thesis is brought to you for free and open access by the Digitized Special Collections at Scholarship@Western. It has been accepted for inclusion in Digitized Theses by an authorized administrator of Scholarship@Western. For more information, please contact wlswadmin@uwo.ca.

DESIGN AND MICROFABRICATION OF EDGE-LIT OPTICAL LIGHT CURTAINS

(Spine title: Design and Microfabrication of Edge-Lit Optical Light Curtains)

(Thesis format: Monograph)

by

Rahima Afrose Ronny

Graduate Program in Engineering Science
Department of Mechanical & Materials Engineering

A thesis submitted in partial fulfillment
of the requirements for the degree of
Master of Engineering Science

The School of Graduate and Postdoctoral Studies
The University of Western Ontario
London, Ontario, Canada

© Rahima Afrose Ronny 2011

THE UNIVERSITY OF WESTERN ONTARIO
SCHOOL OF GRADUATE AND POSTDOCTORAL STUDIES

CERTIFICATE OF EXAMINATION

Supervisor

Dr. George K. Knopf

Co-Supervisors

Dr. Evgueni Bordatchev

Dr. Suwas Nikumb

Examiners

Prof. Jayshri Sabarinathan

Prof. Sam Asokanthan

Prof. Michael Naish

The thesis by

Rahima Afrose Ronny

entitled:

Design and Microfabrication of Edge-Lit Optical Light Curtains

is accepted in partial fulfillment of the
requirements for the degree of
Masters of Engineering Science

Date

Chair of the Thesis Examination Board

ABSTRACT

Plastic optical light guides can be used for a variety of interior and exterior vehicle light curtains such as cabin illuminators and automotive tail lights. The edge-lit wave guide is an optically transparent substrate coupled with one or more energy efficient light emitting diodes (LEDs). The light rays from the source travel through the substrate based on the principle of total internal reflection. If a surface of the optical wave guide is patterned with optical microstructures then the light rays will scatter and refract throughout the medium, primarily exiting opposite to the patterned surface. Uniform illumination over this active surface region is a function of the individual optical microstructure's shape and the spatial distribution of the microstructures. The goal of this research is to investigate the light dispersion characteristics in both smooth and micro-patterned optically transparent substrates, and utilize optical simulation software to develop viable design approaches for fabricating small and medium sized light curtains. The study first identifies an appropriate optical microstructure (i.e. cylindrical indentations) that can be reliably imprinted on the surface of an optically transparent polymethyl-methacrylate (PMMA) substrate using a multi-axis micromilling machine. The optical simulation software "Light Tools" is then used to determine the most appropriate microstructure radius and spatial positioning of elements for uniform light distribution. The key design and fabrication parameters for near optimal performance are summarized and used to establish the process plan for the high-speed precision micromilling operations. Experiments are performed on several 100 mm x 100 mm x 6 mm polymer light guide panels (LGPs) including a customized design with a hexagonal arrangement of microstructures. Both interior and boundary regions of the sample LGPs are investigated for intensity distribution, optical transmission efficiency, and light loss. Although the experiments involve relatively small flat PMMA LGPs, the optical design and microfabrication methods can be readily extended to larger surface areas or curved optically transparent polymer substrates for contoured light curtains.

Keywords *– Edge-lighting, light guide panel, micro-optics, micro-milling, automotive light curtain*

ACKNOWLEDGEMENTS

This project is a result of the collaborative work between the National Research Council of Canada's *Industrial Materials Institute* (NRC-IMI) and The University of Western Ontario. This study was partially supported by the NSERC Discovery Grant.

I would like to acknowledge several individuals who helped to make this research possible. First, I would like to thank my supervisors at IMI, Dr. Evgueni V. Bordatchev and Dr. Suwas Nikumb, for their dedicated guidance, patience, and time over the last two years. Special thanks to Professor George K. Knopf, who has provided unconditional supervision and direction during the course of this project. Without their encouragement, and support, this work could not be possible. Secondly, the staff at IMI's Centre for Automotive Materials and Manufacturing deserves recognition for their help, tips, and suggestions with regard to optical design and microfabrication. There are not enough words to express my gratitude to them. Many people have enriched my research experience during the past two years. Specifically, these people include: Hugo Reshef, Dr. Mohammad Tauhiduzzaman, Craig Dinkel, Mike Meinert and Marco Zeman.

TABLE OF CONTENTS

CERTIFICATE OF EXAMINATION II

ABSTRACT III

ACKNOWLEDGEMENTS IV

TABLE OF CONTENTS V

LIST OF FIGURES VIII

LIST OF TABLES XII

NOMENCLATURE XIII

CHAPTER 1

INTRODUCTION 1

1.1 The Problem 1

1.2 Design and Fabrication of Microstructures in Light Guide Panels 3

1.3 Research Motivation 4

1.4 Objectives of the Research 5

1.5 Overview of the Thesis 5

CHAPTER 2

REVIEW OF EDGE-LIT GUIDE PANELS (LGPS) 7

2.1 Introduction 7

2.2 Light Guide Technology 8

2.3 Structure of Edge-lit LGP 13

2.4 Characteristics of Uniform Illumination 15

2.5 Optical Microstructures 16

2.6 Microfabrication Methods for Creating LGPs 19

2.7 Measures for Evaluating LGP Performance 26

2.8 Concluding Remarks 28

CHAPTER 3

DESIGN OF OPTICAL MICROSTRUCTURES FOR LGP 30

3.1 Introduction 30

3.2 Single Microstructure 32

3.3 Multiple Optical Microstructures 41
    3.3.1 Linear arrays 41
    3.3.2 Non-linear arrays 65

3.4 Optimization using Optical Simulation Tools 69

3.5 Controlled Array for Specific Pattern 72
    3.5.1 Test pattern 1 73
    3.5.2 Test pattern 2 74

3.6 Discussion 76
    3.6.1 Comparison of optical microstructures 76
    3.6.2 Comparison of array arrangements 76
    3.6.3 Advantages of the proposed optimization method 77

3.7 Concluding Remarks 77

CHAPTER 4

MICROFABRICATION METHOD 79

4.1 Introduction 79

4.2 Micromilling 80

4.3 Experimental Verification and Results 82

4.4 Performance of the Fabricated Prototypes 85
    4.4.1 LGP without microstructures 86

4.4.2 LGP with linear array of microstructure....87
4.4.3 LGP with optimized array of microstructure....88
4.4.4 LGP with controlled array of microstructures....89
4.4.5 LGP with patterned logo....90
4.5 General Observations and Discussion....90
4.6 Concluding Remarks....91

CHAPTER 5

CONCLUSION....93
5.1 Concluding Comments....93
5.2 Thesis Summary....94
5.3 Recommendations and Future Work....96

BIBLIOGRAPHY....97

APPENDIX A

MODELING AND SIMULATING LGPS USING LIGHT TOOLS....102
A.1 Light Tools Simulator....102
A.2 Testing and Verification of Light Tools....104

APPENDIX B

AUTOMOTIVE LIGHTING STANDARDS....106

APPENDIX C

PHOTOMETRIC UNITS....114

CURRICULUM VITAE....118

LIST OF FIGURES

Figure 1.1 Examples of interior convenience lighting in an automobile 2

Figure 1.2 Examples of exterior safety lighting in an automobile 2

Figure 2.1 Different possible shapes of light guide panel (LGP)..................................7

Figure 2.2 The behavior of a light ray as it travels from medium A to medium B 8

Figure 2.3 Total internal reflection (TIR) phenomena 9

Figure 2.4 Light guide panel without modification of any surface 11

Figure 2.5 Effect of patterning the bottom surface of light guide panel (LGP) 11

Figure 2.6 Light propagation in a bend LGP..12

Figure 2.7 Elements in an edge lit LGP [Adapted from Joo et al., 2010] 13

Figure 2.8 Expression of luminance emitted from the light source 14

Figure 2.9 Illumination characteristics with distance...16

Figure 2.10 Different way for distribution of microstructures in LGP 17

Figure 2.11 Microfabrication processes for optical microstructures 20

Figure 2.12 LIGA process [adapted from Banks, 2006] 22

Figure 2.13 State-of-the-art in different methods for creating mold for microstructures for further replication on LGP [adapted from Herzig, 1997].......................23

Figure 2.14 Basics of replication process.(i) photoresist on a substrate, typically glass; exposed pattern, binary or continuous relief; deposition of Au contact layer; electroplating with a Ni master; replication in a polymer using the resultant molding tool [Adapted from Zappe, 2010] 24

Figure 2.15 State-of-the-art in different methods for replication of microstructures on LGP [adapted from B. Stager et al., 2005] 25

Figure 2.16 Illumination...27

Figure 2.17 Illumination uniformity measurement by 9-point test method 28

Figure 3.1 Parameters for a hemispherical-tip cylindrical shape microstructure...........32

Figure 3.2 Effect of using source housing for light source 33

Figure 3.3 Illumination behavior for LGP without patterning any surface....................35

Figure 3.4 LGP with single concave shape optical microstructure. Dimension of LGP: 100 mm (L) x 100 mm (W) x 6 mm (H). Location of microstructure is at the middle of LGP, radius and depth of microstructure are 0.5 mm and 0.5 mm respectively 38

Figure 3.5 LGP with single convex shape optical microstructure. Dimension of LGP: 100 mm (L) x 100 mm (W) x 6 mm (H). Location of microstructure is at the middle of LGP, radius and depth of microstructure are 0.5 mm and 0.5 mm respectively 40

Figure 3.6 Basic design for analyzing the effect of horizontal line of concave microstructures on a flat back surface. Location of line of microstructures is at X-X' cross-section..42

Figure 3.7 Optical performance of one horizontal line of concave microstructure on a flat back surface (three microstructures in a line)......................................44

Figure 3.8 Optical performance of one horizontal line of concave microstructure on a flat back surface (five microstructures in a line) 46

Figure 3.9 Optical performance of one horizontal line of concave microstructures on a flat back surface (nine microstructures in a line)..48

Figure 3.10 Basic design for analyzing the effect of vertical lines of concave microstructures on a flat back surface. Location of line of microstructure is at Y-Y' cross-section..49

Figure 3.11 Optical performance of one vertical line of concave microstructures on a flat back surface 51

Figure 3.12 Optical performance of three vertical lines of concave microstructures on a flat back surface. Gap between each microstructure and each line are 2 mm and 10 mm respectively 53

Figure 3.13 Optical performance of five vertical lines of concave microstructures on a flat back surface. Gap between each microstructure and each line are 2 mm and 5 mm respectively 55

Figure 3.14 Design for nine vertical lines of concave microstructures on a flat back surface. Gap between each microstructure and each line are 2 mm and 2.5 mm respectively 57

Figure 3.15 Fill factor calculation for rectangular and hexagonal array arrangement of microstructures [adapted from Nussbaum et al., 1997] 59

Figure 3.16 Illumination for rectangular array arrangement 61

Figure 3.17 Illumination for hexagonal array arrangement 63

Figure 3.18 Illumination when depth of microstructure is varying along each column of LGP 68

Figure 3.19 Explanation for decreasing illumination far from light source 69

Figure 3.20 Distribution of microstructures for the proposed optimization approach 70

Figure 3.21 Illumination for the optimized distribution of microstructures in LGP 72

Figure 3.22 Guiding the light for test pattern one 74

Figure 3.23 Guiding the light for test pattern two 75

Figure 4.1 Fabrication of microstructures by micromilling 82

Figure 4.2 Surface analysis of the fabricated cylindrical microstructure 84

Figure 4.3 Illumination performance test set-up for LGP 85

Figure 4.4 Illumination performance for a LGP without any microstructures 86

Figure 4.5 Illumination performance for a LGP with linear array of microstructures (fixed radius and depth of microstructure, uniform pitch between microstructures) 87

Figure 4.6 Illumination performance for a LGP with optimized array of microstructures (with varying depth of microstructure) 88

Figure 4.7 Illumination performance for a LGP with test pattern two 89

Figure 4.8 Illumination performance for a LGP with patterned logo 90

Figure 4.9 Technique for mass production of LGP with microstructures 92

Figure A.1 Verification of the "Light Tools" software 105

Figure B.1 Photometric requirements for Tail lamp with LED light sources according to SAE J1889 for use on vehicles less than 2032 mm in overall width 109

Figure C.1 Luminous Intensity 115

Figure C.2 Solid Angle 117

LIST OF TABLES

Table 3.1 Summary from Figure 3.16 and Figure 3.17 64

Table B.1 Photometric requirements for Fog tail lamp as per SAE J575 for use on vehicles less than 2032 mm in overall width 110

Table B.2 Photometric requirements for rear cornering lamps as per SAE J575 for use on vehicles less than 2032 mm in overall width 111

Table B.3 Photometric Requirements for auxiliary upper beam lamp according to the requirements of SAE J575 for use on vehicles less than 2032 mm in overall width 111

Table B.4 Photometric Requirements for auxiliary upper beam lamp according to the requirements of SAE J2139 for use on vehicles 2032 mm or more in overall width 112

NOMENCLATURE

BLU	Backlight unit
cd	Candela
CCFL	Cold cathode fluorescent lamp
DOE	Design of experiments
FIB	Focused ion beam
GRIN	Gradient-index
LGP	Light guide panel
LCD	Liquid crystal display
LED	Light emitting diode
LIGA	Lithography, galvanoforming-electroplating and plastic molding
MO	Micro-optical
MD	Molecular dynamics
mm	Millimetre
µm	Micrometre
MEMS	Micro-electro-mechanical systems
MLA	Micro-lens array
nm	Nanometer
PMMA	Polymethylmethacrylate
PC	Polycarbonate
PDMS	Polydimethylsiloxane
PQRSM	Progressive quadratic response surface modeling
SU-8	Photoresist for UV photolithography application
RIE	Reactive ion etching
RPM	Revolution per minute
2D	Two-dimensional
3D	Three-dimensional
TIR	Total internal reflection
WC	Tungsten carbide
UV	Ultraviolet

CHAPTER 1

INTRODUCTION

1. 1 The Problem

Light guide technology is popular as a way of transmitting the incident light for a variety of applications. Optical microstructures, created on the bottom or top surface of the light guide panel (LGP) act as light scattering elements. These microstructures scatter the incident light from light sources at different angles, frustrate total internal reflection (TIR) and redistribute the light uniformly across the surface opposite to the patterned surface with minimal optical losses along the edges. The surface with uniform illumination appears as a surface illuminator. Linear, i.e., Cold Cathode Fluorescent Lamp (CCFL) or multiple point i.e., Light Emitting diode (LEDs) light sources are attached to either in the backside (named as Direct-lit) or along the edge (named as edge-lit) of the light guide panel (LGP). In terms of light weight and reduced thickness, edge-lit LGP are generally preferred. Some common devices that use this technology are mobile phones, monitors or minitubes (TV) [Jeong et al., 2008; Feng et al., 2005]. In addition to these, a new area of application is convenience lighting or style (cosmetic) features such as signature lighting.

Lighting and signaling devices are integrated in vehicle exteriors in order to provide illumination for the driver to operate the vehicle safely after dark, in fog, to increase the vehicle conspicuity, and to display information about the vehicle's presence, position, size, direction of travel, and driver's intentions regarding direction and speed of travel to other drivers on the road. Exterior lights (forward and rear lighting) convey a *distinct appearance for the vehicle. Since the response of the human visual system to different wavelengths is different at high light level, i.e., day time, and low light level, i.e.,* night time, therefore in traffic, contour lighting requires spatial orientation and the maximum illuminance level as well as uniformity of the illuminance is an important factor in this case [Wördenweber et al., 2007]. Generally a lamp (e.g., fluorescent, neon) and a reflector are used for automotive lighting. The reflector surrounding the bulb reflects the light in the desired direction. However, these types of linear and point light sources are only suitable for distributing light over a small area. Light guide panel technology using light sources at the edge represent a new approach to developing small and medium-size illumination sources for automotive applications such as interior cabin lighting, dashboard lighting and exterior safety side lights and even rear tail lights instead of conventional lighting system as shown in Figure 1.1 and Figure 1.2.

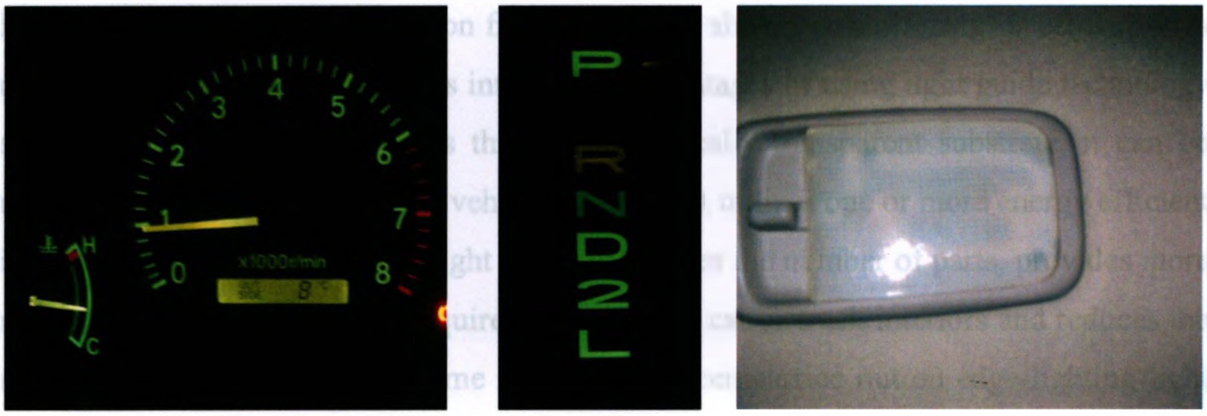

Figure 1.1 Examples of interior convenience lighting in an automobile.

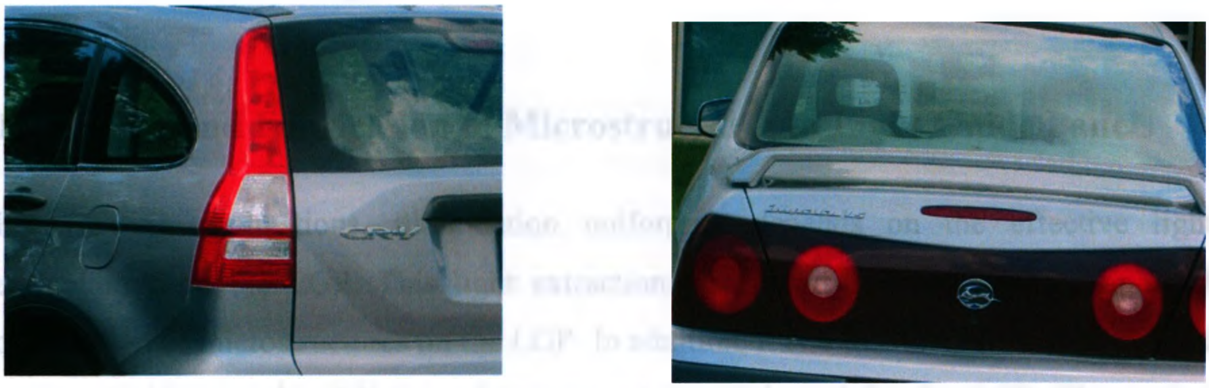

(a) Rear tail light of Honda CR-V

(b) Rear tail light arrangement on Chevrolet Impala.

Figure 1.2 Examples of exterior safety lighting in an automobile.

Light guide with microstructures patterned on the bottom surface offer great opportunities to design attractive exterior lamps, e.g. front position lights, tail lamps or side lights. Incident light can be guided in a controlled direction through the selective distribution of microstructures and the illuminating surface of the LGP appears as a light curtain that can be also used for signature lighting in order to highlight important styling lines, contours around lighting chambers or the edges of a lamp. For example, tail lamps mark the vehicle position in traffic particularly in twilight (low contrast) and darkness. In this manner the output illumination from a tail light should be sufficient for other drivers to visually understand the driver's intent. The advantages of using light guide technology is that the illuminator can be as thin as the optically transparent substrate, it can be molded to fit the geometry of the vehicle body and it utilizes one or more energy efficient light emitting diodes (LEDs) as light sources, reduces the number of parts, provides more opportunity for style changes, requires less space in car or truck interiors and reduces the manufacturing cost. Although some research has been carried out on edge-lighting light guide panel for light curtain applications, these works do not explain clearly what features were used to achieve uniform illumination for light curtains and how the microstructures redirect light.

1.2 Design and Fabrication of Microstructures in Light Guide Panels

For lighting applications, illumination uniformity depends on the effective light extraction from the LGP. This light extraction is primarily related to the shape and distribution of microstructures on the LGP. In addition, it is a function of the type of light source, incident angle of light and transparent material used for the LGP. The optical efficiency of the LGP and reduction in "light loss" through the edges of the substrate can be controlled by the proper design of the individual optical microstructure shape and the spatial distribution of microstructures in the LGP. In general, these factors affect the illumination pattern over the whole area of the LGP. Optical simulation software is generally used to observe the performance of the system by ray tracing. After the design and simulation is complete, it is usually necessary to fabricate the prototype and compare it with the simulation results. The common method to obtain prototypes involves fabrication of a master mold by available fabrication technology, i.e., LIGA (lithography, galvanoforming-electroplating and plastic molding), e-beam writing, laser writing and mechanical micromachining (micromilling) followed by replication in polymethylmethacrylate (PMMA) by means of hot embossing or injection molding. Moreover, these are multistep and batchwise processes. Therefore, it becomes a matter of cost and time to get a prototype right after the design before undertaking mass production. In addition, in most cases, to fabricate a prototype by micromilling requires different diameters of tools due to the specification of different size of microstructures in the LGP according to the design.

1.3 Research Motivation

Efficient design of the LGP depends on an optimized design of the microstructure array on the LGP in order to extract the maximum amount of light and to produce homogeneous illumination over the whole area of the LGP. Successful design is also related to the choice of fabrication method with a few processing steps in a relatively short time and at a low cost. Available fabrication methods for microstructures, which include photo resist reflow technique, deep X-ray lithography, etc., are not a direct process to fabricate different shaped microstructure array on the LGP, in less processing time with an optical-quality surface finish. Mechanical micromachining, i.e., micromilling is capable of creating microstructures directly in the LGP. In order to create microstructures with varying size (different diameter) and pitch by micromilling calls for tools of different diameter during the fabrication process, which is time consuming and expensive as well. Therefore, an optimized distribution of microstructures array in the bottom surface of the LGP and a direct fabrication method (without the need for a mold and different diameter tools) to fabricate the microstructures in the final substrate of the LGP (PMMA) is necessary.

1. 4 Objectives of the Research

The primary goal of this thesis is to design an optimized distribution of microstructures in the bottom surfaces of the LGP in order to obtain homogeneous illumination over the entire active area of the LGP. The design issues are related to the radius and depth of the cylindrical shaped microstructures, pitch between adjacent microstructures, arrangement of the microstructures in the LGP, the type of material for the LGP and the type of light source. Illumination simulation software "Light Tools" will be used to understand the effect of different distributions of microstructure array on the LGP prior to the fabrication of the final product. After the design has been completed, a novel microfabrication method will be introduced to fabricate the microstructure array on the LGP, which will meet the following requirements:

1. Direct high quality fabrication of the microstructure array on the LGP substrate (PMMA) without the need for different diameter milling tools.
2. Minimal number of operational steps.
3. Enable the production of different size microstructures with dimensions in micrometer range and also permit various arrangements of microstructure arrays to be created for a wide range of applications.

1. 5 Overview of the Thesis

The remainder of this thesis is organized into four chapters. Chapter 2 provides a detailed review about the fundamental principles of light traveling through a transparent light guide, edge-lit light guide panel (LGP) technology with optical microstructures and the characteristics of uniform illumination for such LGPs. This chapter also involves a detailed description of the available design and microfabrication methods for creating LGPs and measures for evaluating LGP performance. The primary focus of this discussion will be on characteristics of uniform illumination for LGPs and the methods that support the design and fabrication of optical microstructures in LGPs.

Chapter 3 illustrates the design concept for distribution of optical microstructures and arrays of optical microstructure in the LGP and a detailed analysis of how the parameters of each microstructure and its distribution in an array affect the output illumination pattern. This chapter also includes the simulation results based on the design and optimization technique in order to obtain a near homogeneous illumination over the whole area of the LGP.

Chapter 4 discusses the proposed microfabrication method for creating the optical microstructure in the LGP and supports the advantages of the proposed fabrication method. The fabrication method involves micromilling to create cylindrical microstructures by varying only the depth of the microstructures directly on the LGP made from polymethylmethacrylate (PMMA). This chapter also describes the performance testing of the LGPs by a digital lux meter and compares the illumination behavior with the simulated results. Finally, a summary of the research contributions, conclusions and recommendations for future work are provided in Chapter 5.

CHAPTER 2

REVIEW OF EDGE-LIT LIGHT GUIDE PANELS (LGPs)

2. 1 Introduction

Guiding light using a solid transparent substrate has been well-known for hundreds of years [Zappe, 2010]. The concept of light-guiding was analyzed scientifically as early as 1842. Today the light guide panel is an important component for backlight panels where ultimate goal is to achieve uniform illumination and high luminance across the Liquid Crystal Display (LCD) surface. The condition of homogeneous illumination in a LGP greatly depends on the size of the optical microstructure and how they are distributed in the LGP. LGP is an optically transparent substrate, which can be of different shapes such as rectangular or wedge as shown in Figure 2.1. Radiated light from the source is coupled into the LGP and propagates inside the LGP based on the principle of total internal reflection. This propagated light starts reflecting as soon as it comes in contact with microstructures patterned on the bottom surface of the LGP and is emitted out from the front face of the LGP.

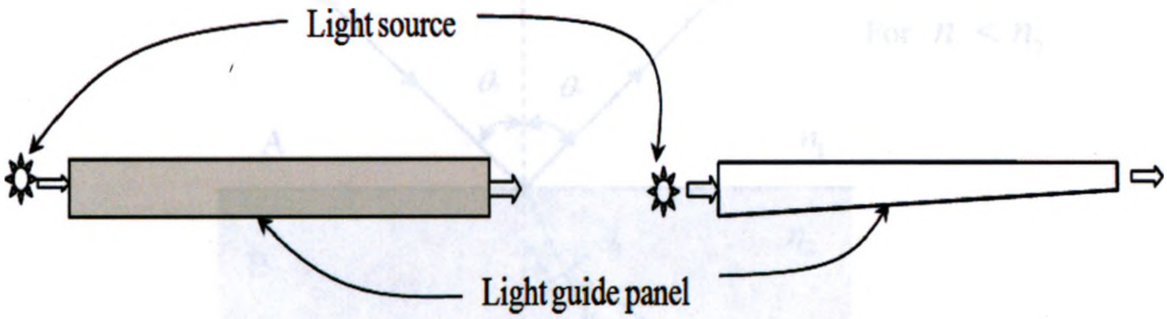

(a) Rectangular LGP (b) Wedge shape LGP

Figure 2.1 Different possible shapes of light guide panel (LGP).

In this chapter, a detailed review about edge-lit Light Guide Panel (LGP) with optical microstructures, characteristics of uniform illumination for such LGP, a detailed description of available designs and microfabrication method for creating optical microstructures in the LGP and available measures for evaluating LGP performance will be presented. The primary focus of this discussion will be on the distribution of optical microstructures with respect to the characteristics of uniform illumination for LGP and microfabrication methods that support the design and microfabrication of such optical microstructures in the LGP, followed by the limitations of this available microfabrication method.

2.2 Light Guide Technology

According to the basic geometric optics, when light travels from a medium A of lower refractive index, n_1 (e.g., air) into a medium B of higher refractive index, n_2 (glass or PMMA), as shown in Figure 2.2, a fraction of incident light is reflected from the interface, and the remainder of it bends at that boundary into the medium of higher refractive index, n_2. This case is known as external incidence and usually occurs when light is coupled into a material [Iga et al., 1984].

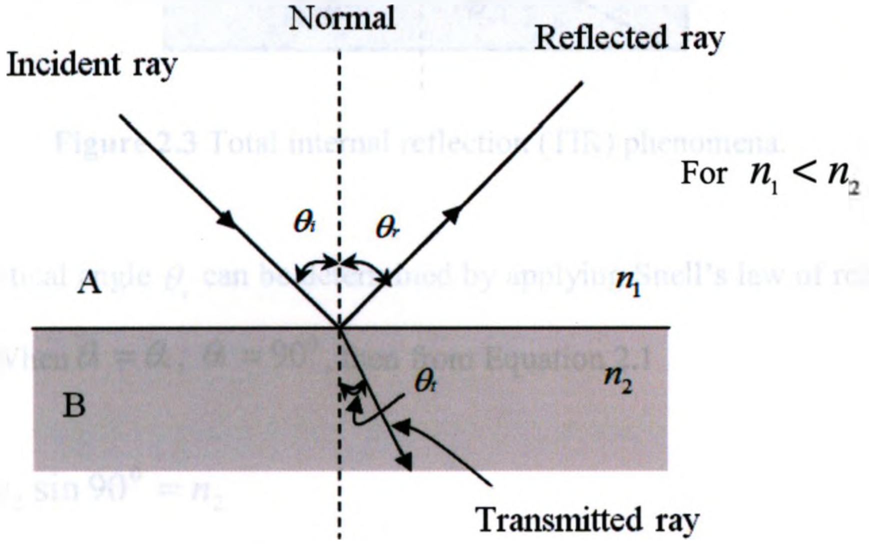

Figure 2.2 The behavior of a light ray as it travels from medium A to medium B.

In the above diagram, θ_i, θ_r and θ_t are the incident angle, reflected angle and transmitted angle respectively with the normal to the surface. According to Snell's law,

$$n_1 \sin\theta_i = n_2 \sin\theta_t \tag{2.1}$$

Internal incidence of light occurs when light travels from a medium of higher refractive index, n_2 (glass or PMMA) to a medium of lower refractive index, n_1 (e.g., air). In internal incidence, as the value of incident angle θ_i increases, transmitted angle θ_t will be reached at 90^0 for $\theta_i < 90^0$, as in Figure 2.3 and no light will be transmitted at the boundary. The value of incident angle at which the transmitted angle, θ_t reached at 90^0 is known as critical angle (θ_c) and this phenomena is known as "total internal reflection" (TIR).

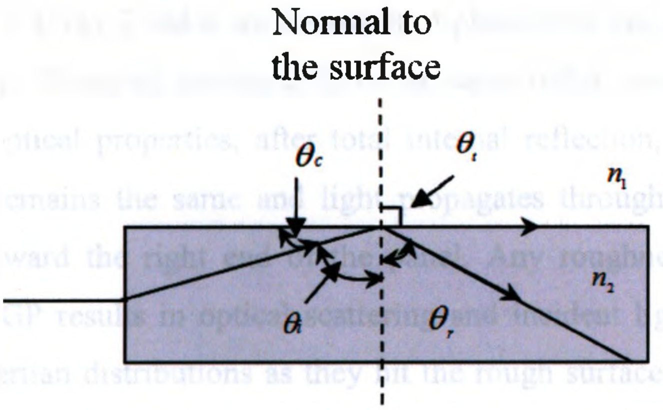

Figure 2.3 Total internal reflection (TIR) phenomena.

The critical angle θ_c can be determined by applying Snell's law of refraction [Iga et al., 1984] .When $\theta_i = \theta_c$, $\theta_t = 90^0$, then from Equation 2.1

$$n_1 \sin\theta_c = n_2 \sin 90^0 = n_2 \tag{2.2a}$$

$$\sin\theta_c = \frac{n_2}{n_1} \text{ (For } n_1 > n_2\text{)} \tag{2.2b}$$

The critical angle that causes the total internal reflection defines the numerical aperture, which can be expressed in terms of the refractive index difference of the two media. Propagation in a light guide panel is considerably different from propagation in free space. In a light guide panel the light propagates in different paths and each path has different wavelength, propagation constant and effective index [Malacara, 2001]. Total reflection in a light guide panel results in zero transmission with no energy transmitted across the interface. When total internal reflection occurs, a phase shift occurs between the incident and reflected beams. Phase shift is a function of the refractive indices of the two mediums, the angle of incidence and the polarization of light.

When due to TIR many paths of light rays propagate through a panel along different directions with the same intensity, the output luminous flux is the result of interference of these rays in different directions. The intensity of light rays deteriorates as the panel length increases. In a planar light guide panel without patterning on any surface, shown in Figure 2.4, ray 2 and 4 are the result of phase shift due to TIR of incident ray 1 and 3 respectively. Since all interfaces have the same index step and all of the surfaces have the same optical properties, after total internal reflection, the incident angle and reflected angle remains the same and light propagates through the panel without any optical losses toward the right end of the panel. Any roughness associated with any surface of the LGP results in optical scattering and incident light undergoes reflection following Lambertian distributions as they hit the rough surface [Malacara, 2001]. This roughness can be applied to the bottom surface of a LGP by patterning optical microstructures as in Figure 2.5. In this case, the two interfaces (top and bottom) will be different and the resultant phase shift will be different. Light will be reflected from the patterned interface at wider angles and thus the incident angle and reflected angle will be different.

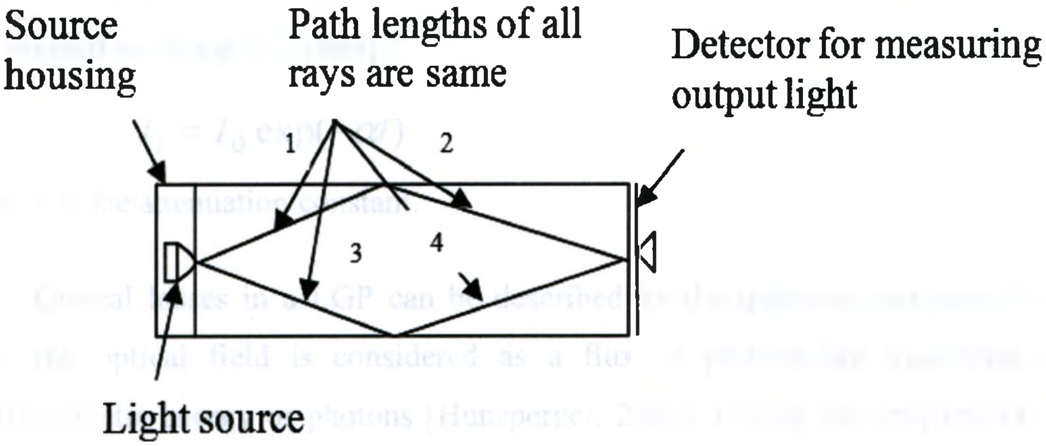
Source housing
Path lengths of all rays are same
Detector for measuring output light
1
2
3
4
Light source

Figure 2.4 Light guide panel without modification of any surface.

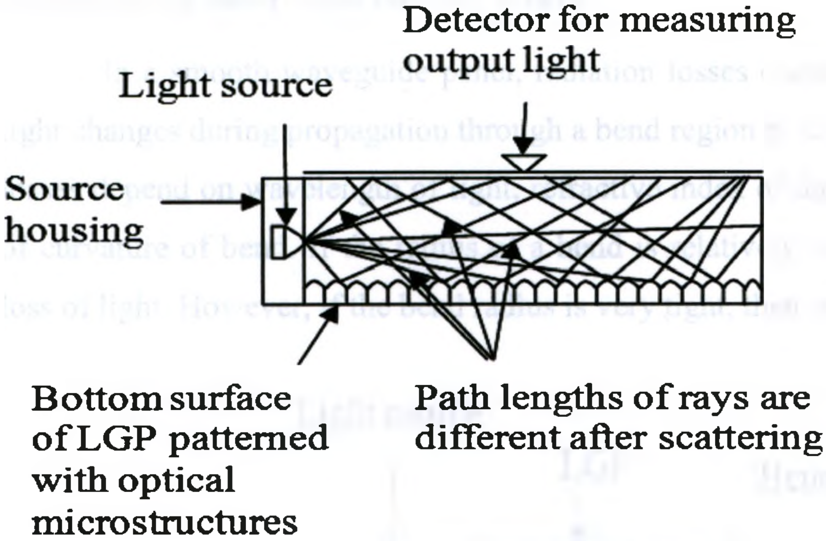
Detector for measuring output light
Light source
Source housing
Bottom surface of LGP patterned with optical microstructures
Path lengths of rays are different after scattering

Figure 2.5 Effect of patterning the bottom surface of light guide panel (LGP).

This difference in phase shift will frustrate the total internal reflection and light can be transmitted in a direction perpendicular to the direction of propagation. A detector or receiver mounted on the output surface of the LGP measures the output illumination. The output illumination is mostly influenced by the geometry (size and shape) and distribution of these microstructures. When light propagates through the LGP, it loses its intensity over distances, an effect known as optical loss or attenuation. If I_0 is the intensity of light ray at the entrance of a LGP, transmitted intensity I_t at a distance l can be expressed as [Iga et al., 1984]:

$$I_t = I_0 \exp(-\alpha l) \tag{2.3}$$

where α is the attenuation constant.

Optical losses in a LGP can be described by the quantum mechanical concept, where the optical field is considered as a flux of particle-like quantized units of electromagnetic energy or photons [Hunsperger, 2009]. During the propagation of light through the LGP, photons reduce their energy either by scattering, radiation or absorption. Optical losses by scattering is a dominant issue in glass or dielectric waveguides, absorption losses are most important in semiconductors and radiation losses are significant factor when the LGP is bent.

In a smooth waveguide panel, radiation losses occur when the incident angle of light changes during propagation through a bend region as shown in Figure 2.6. Radiation losses depend on wavelength of light, refractive index of the two medium and the radius of curvature of bend. If the radius of a bend is relatively large, there will be almost no loss of light. However, if the bend radius is very tight, then some light will be lost.

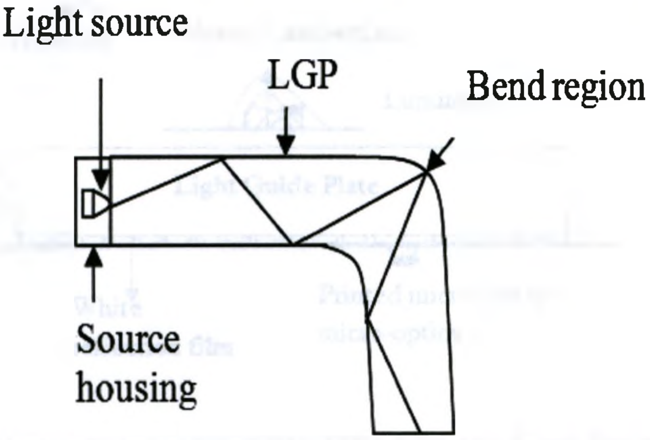

Figure 2.6 Light propagation in a bend LGP.

As propagation of light in a medium depends on the refractive index, wavelength, therefore selection of material is also an important factor for a particular application.

Usually glass, semiconductors, dielectrics, polymers and specialized crystals are used as LGP material. Among these, polymers are less expensive and have flexibility in manufacturing either by molding or embossing process. The refractive index of polymers is typically around 1.5 for visible wavelengths.

2. 3 Structure of Edge-lit LGP

In a typical edge-lit light guide panel used for display applications, different layers are used above the outer surface and under the bottom surface, as in Figure 2.7. The effective positioning of the light source is important as it controls the incidence angle of light.

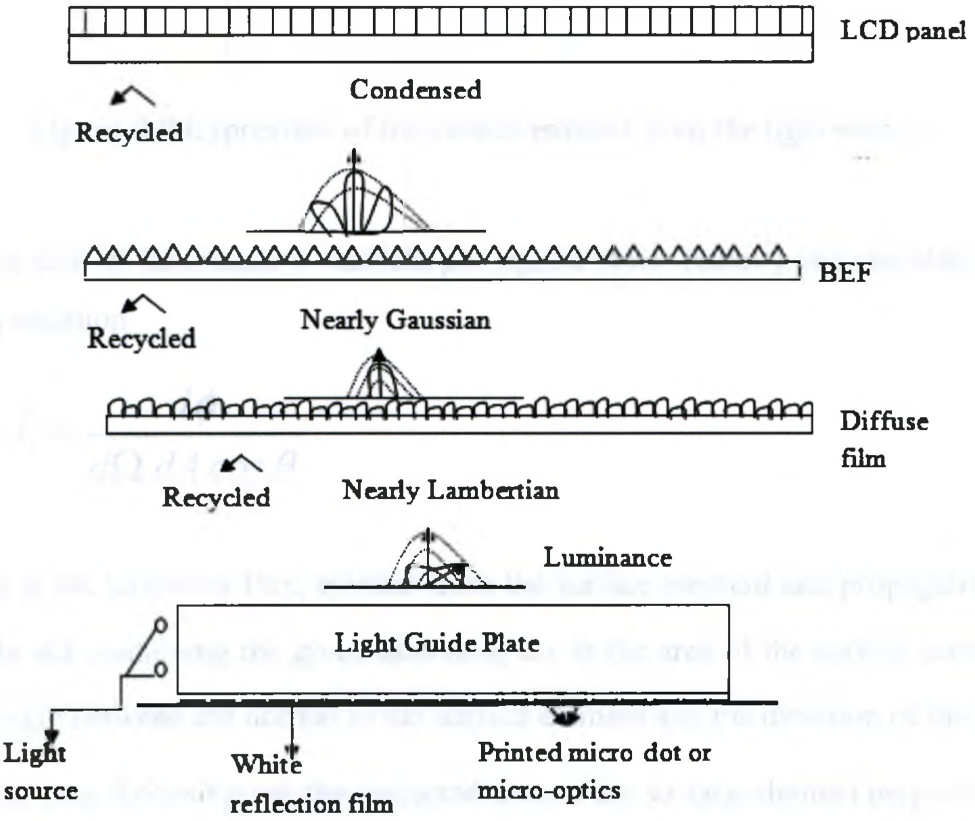
LCD panel
Recycled
Condensed
BEF
Recycled
Nearly Gaussian
Diffuse film
Recycled
Nearly Lambertian
Luminance
Light Guide Plate
Light source
White reflection film
Printed micro dot or micro-optics

Figure 2.7 Elements in an edge lit LGP [Adapted from Joo et al., 2010].

Luminance, L (defined as flux per unit projected area and per solid angle) is emitted from the source by its surface elements as shown in Figure 2.8.

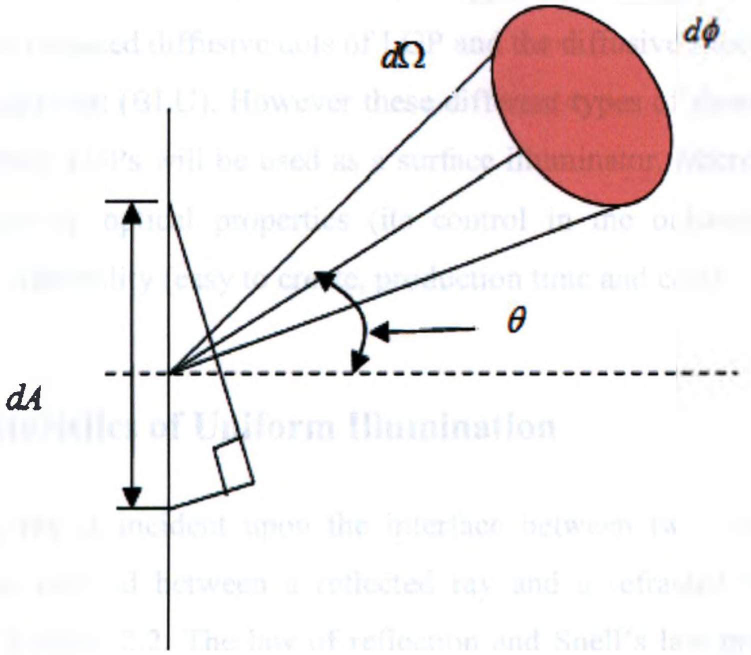

Figure 2.8 Expression of luminance emitted from the light source.

The unit of luminance is candela per square meter (cd/m^2) and calculated by the following equation

$$L = \frac{d\phi}{d\Omega\, dA \cos\theta} \tag{2.4}$$

where $d\phi$ is the luminous flux, emitted from the surface element and propagating in the solid angle $d\Omega$ containing the given direction, dA is the area of the surface element and θ is the angle between the normal to the surface element and the direction of the ray.

The term $dA\cos\theta$ gives the projected area of the surface element perpendicular to the direction of measurement. A finite number of rays are traced from the light source. The emitted light is coupled into the LGP, continues to propagate until they hit the optical microstructures patterned on the bottom surface of the LGP and then leaves the LGP via multiple total internal reflections. Light scattering microstructures guide the propagating light by scattering and frustrating the total internal reflection (TIR), direct the light in a direction perpendicular to the direction of propagation and produce the effect of a homogeneously illuminated surface. Different types of back light unit (BLU) have been reported which replaced diffusive dots of LGP and the diffusive sheet with a modification on the back light unit (BLU). However these different types of sheets are not significant in the case where LGPs will be used as a surface illuminator. Microstructures should be chosen considering optical properties (its control in the outcoupling direction) and manufacturing feasibility (easy to create, production time and cost).

2. 4 Characteristics of Uniform Illumination

When a light ray is incident upon the interface between two transparent media, the incident ray is divided between a reflected ray and a refracted (transmitted) ray, as mentioned in Section 2.2. The law of reflection and Snell's law predict the path of the resulting rays, and Fresnel's law of reflection predicts the amount of intensity carried by each ray [Choi et al., 2004]. Inverse square law defines the relationship between luminance from a point source and the distance to the measurement surface. It states that the intensity per unit area varies inversely proportional to the square of the distance between the source and the surface. According to this law, illuminance (*E*) and intensity (*I*) are related as follows:

$$E = \frac{I}{l^2} \tag{2.5}$$

where l = the distance from the light source. This equation quantifies the effect that, a surface that is illuminated by a light source appears dimmer as it moves away from the light source. In fact, it becomes dimmer much faster than it moves away from the source. Therefore, this characteristic of uniform illumination for a LGP can be illustrated in Figure 2.9.

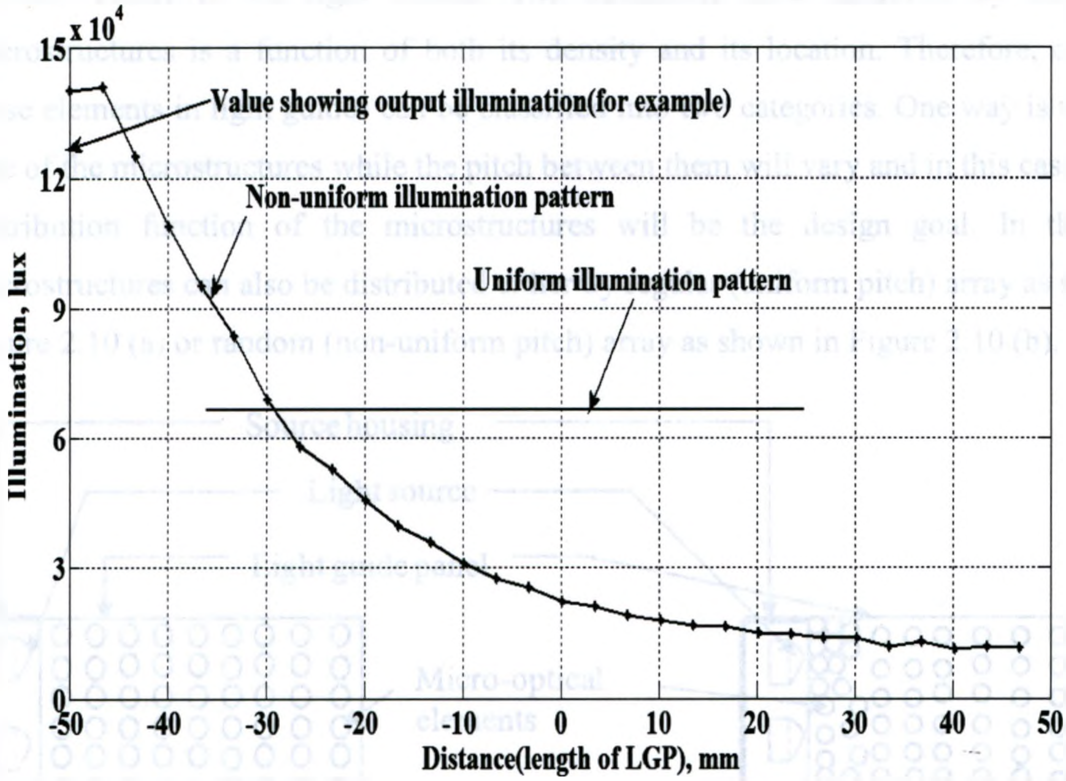

Figure 2.9 Illumination characteristics with distance.

2. 5 Optical Microstructures

In order to achieve a homogeneous illumination from an LGP, it is necessary to properly distribute the optical microstructures and reduce the amount of losses in the LGP. Optical microstructures, both, refractive and diffractive type are used to couple the light in an LGP. Microstructures are small elements, such as a lens or any geometric shape (spherical, cylindrical, triangular, prism, pyramid, inverse-trapezoidal, conic etc) generally with diameters less than a millimeter and often as small as 10 µm. The LGP needs to be thick enough to support these small microstructures.

Design of optical microstructures plays a key role in achieving an equal-luminance (EL) condition due to their outstanding redirecting ability. For example, a high-luminance level can be achieved for a high-density configuration of optical microstructures at a specific position or for a configuration of the same density at a position closer to the light source. The luminance level achieved by the optical microstructures is a function of both its density and its location. Therefore, design of these elements in light guides can be classified into two categories. One way is to fix the size of the microstructures while the pitch between them will vary and in this case density distribution function of the microstructures will be the design goal. In this case, microstructures can also be distributed either by regular (uniform pitch) array as shown in Figure 2.10 (a) or random (non-uniform pitch) array as shown in Figure 2.10 (b).

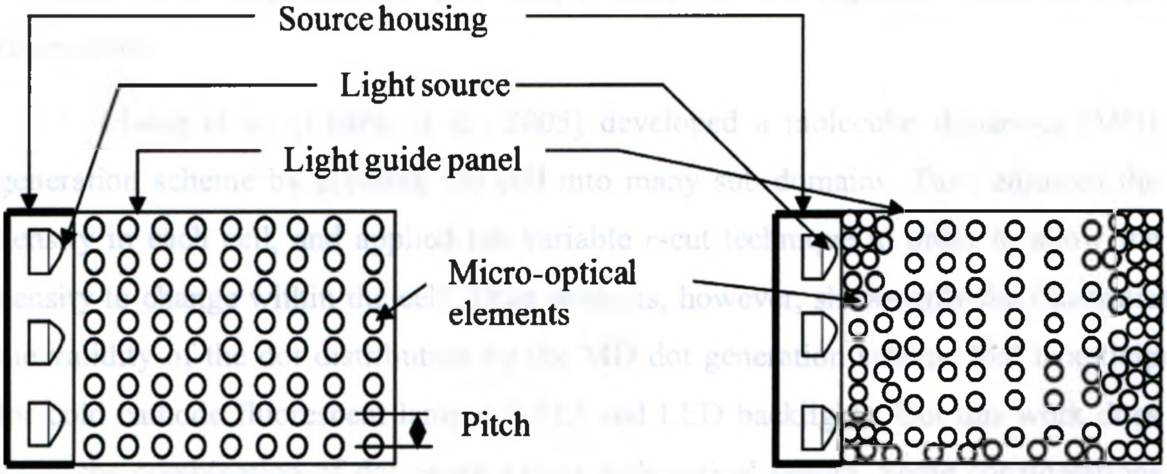
Source housing
Light source
Light guide panel
Micro-optical elements
Pitch

(a) Uniform array

(b) Random array

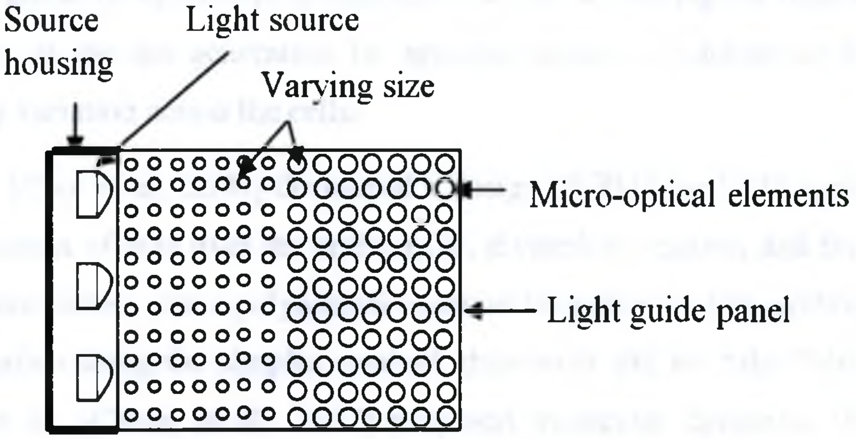
Source housing
Light source
Varying size
Micro-optical elements
Light guide panel

(c) Array with varying size of microstructure

Figure 2.10 Different way for distribution of microstructures in LGP.

Another way is to fix the pitch between microstructures while varying their size as shown in Figure 2.10 (c) and the distribution of microstructure size is the design goal here [Ide et al., 2003; Chang et al., 2005]. Each method has its own advantages and disadvantages. The first method is easy to control and permits direct fabrication of the array of microstructures in a relatively short time with lower cost. The later method can increase the tooling cost in fabrication because of the requirement of different diameter tool. Random distribution of microstructures can eliminate the "Moiré" effect [Ide et al., 2003]. "Moiré" effect is an optical phenomenon that can occur with an overly regular arrangement of microstructures and causes defects by producing distinct dark and light bands on the display. However this "Moiré" effect is not a significant issue for a surface illuminator.

Chang et al. [Chang et al., 2005] developed a molecular dynamics (MD) dot generation scheme by dividing the cell into many sub domains. They adjusted the dot density in each cell, and applied the variable *r*-cut technique in order to allow the dot density to change within the cell. Their analysis, however, shows only the illustration of the validity of the dot distribution by the MD dot generation scheme that is anticipated for cold cathode fluorescent lamp (CCFL) and LED backlights. But this work does not show the combination of dot optimization with optical design. Some considerations are still lacking in the dot generation scheme's ability to accommodate the optical design phase, such as the arbitrary addition to or removal from the cell during the optical design phase, localization of the dot generation for specific regions, or achieving high and distinct dot density variation across the cells.

Choi et al. [Choi et al., 2004] developed a design of BLU for LCD applications. They fixed the location of dots over the entire LGP, divided its regions, and formulated the density of the dot pattern into a polynomial equation for radius of dots. Although they optimized the equation using the simplex method, their work did not take "Moiré" into account. Chang et al. [Chang et al., 2007] proposed molecular dynamics (MD) dot generation schemes by applying variable *r*-cut technique with reflective boundary condition and adjusted the dot density in each cell in order achieve a high dot density variation of dot distribution. They also used the add-on and remove-from techniques to increase or lower the cell dot density locally.

Chang and Fang [Chang and Fang, 2007] developed an optical model by providing a gap between the microstructure and the bottom surface of the LGP in order to specify the optical properties for the microstructures and bottom surface of the LGP. The light guide was divided into an array of equal-size rectangular partitions where all microstructures had an equal initial radius and then the model was optimized by varying the microstructure radius according to the difference between the illumination output of each region and the average illumination across the entire light guide plate. Jeong et al. [Jeong et al., 2008] introduced the design of incoupling part of LGP by design of experiments (DOE) to increase the average illumination and uniformity. In their work, they also created microstructure in the light entering surface of LGP in order to reflect the emitted light from light source. The microstructure distribution in the outcoupling part was determined by progressive quadratic response surface modeling (PQRSM) to resolve the numerical noise problem of the simulation.

2. 6 Microfabrication Methods for Creating LGPs

Light guiding in a panel depends on the spatially distributed microstructures and the difference in refractive index between the panel and outside medium, (i.e., air). Proper selection of the fabrication method for creating microstructures in the LGP is necessary, depending upon the particular application and the resources available to do so. Optical microstructures can be created in the LGP in several ways as shown in Figure 2.11.

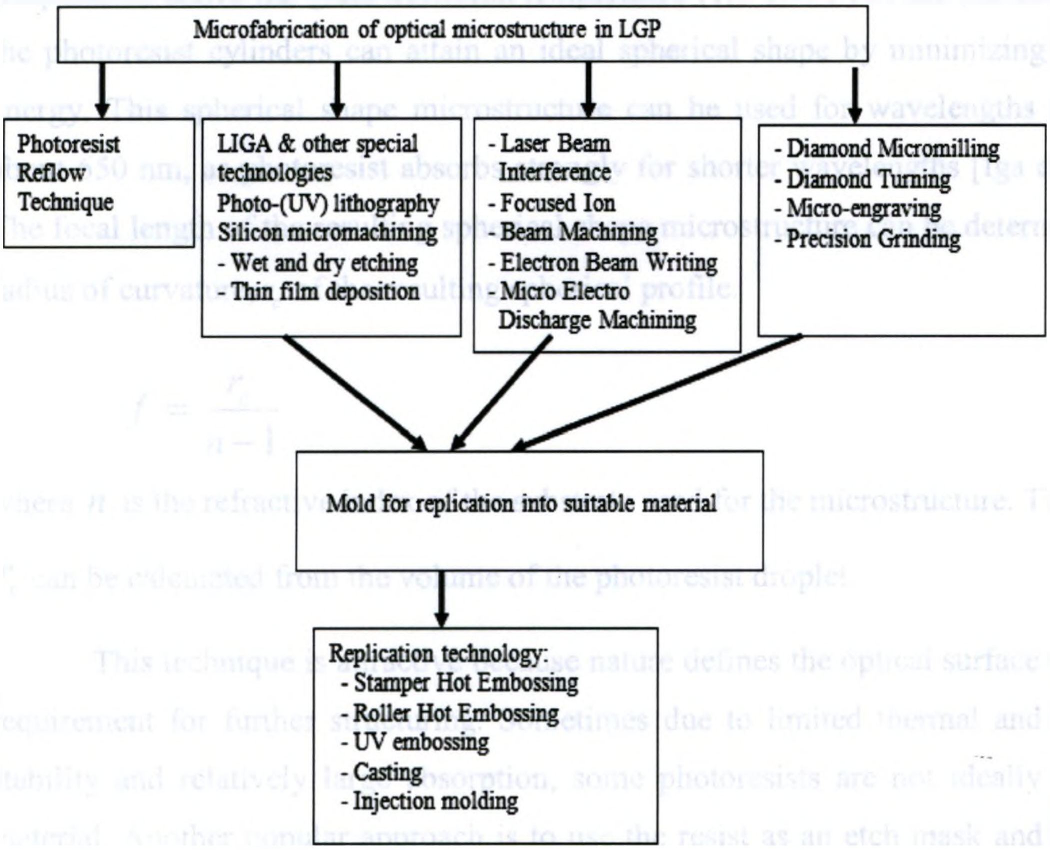
Microfabrication of optical microstructure in LGP
Photoresist Reflow Technique
LIGA & other special technologies
Photo-(UV) lithography
Silicon micromachining
- Wet and dry etching
- Thin film deposition
- Laser Beam Interference
- Focused Ion Beam Machining
- Electron Beam Writing
- Micro Electro Discharge Machining
- Diamond Micromilling
- Diamond Turning
- Micro-engraving
- Precision Grinding
Mold for replication into suitable material
Replication technology:
- Stamper Hot Embossing
- Roller Hot Embossing
- UV embossing
- Casting
- Injection molding

Figure 2.11 Microfabrication processes for optical microstructures.

Fabrication of a LGP primarily involves the creation of microstructures on the LGP. Different types of fabrication methods are reported for LGPs with microstructures and most of the available methods are related to the needs of the cell phone and display industries. Photoresist reflow is the most common technique. In micro-electro-mechanical systems (MEMS) process, silicon is used as the mold for microstructure. The mold is created by using photolithography, anisotropic etching technology [Chao et al., 2008], electro-plating or ultra precision machining and then silicon mold is passed through the hot-embossing process or UV imprinting for replication into the PMMA material [Ta-Wei et al., 2008] .

The photoresist reflow technique utilizes the effect of surface tension. Photoresist or similar polymer materials are melted and the surface tension in the melted materials creates cylindrical "islands" of microstructures. The photoresist layer is then patterned lithographically to form small cylinders on a substrate and the structure is heated to a temperature above the glass transition temperature (T_G~160^{0}C) of the photoresist so that the photoresist cylinders can attain an ideal spherical shape by minimizing the surface energy. This spherical shape microstructure can be used for wavelengths longer than about 650 nm, as photoresist absorbs strongly for shorter wavelengths [Iga et al., 1984]. The focal length of the resulting spherical shape microstructure can be determined by the radius of curvature, r_c of the resulting spherical profile.

$$f = \frac{r_c}{n-1} \tag{2.6}$$

where n is the refractive index of the substrate used for the microstructure. The radius r_c can be calculated from the volume of the photoresist droplet.

This technique is attractive because nature defines the optical surface without any requirement for further structuring. Sometimes due to limited thermal and mechanical stability and relatively large absorption, some photoresists are not ideally suited as a material. Another popular approach is to use the resist as an etch mask and transfer the lens shape into the underlying substrate using directional dry etch, e.g. reactive ion etching (RIE), reactive ion beam etching (RIBE) or ion beam milling (IBM) [Iga et al., 1984]. But the RIE process is slow (20 nm/min for quartz and 5 nm/min for CaF_2) and this requires high control of the proportional etching and resist characteristics. The LIGA process as shown in Figure 2.12 uses lithography, electroplating, and molding processes to produce high-aspect-ratio microstructures. In this process, deep X-ray lithography, as in Figure 2.12(a), is first applied to produce a high-aspect-ratio microstructure (master) in very thick layers of photoresist, usually PMMA-based resists as in Figure 2.12(a); after the developing process, a metal replica is produced by electroforming with metal for use as a structural component itself, or as a mold insert for further replication in plastic, glass or ceramic as shown in Figure 2.12(f). Synchrotron light with high energy (3 to 20 keV) is exposed to penetrate deep X-rays into the resist in order to produce microstructures with high aspect ratios.

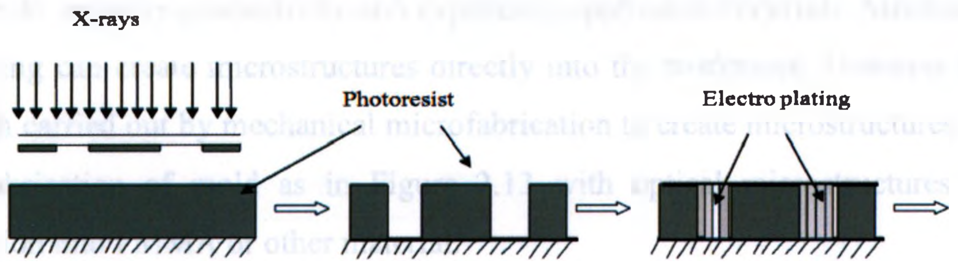

(a) X-ray exposure (b) Photoresist developed (c) Electroplating to fill gaps in photoresist

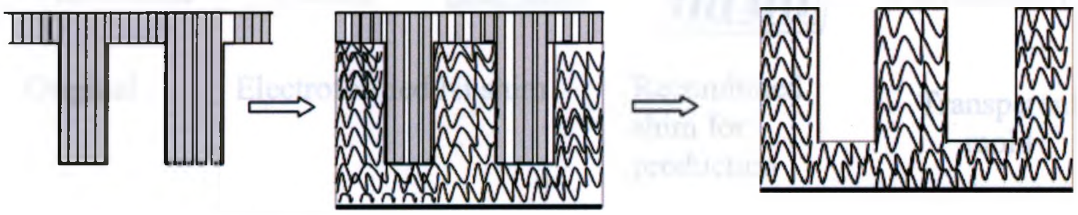

(d) Electroplating is continued to create a metal mold insert (e) Injection molding (f) Final structure in plastic

Figure 2.12 LIGA process [adapted from Banks, 2006]

The microstructures formed by the LIGA technique are planar shape in most cases. Although there is freedom to choose X-ray energy with different wavelength (0.01nm-1nm), but this requires very thick layers of photoresist for exposure. Corresponding thermal expansion can also limit resolution and performance of the process, which is quite often for masks that incorporate polymer membranes. X-ray sources used in this process are relatively small, which requires several exposures in order to scan the mask and substrate across the source, which means that little time is available for cooling during the process and the mask may heats up in some cases. Considering high-energy x-rays, X-ray lithography is a relatively expensive process [Banks, 2006].

Laser or e-beam writing is often used to create lithographic masks and is also applicable for profiling in a direct writing mode with quasicontinuous intensity modulation. This technique is used mainly for the generation of masters for replication.

Mechanical micromachining is another alternative method of non-traditional machining in order to improve productivity and expanding applicable materials. Mechanical micromachining can create microstructures directly into the workpiece. However most of the research carried out by mechanical microfabrication to create microstructures was related with fabrication of mold as in Figure 2.13 with optical microstructures for further replication into PMMA or other material.

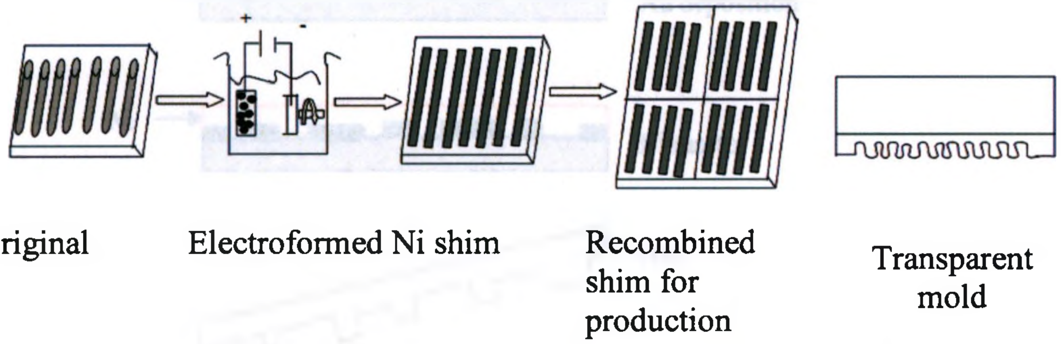

Figure 2.13 State-of-the-art in different methods for creating mold for microstructures for further replication on LGP [adapted from Herzig, 1997].

Mechanical micromachining can be done either by milling or turning operation. In turning method, the work piece is held in the rotary chuck and a fixture is used to hold the fly cutter in the rotary chuck for micro-groove cutting. In micromilling, either diamond tools or tungsten carbide (WC) micro-end mills are generally used as micro-cutting tools, especially for complex micropatterns, functional shapes, and three-dimensional features. In each case parameter, e.g. spindle speed (rpm), feed rate (mm/min), axial depth of cut (µm), center distance of adjacent microstructures (µm), cutting fluid need to be selected carefully. The material for creating mold can be metal or PDMS as reported by Chang et al. [Chang et al., 2007].

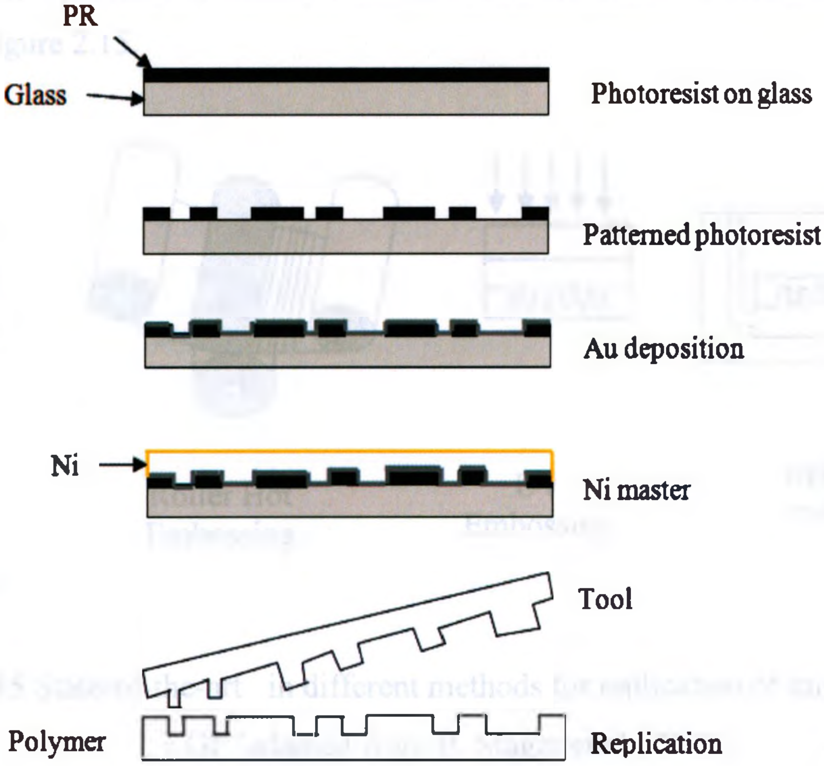

Figure 2.14 Basics of replication process.(i) photoresist on a substrate, typically glass; exposed pattern, binary or continuous relief; deposition of Au contact layer; electroplating with a Ni master; replication in a polymer using the resultant molding tool.

[Adapted from Zappe, 2010]

Replication techniques are capable of copying microstructure features with nanometric resolution over large areas at low cost and have become a key technology for mass production in industry. The basic replication process as shown in Figure 2.14 involves the copying of a surface-relief microstructure from a metal form, the replication stamper, into a formable material such as thermoplastic or curable polymer [Herzig, 1997]. The original micro-relief can be fabricated in any material by any of the techniques or using one or a combination of suitable high-resolution lithographic processes as described in previous section. The original surface microstructure is then electroformed to produce a first-generation metal copy, usually in nickel (Ni), from which further generations can be electroformed. The Ni copy can then be used for replication into polymer or another material. Different available replications set up are as shown in Figure 2.15.

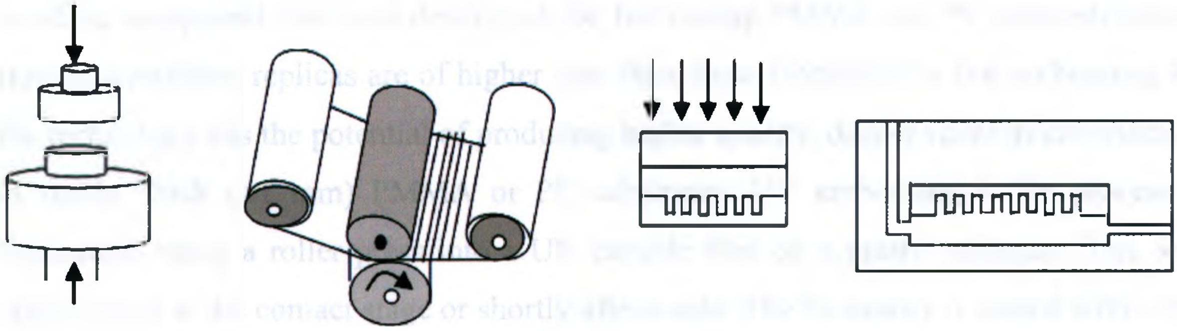

Stamper Hot Embossing

Roller Hot Embossing

UV Embossing

Injection molding

Figure 2.15 State-of-the-art in different methods for replication of microstructures on LGP [adapted from B. Stager et al., 2005].

Stamping, roller or reciprocating systems are used for hot embossing of surface relief microstructures into thermoplastic. Replication of microstructures with relief amplitudes in excess of about 1µm by commercial roller systems creates considerable problems [Herzig, 1997]. Reciprocating or stamping hot press, which is also capable of relatively high throughput, is also applicable for replication of deeper microstructures. Embossing can be also done into a thin, customized thermoplastic layer coated onto a stable substrate film such as polyester. However this works extremely well for shallow microstructures (relief depths of less than about 1 µm) and for deeper structures with no features and high aspect ratio (<1 depth to width ratio). Injection molding is another standard technology for replication of microstructures. Generally molding involves the stepwise forming of molten plastic under high pressure in a temperature controlled mould, containing the relief microstructure to be replicated. The plastic is then cooled and solidified in the mold before removal, resulting in a very high fidelity copy of microstructure. In injection moulding, plastic material is injected as a pre-heated molten resin into the mold which results in short cycle times; whereas compression molding introduces plastic in either powder or sheet form that is pressed between two heated dies, resulting in longer cycle times. For better reproduction of deeper structures, a combination of injection-compression molding is also possible. Customized injection molding equipment has been developed for fabricating PMMA and PC microstructures. Injection molding replicas are of higher cost than those fabricated by hot embossing, but the technology has the potential of producing higher quality, deeper relief microstructures in stable, thick (>1 mm) PMMA or PC substrates. UV embossing is the process of replication using a roller press into a UV curable film on a plastic substrate film, with rapid curing at the contact stage or shortly afterwards. The Ni master is coated with a thin layer of UV-curable material (photopolymer) and pressed against a glass substrate. The sandwich is then cured under pressure and separated after hardening. UV embossing has the advantage of producing a replicated film which can be highly resistant to a subsequent solvent coating step and therefore suited to the replication of deep or high aspect ratio microstructures.

The most common materials suitable for replication are polycarbonate, PVC and PMMA for hot embossing and photopolymer for UV-casting. The fidelity of replicated microstructures is very dependent upon the aspect ratio (feature width to height ratio). The main limitation of replication technology is the effective cycle time. The release of polymer from the shim or mould is a critical process for high fidelity optical structures that can affect the surface roughness and feature resolution at the nanometer scale. The set up for replication technique is expensive as well [Herzig, 1997].

2. 7 Measures for Evaluating LGP Performance

In display technologies such as in LCD TV, the outcoupling efficiency of light from LGP depends on the direction and polarization state of illumination. In automotive exterior lighting, light goes directly from source (in this case, LGP) to the detector (eye), performance of the LGP includes how much ray can be outcoupled from LGP and are measured in terms of lux or W/steredian. Design parameters such as accuracy of the light path, the intensity of the reflected light and the light density distribution etc. need to be considered in order to having homogeneous light intensity and distribution from the LGP. Illumination, E as shown in Figure 2.16 is the amount of luminous flux incident per unit area of a surface and expressed by

$$E = \frac{d\phi}{dA} \tag{2.7}$$

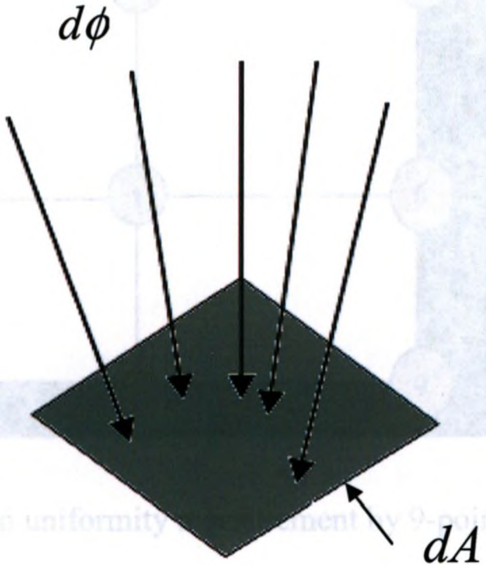

Figure 2.16 Illumination.

Luminance meter or digital lux meter can be used to measure the illuminance and uniformity of the LGP. Performance of LGP means measurement of illumination over the LGP. The performance of LGP is related to various factors, e.g., how the light dispersing elements are arranged, measurement of surface finish of the fabricated light dispersing elements, type and location of light source. One key parameter in evaluating LGP performance is coupling efficiency, the fraction of available light that is coupled into the LGP. The calculations of illumination uniformity for the LGP are often done using 5-point or 9 point test method as shown in Figure 2.17. By "Digital Lux Meter", illumination data is taken at 5, 9 or more points to get the minimum, $E_{\min}$ and maximum illumination, $E_{\max}$. Once the minimum and maximum illumination is measured by using a digital lux meter, illumination uniformity (U_E) can be calculated by using the following equation

$$U_E = \frac{E_{\min}}{E_{\max}} \tag{2.8}$$

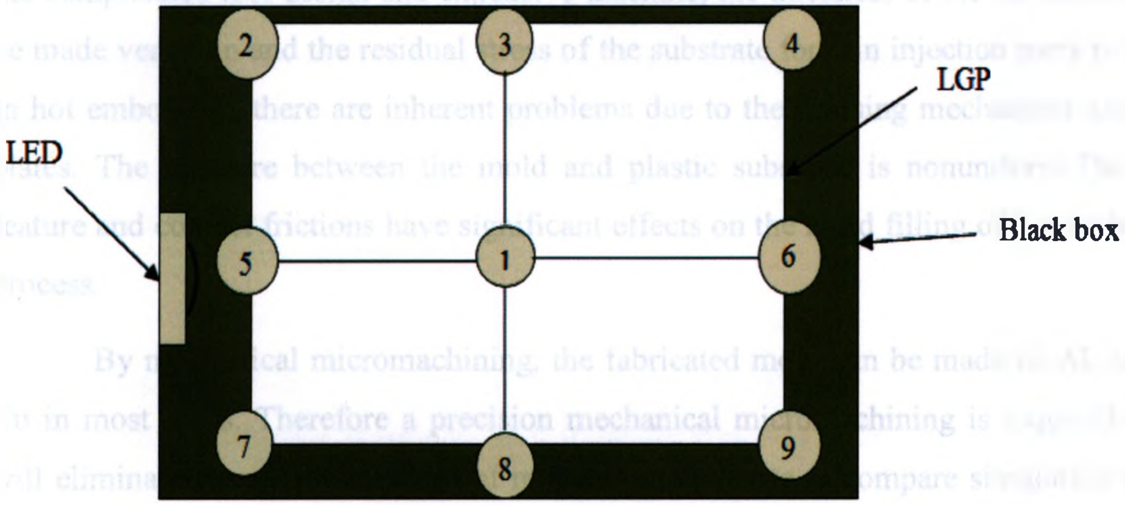

Figure 2.17 Illumination uniformity measurement by 9-point test method.

2. 8 Concluding Remarks

From the review presented in this chapter, it is essential to have an optimized design for the geometry and array of optical microstructures and a proper choice of fabrication method in order to obtain a homogeneous illumination from the LGP for desired applications. In most cases, the resist reflow process is used. To create a mold or master, micro-stereo lithography, moving mask X-ray lithography, and inclined UV lithography methods have been used, which have strengths for specific applications but require very specialized equipment such as a stereo lithography machine, X-ray source, and inclined stages in the mask aligner. However, the cost of synchrotron radiation facility is considerably more expensive than ultraviolet (UV) exposure system. The FIB and modified LIGA techniques are expensive, time-consuming and not easily accessible.

Injection molding and hot embossing are regarded as the best mass-production method to replicate microstructures; however, the processes involve high temperature and high pressure. These are time-consuming, often repetitive processes and introduce additional defects that could be doubled due to the repeated pattern transfer of photoresist to metal master, then metal master to polymer substrate. Thus fabrication by hot embossing or injection molding is still challenging since a high-definition mold is required prior to the molding procedure. The injection molding process is also limited by the complicated tool design and expensive machine, the thickness of the substrate cannot be made very thin and the residual stress of the substrate for thin injection parts is larger. In hot embossing, there are inherent problems due to the pressing mechanism using hot plates. The pressure between the mold and plastic substrate is nonuniform.The mold feature and contact frictions have significant effects on the mold filling of hot embossing process.

By mechanical micromachining, the fabricated mold can be made of Al, steel or Cu in most cases. Therefore a precision mechanical micromachining is required which will eliminate the additional steps of replication, facilitate to compare simulation results with the fabricated part in a relative short time with low cost and can create optical microstructures on PMMA directly with optical quality surface finish.

CHAPTER 3

CYLINDRICAL OPTICAL MICROSTRUCTURES FOR LGP

3.1 Introduction

The edge-lit LGP is an optically transparent substrate, coupled with one or more energy efficient light emitting diodes (LEDs). The light rays from the source travelling through the substrate experience frustrated total internal reflection (TIR) and consequently, are redistributed such that the emitted light has near equal luminance across the entire active surface. In most cases, the substrate is a molded optically transparent plastic called polymethylmethacrylate (PMMA) with a refractive index of 1.49. PMMA is used as the material for LGP as polymer offers more flexibility for optical component design compared to glass. Moreover polymer optics has also some unique advantages such as high production numbers at low cost, lightweight and hardiness, impact and abrasion resistance, temperature resistance and thermal expansion [Iga et al., 1984]. More specifically the transparency of PMMA is greater than that of most optical glasses and additives to acrylic as well as to several other plastics which considerably improve its ultraviolet transmittance and stability. Also with PMMA material, it is possible to maintain a high performance level with low cost. The microstructures are fabricated on only one side of the LGP substrate. The opposite side of the LGP is unaltered and is usually transparent. LED are positioned at the side of the LGP, emitted light is coupled into the panel and propagates by means of multiple total internal reflections. Optical microstructures fabricated on any side of this plate frustrate this total internal reflection, direct the light forward by scattering the light at different angles and produce the effect of a homogeneously illuminated surface.

Various techniques that have been described in the literature for modeling the optical microstructures on the LGP were discussed in Chapter 2. For example, creating dot design on the LGP is the most common techniques [Ide et al., 2003; Chang et al., 2005; Choi et al., 2004]. Patterning of optical microstructures in either the top or bottom surface of the LGP was also discussed [Chang and Fang, 2007]. However in most cases, optical microstructures were distributed in the LGP by either varying radius of microstructures or density of microstructures or combination of both. State-of-the-art in fabrication methods to validate the proposed design involve photoresist reflow process, injection molding or hot embossing where the master mold is prepared by mechanical micromachining or some other process mentioned in Figure 2.11 followed by a replication process to get the final structure. During fabrication of the mold, creating microstructures by varying radius technique requires frequent change of tools. As a result the whole process becomes expensive and time consuming and often it is not possible to compare the simulation result with the real set up right away.

In the research presented in this thesis, the cylindrical shape of optical microstructure with hemispherical or rounded tip has been chosen as their curvature would scatter the incident light well and thus resulting in better exiting-light uniformity of LGP's. This shape is also based on a standard ball-end milling tool for manufacturing features directly onto the PMMA substrate. An analysis is carried out to select the geometry (concave or convex) of the cylindrical microstructure and arrangement of array of these microstructures over the LGP is discussed. To verify this, the optical simulation tool "Light Tools" is used to determine the shape of the optical microstructures and arrangement of arrays respectively. A new optimization technique is discussed by varying only the depth of cylindrical microstructures in order to obtain near optimal illumination uniformity for the LGP. The microstructures by only varying the depth will be easier to create directly in PMMA by the use of ball end tool of fixed diameter in micromilling. This will assist for examining the simulation results with the fabricated prototype right away without the requirement of any mold and any expensive set-up. The technique for controlling the light for any specific pattern within any area of the LGP is also presented in this chapter. Advantages for using the proposed optimization technique are also discussed in this chapter.

3.2 Single Microstructure

Since the objective is to transform multiple point light source into an area of uniform illumination, refractive optical microstructures were chosen because they have higher efficiency and offer substantial properties such as less stray light, larger numerical apertures and reduced wavelength sensitivity [Herzig, 1997].

When the light rays strike the cylindrical microstructures on the LGP surface, the angles of incidence would vary greatly with the incident positions due to the curvature of the cylindrical microstructures. As a result, the light rays would be scattered out of the exiting light surface of the LGP along a wide range of directions [Chen et al., 2008]. Also this type of structure would be easier to create in an LGP by using a ball end milling tool where only radius and depth will be the only two parameters as shown in Figure 3.1.

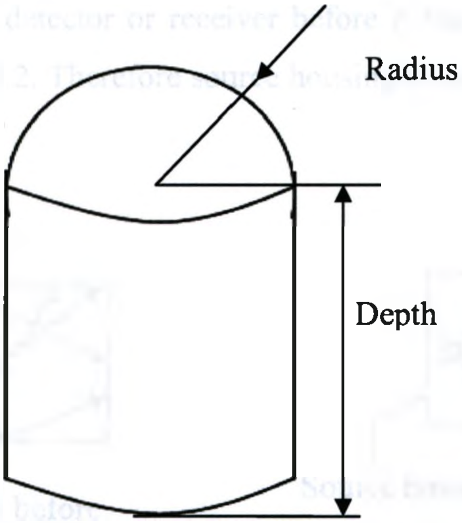

Figure 3.1 Parameters for a hemispherical-tip cylindrical shape microstructure.

From an automotive lighting perspective, the shape of the interior convenience lights or exterior tail lamps must reflect the aesthetic style and contour of the vehicle while emitting high luminous intensity uniformly across the active surface. Thus the change in luminance with curvature is an important design parameter and the cylindrical microstructures could result in better exiting-light uniformity. Concave microstructures (cylindrical microstructures) can be micromachined directly on the transparent substrate with the radius and depth of surface penetration being the two defining parameters to minimize fabrication steps and reduce manufacturing errors. High speed micromilling is capable of producing microstructures with high profile accuracy and outstanding optical quality surface finish. In addition, this form of microfabrication permits a variety of microfeature parameters and array patterns to be examined.

For the simulation, light emitting diode (LED) was used as light source. Nine LED's are placed 12 mm apart along the left edge of the LGP, termed as "edge-lit" which provides better optical control, reduced power consumption, requires fewer LEDs, and reduce the number of layers of light management film. Each LED exhibits nearly Lambertian, wide angle distribution and equivalent to the model LHR974 from OSRAM. Source housing was used to minimize light flux loss at the entrance of LGP. Because if the source radiation pattern angle doesn't match with the acceptance pattern angle of the LGP, there will be loss of light flux at the entrance surface of the LGP and some of the rays may directly hit the detector or receiver before it transmitted and guided into the LGP as shown in Figure 3.2. Therefore source housing is useful for effective in-coupling of light into the LGP.

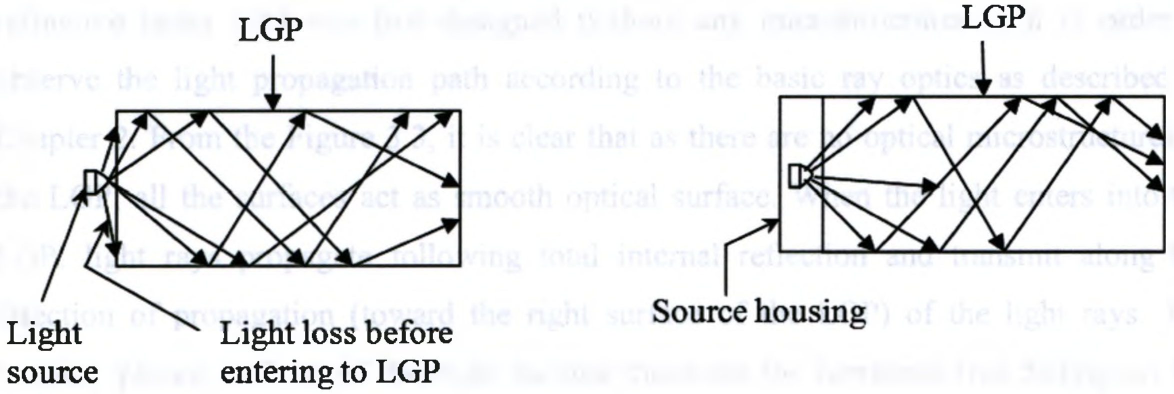

(a)Without source housing
(Right side view)

(b) With source housing, No light loss at
the entrance face of LGP (Right side view)

Figure 3.2 Effect of using source housing for light source.

When a light ray is incident upon the interface between two transparent media, the incident ray is divided between a reflected ray and a refracted (transmitted) ray, as discussed in Section 2.2. The law of reflection and Snell's law predict the path of the resulting rays, and Fresnel's law of reflection predicts the amount of intensity carried by each ray. In order to provide maximum light intensity on top surface, either reflective film or antireflective coating is used under the bottom surface to recycle the light. Generally reflective films are easier to use and far less expensive than antireflective coating. In this research, no reflective film or antireflective coatings were used in order to develop a system with near optimal illumination uniformity without any additional layer, which will reduce the cost as well. Light propagation characteristics in a LGP with smooth optical surface and in a LGP with patterned bottom surface were discussed in the previous chapter. In a LGP without patterning bottom surface, output rays are parallel to the direction of propagation of incident rays. Whereas after patterning or modifying the bottom surface of the LGP, optical microstructures spread the incident light in a wider angle and thus output rays follow a direction perpendicular to the direction of propagation of incident rays.

A LGP of (100 mm x 100 mm x 6 mm) (L *x* W x H) made from PMMA of refractive index 1.49 was first designed without any microstructures in it in order to observe the light propagation path according to the basic ray optics as described in Chapter 2. From the Figure 3.3, it is clear that as there are no optical microstructures in the LGP, all the surfaces act as smooth optical surface. When the light enters into the LGP, light rays propagate following total internal reflection and transmit along the direction of propagation (toward the right surface of the LGP) of the light rays. The receiver placed in front of the right surface measures the luminous flux falling on the right surface (illumination), in terms of photometric units, lux.

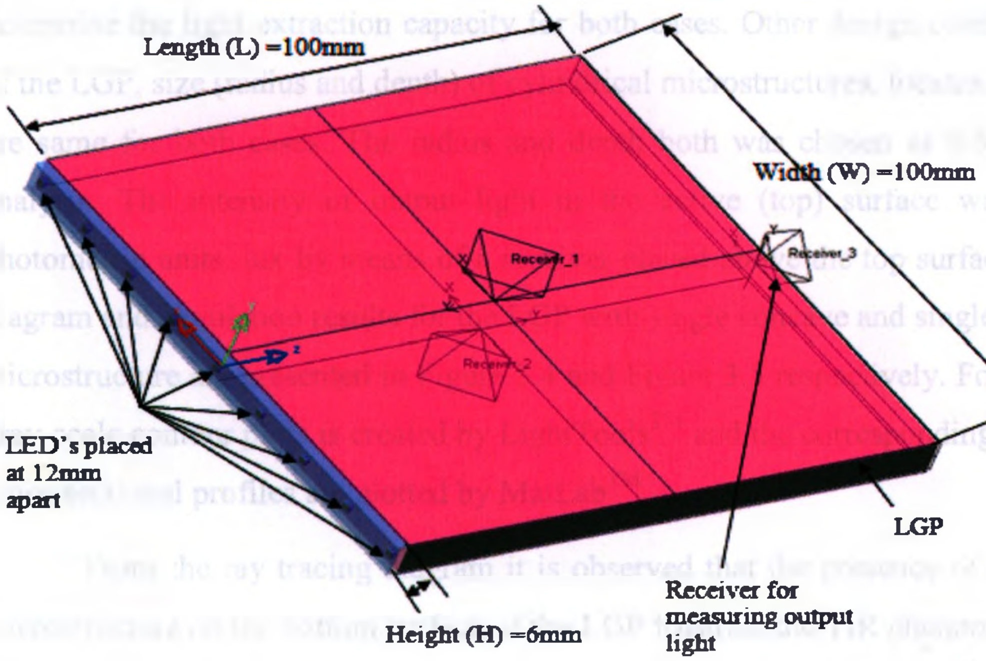
Length (L) =100mm
Width (W) =100mm
Receiver_1
Receiver_3
Receiver_2
LED's placed at 12mm apart
LGP
Receiver for measuring output light
Height (H) =6mm

(a) Design

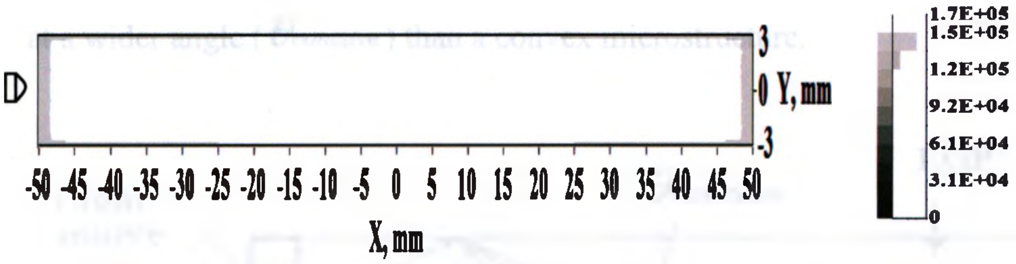

(b) Illumination on the active (right) surface of the LGP

Figure 3.3 Illumination behavior for LGP without patterning any surface.

To observe the effect of patterning the bottom surface of the LGP, a single concave and convex optical microstructure was placed on the bottom surface of the LGP in two different cases. The purpose of placing both the single microstructure in concave and convex shape was to select the geometry of microstructure for further analysis by drawing a comparison of light extraction capacity between concave and convex shape.

Since light intensity decreases as it travels away from the source, as discussed in Section 2.2, location of the single microstructure was chosen at the middle of the LGP to determine the light extraction capacity for both cases. Other design conditions, i.e., size of the LGP, size (radius and depth) of cylindrical microstructures, locations of LED's, etc. are same for both cases. The radius and depth both was chosen as 0.5 mm for initial analysis. The intensity of output light in the active (top) surface was measured in photometric units, lux by means of a receiver placed above the top surface. Ray tracing diagram and simulation results for the LGP with single concave and single convex optical microstructure are presented in Figure 3.4 and Figure 3.5 respectively. For simulations, a gray-scale contour plots is created by LightTools^{TM} and the corresponding X-X' and Y-Y' cross-sectional profiles are plotted by MatLab^{TM}.

From the ray tracing diagram it is observed that the presence of a single optical microstructure on the bottom surface of the LGP frustrate the TIR phenomenon inside the LGP and direct the light in a direction perpendicular to the direction of propagation of light (top surface in this case). Also from the ray tracing diagram as shown in Figure 3.4(a), it can be explained that a concave microstructure can spread the incident light rays at a wider angle ($\theta_{concave}$) than a convex microstructure.

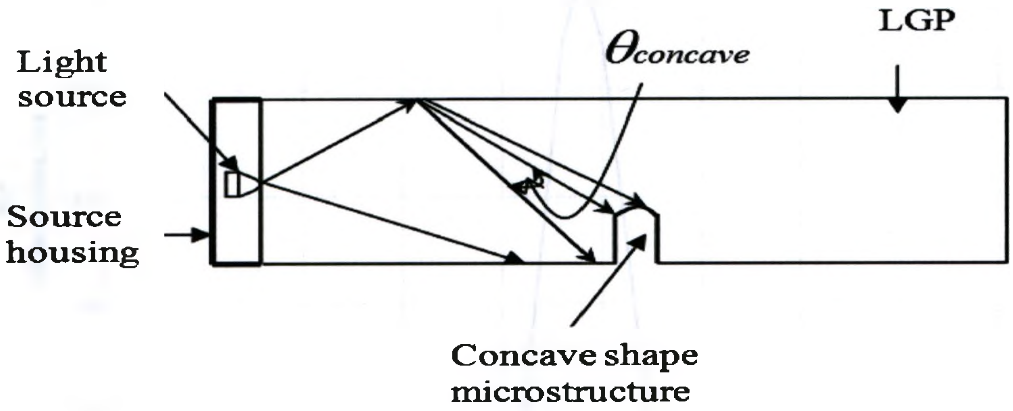

(a) Ray tracing diagram

Figure 3.4 (continued)

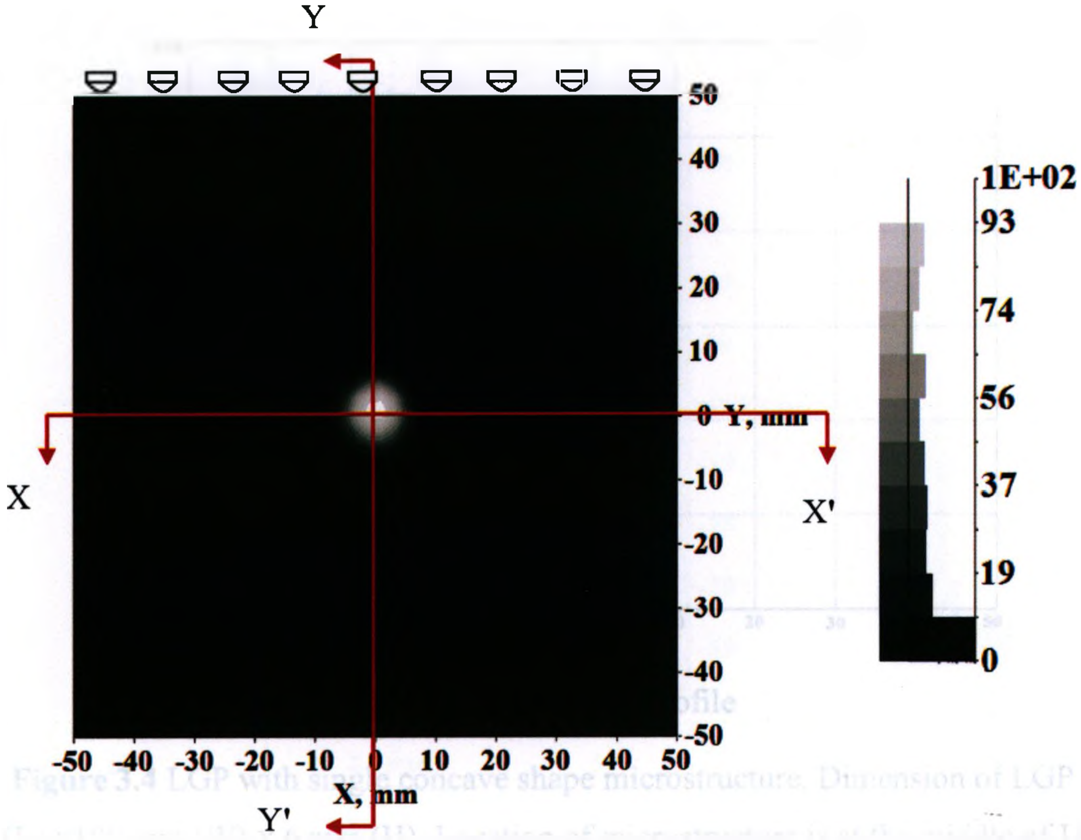

(b) Illumination on active (top) surface

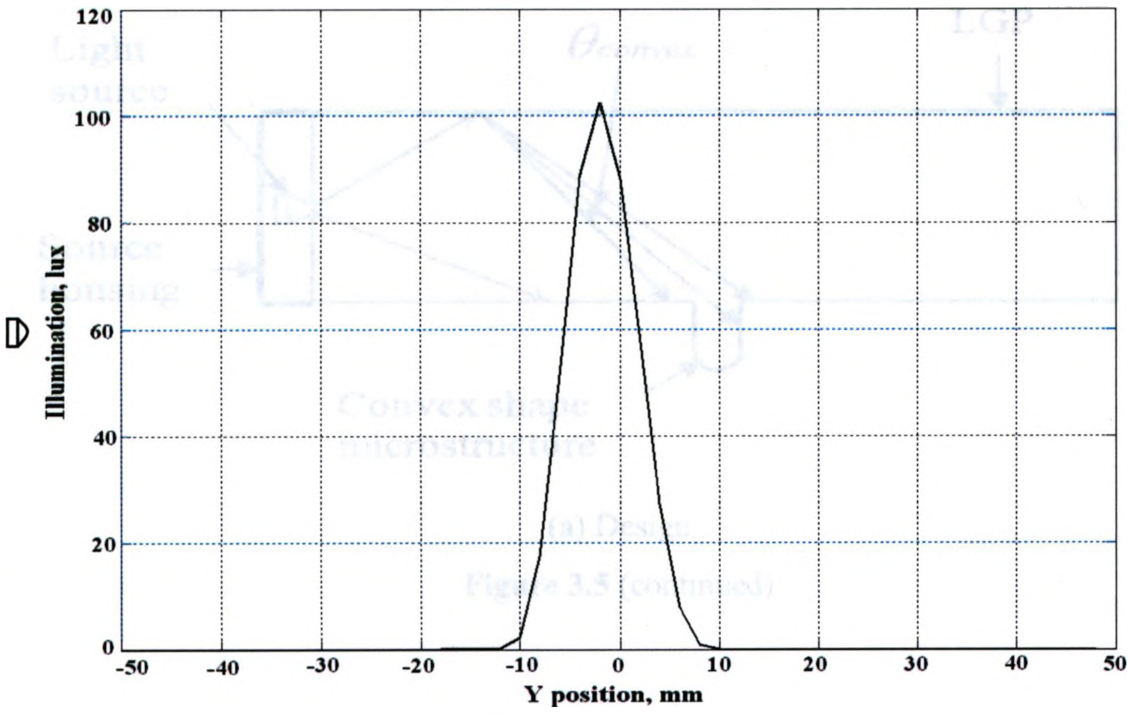

(c) Y-Y' illumination profile

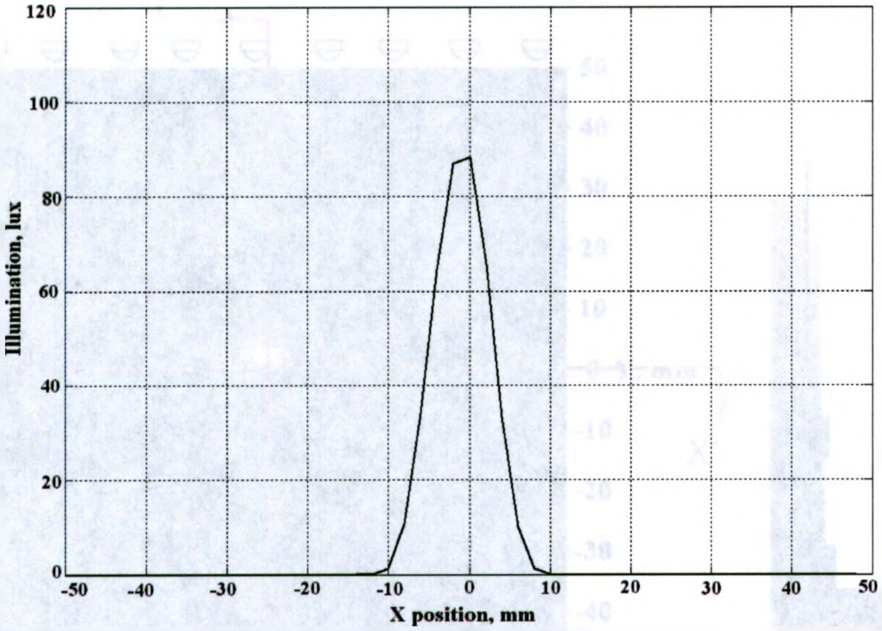

(d) X-X' illumination profile

Figure 3.4 LGP with single concave shape microstructure. Dimension of LGP: 100 mm (L) x100 mm (W) x 6 mm (H). Location of microstructure is at the middle of LGP, radius and depth of microstructure are 0.5 mm and 0.5 mm respectively.

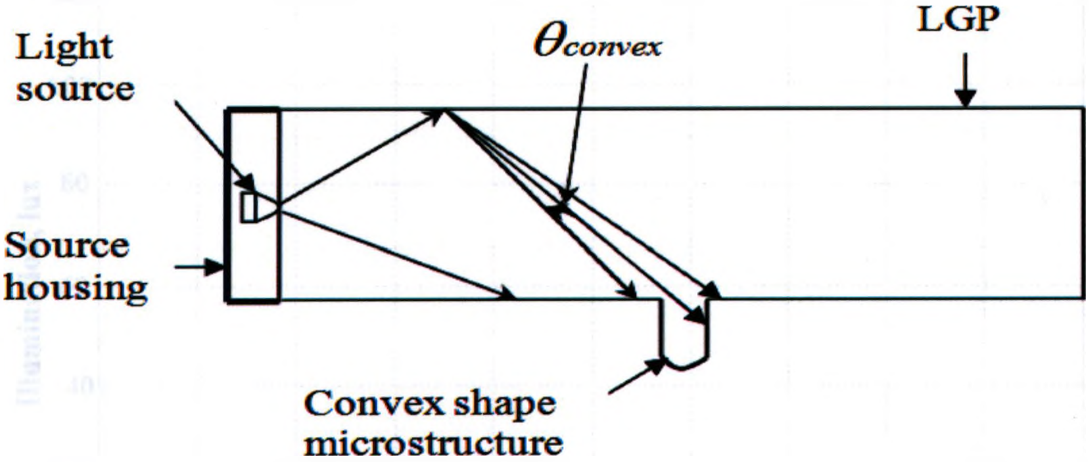
Light source
θ_{convex}
LGP
Source housing
Convex shape microstructure

(a) Design

Figure 3.5 (continued)

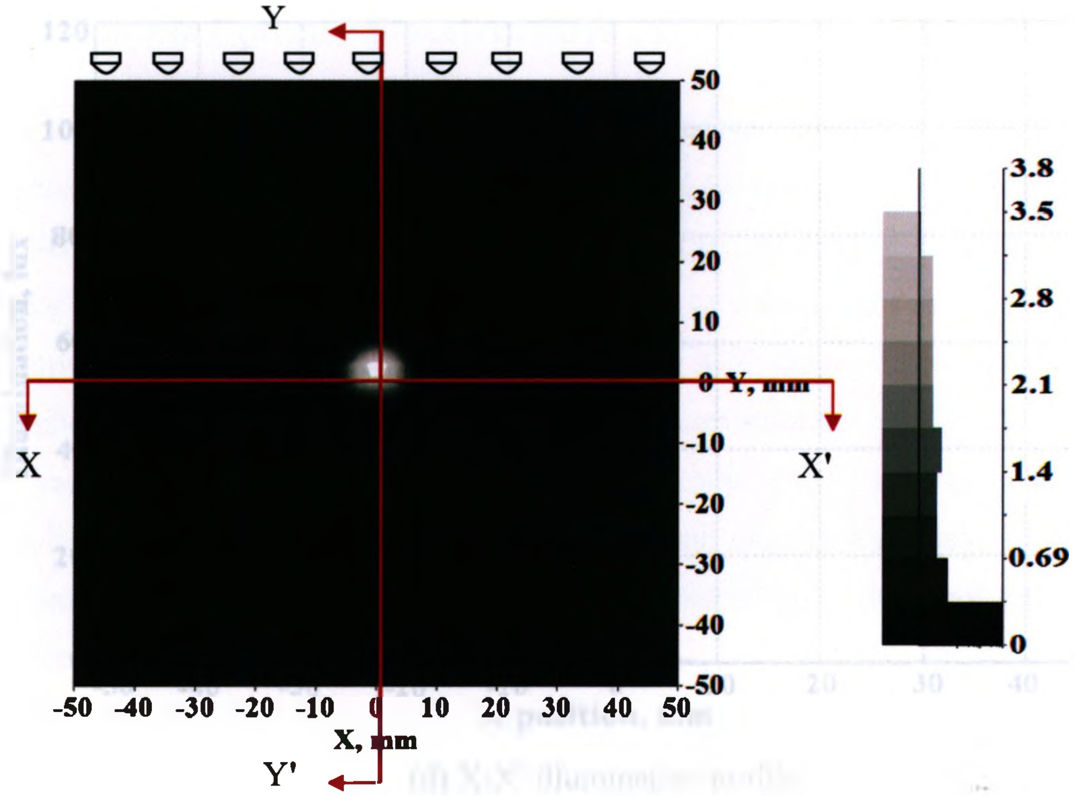

(b) Illumination on active (top) surface

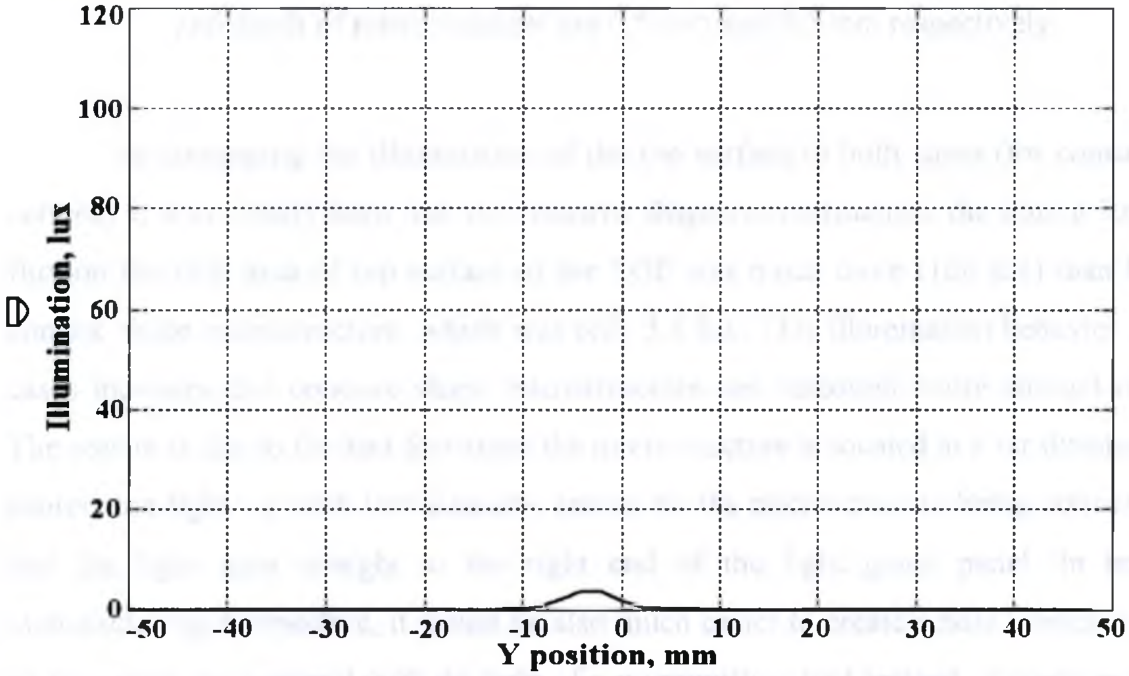

(c) Y-Y' illumination profile

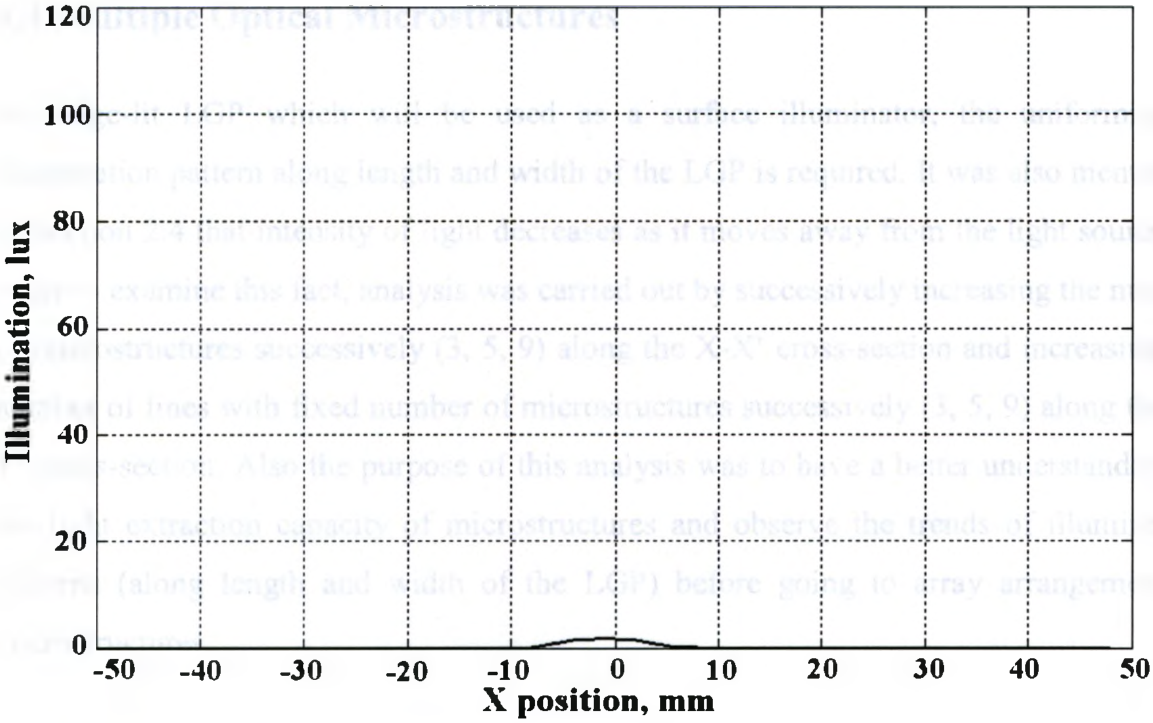

(d) X-X' illumination profile

Figure 3.5 LGP with single convex shape microstructure. Dimension of LGP: 100 mm (L) x100 mm (W) x 6 mm (H). Location of microstructure is at the middle of LGP, radius and depth of microstructure are 0.5 mm and 0.5 mm respectively.

By comparing the illumination of the top surface in both cases (for concave and convex) it was clearly seen that for concave shape microstructure, the output luminous flux on the total area of top surface of the LGP was much more (100 lux) than that for convex shape microstructure, which was only 3.8 lux. This illumination behavior in both cases indicates that concave shape microstructure can outcouple more amount of light. The reason is due to the fact that since the microstructure is located at a far distance from source, the light ray with low intensity cannot hit the microstructure being convex shape and the light goes straight to the right end of the light guide panel. In terms of manufacturing perspective, it would be also much easier to create a hole (concave shape) by removing the material with the help of a micromilling tool instead of creating a bump (convex shape). Based on the above analysis, concave shape cylindrical microstructure was chosen as a light scattering element in the LGP.

3.3 Multiple Optical Microstructures

An edge-lit LGP which will be used as a surface illuminator, the uniformity of illumination pattern along length and width of the LGP is required. It was also mentioned in Section 2.4 that intensity of light decreases as it moves away from the light source. In order to examine this fact, analysis was carried out by successively increasing the number of microstructures successively (3, 5, 9) along the X-X' cross-section and increasing the number of lines with fixed number of microstructures successively (3, 5, 9) along the Y-Y' cross-section. Also the purpose of this analysis was to have a better understanding of the light extraction capacity of microstructures and observe the trends of illumination patterns (along length and width of the LGP) before going to array arrangement of microstructures.

3.3.1 Linear array of microstructures

Linear arrays are defined as where the size of microstructures and pitch (centre to centre distance between microstructures) between each microstructure are uniform throughout the whole area of the LGP. In the first illustrated case as shown in Figure 3.6, the number of microstructures will be increased at a fixed location along the Y-Y' cross-section. The number of microstructures will be increased at different positions along the X-X' cross-section. The pitch between microstructures is 10 mm for 3 microstructures as in Figure 3.7, 5 mm for 5 microstructures as in Figure 3.8, and 2.5 mm for 9 microstructures as in Figure 3.9. The line was located at 0 mm along the length (Y-Y' cross-section) and from -10 mm to10 mm along the width (X-X' cross-section).

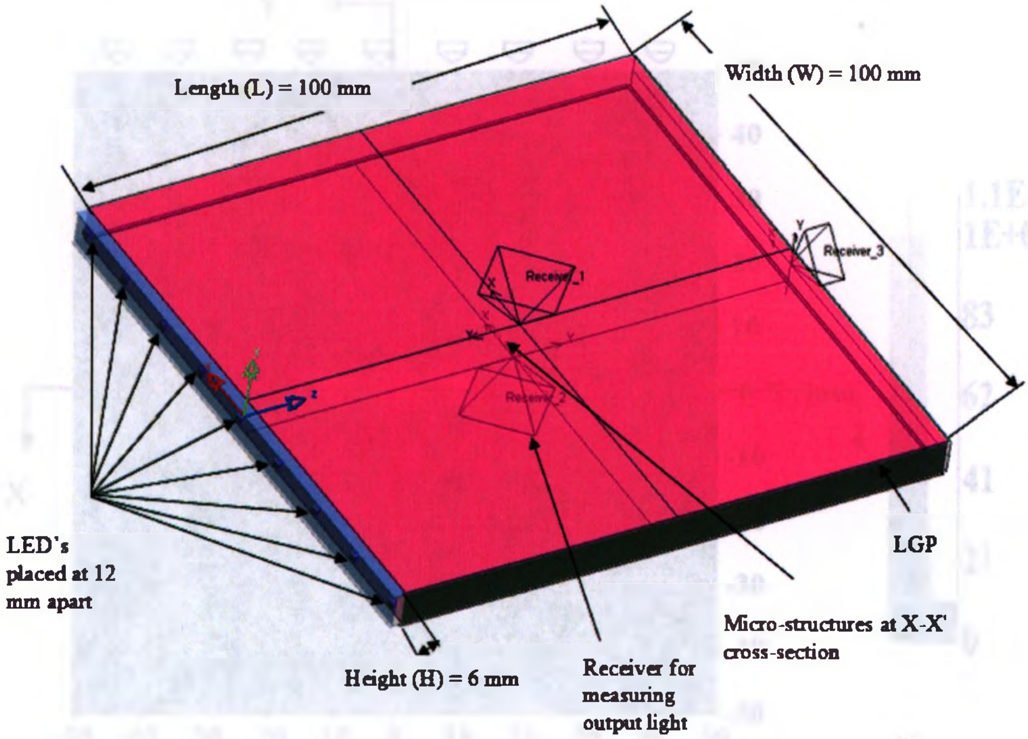
Length (L) = 100 mm
Width (W) = 100 mm
Receiver_1
Receiver_3
Receiver_2
LED's placed at 12 mm apart
LGP
Micro-structures at X-X' cross-section
Height (H) = 6 mm
Receiver for measuring output light

Figure 3.6 Basic design for analyzing the effect of horizontal line of concave microstructures on a flat back surface. Location of line of microstructures is at X-X' cross-section.

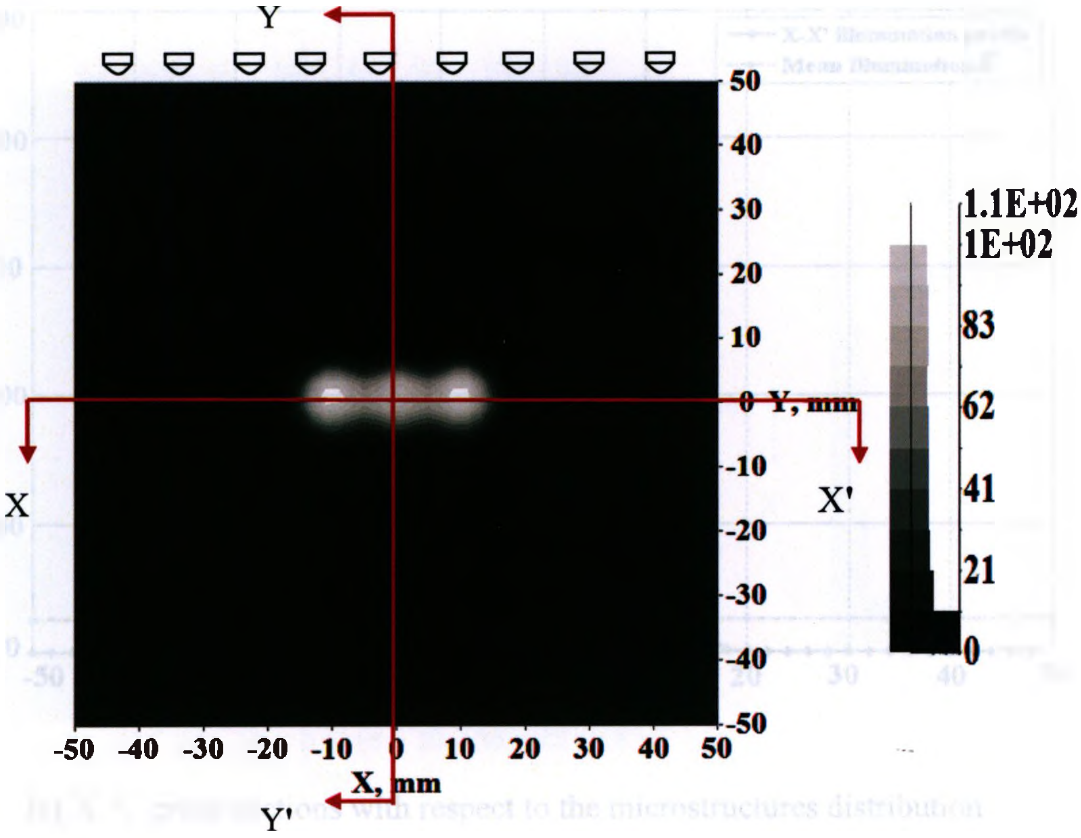

(a) Illumination on active (top) surface

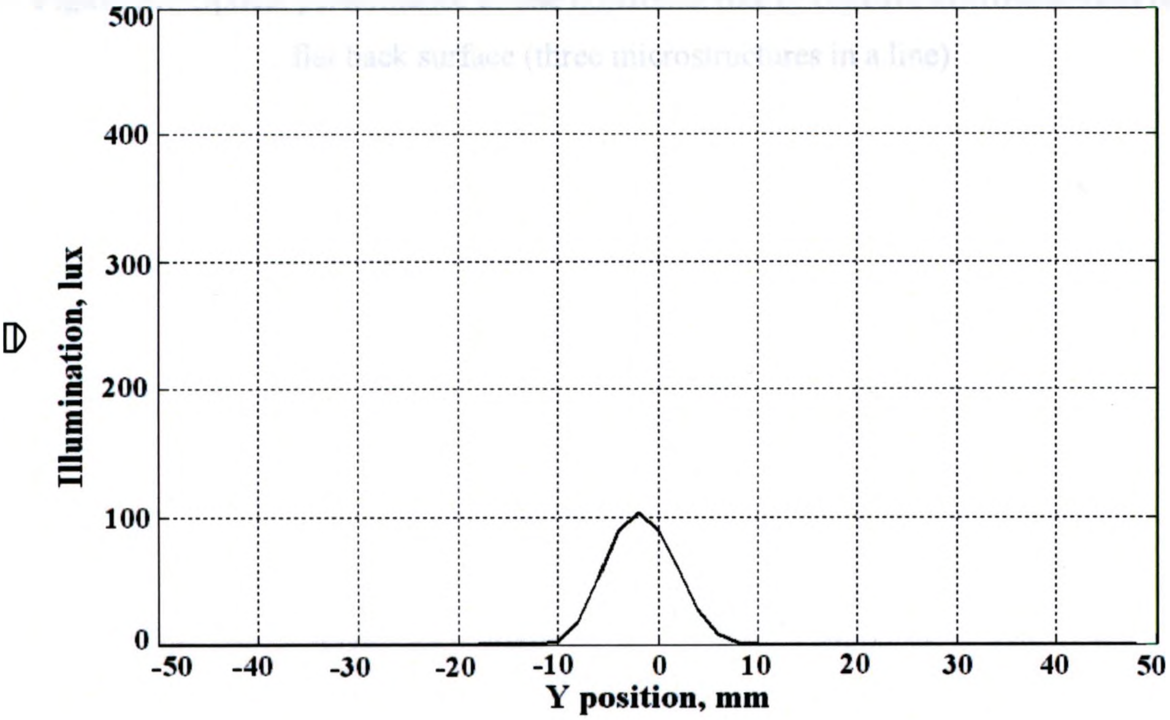

(b) Y-Y' cross-sections with respect to the microstructures distribution

Figure 3.7 (continued)

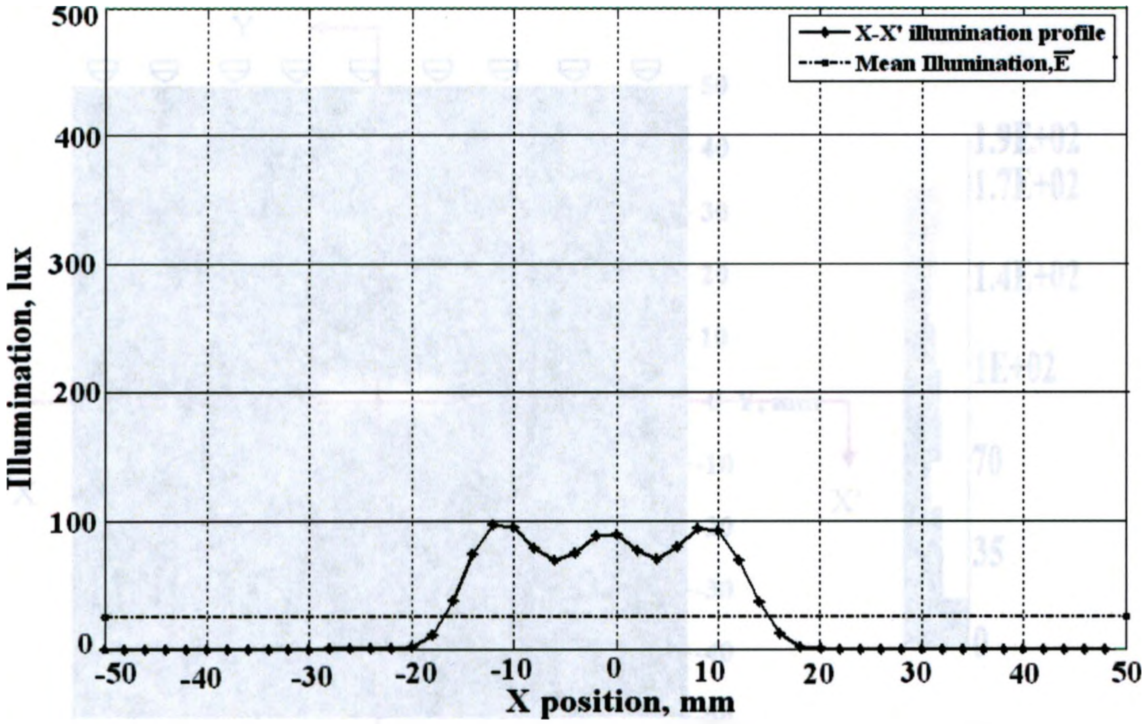

(c) X-X' cross-sections with respect to the microstructures distribution

Figure 3.7 Optical performance of one horizontal line of concave microstructures on a flat back surface (three microstructures in a line)

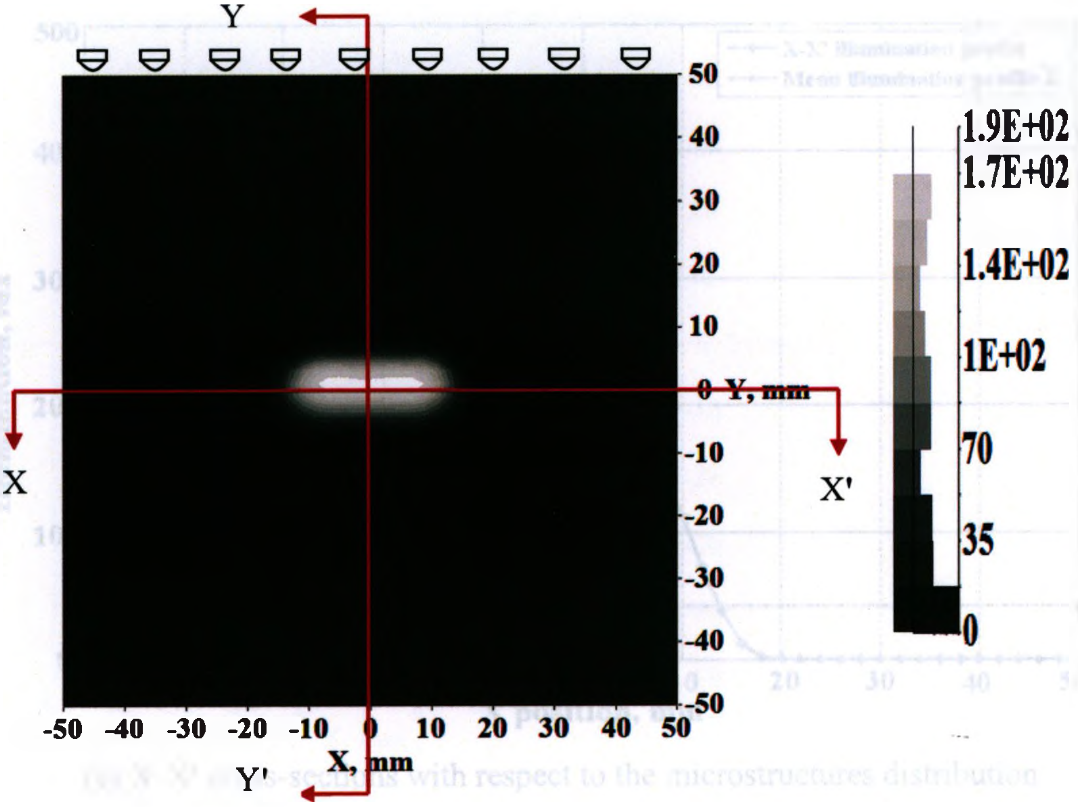

(a) Illumination on active (top) surface

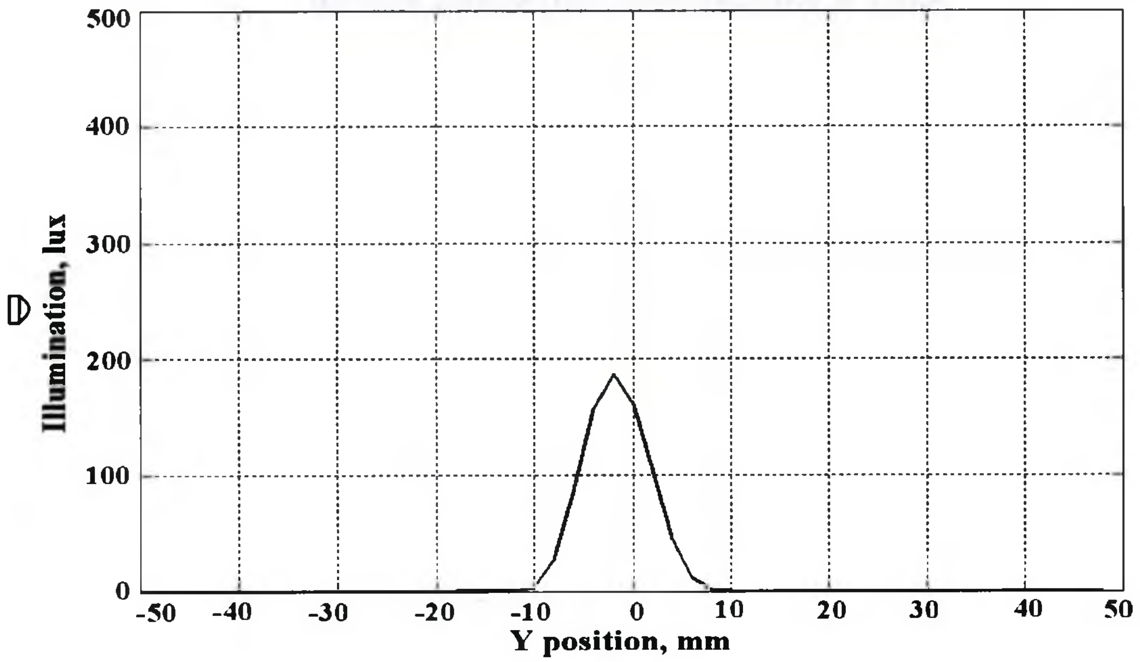

(b) Y-Y' cross-sections with respect to the microstructures distribution

Figure 3.8 (continued)

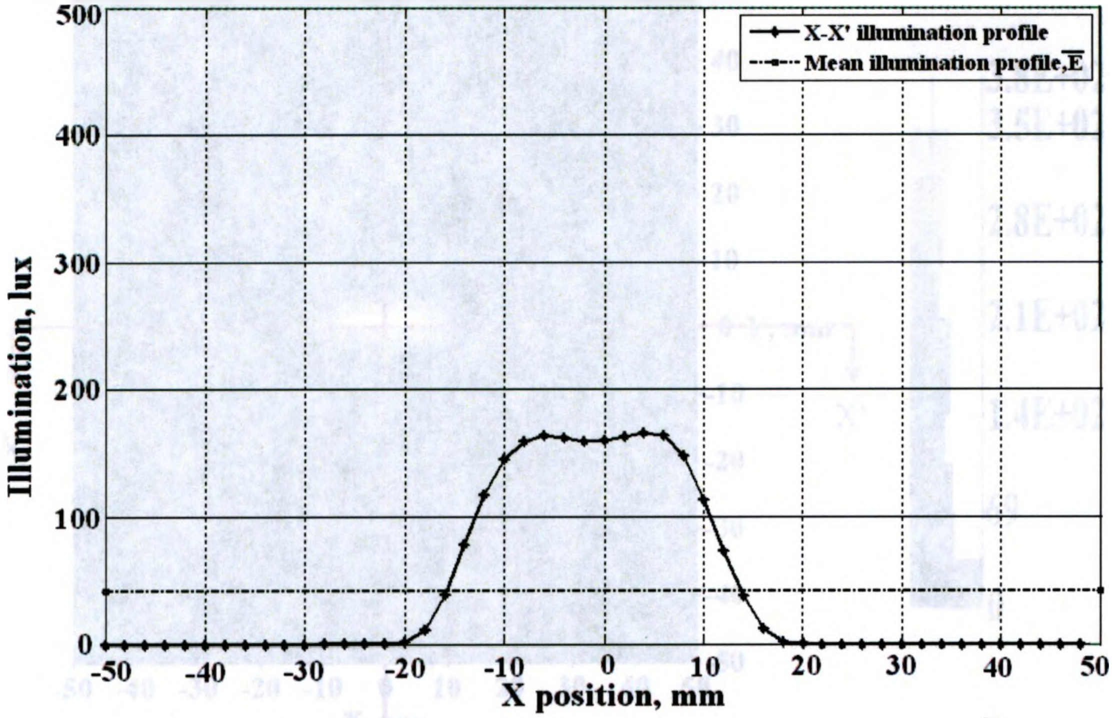

(c) X-X' cross-sections with respect to the microstructures distribution

Figure 3.8 Optical performance of one horizontal line of concave microstructures on a flat back surface (five microstructures in a line)

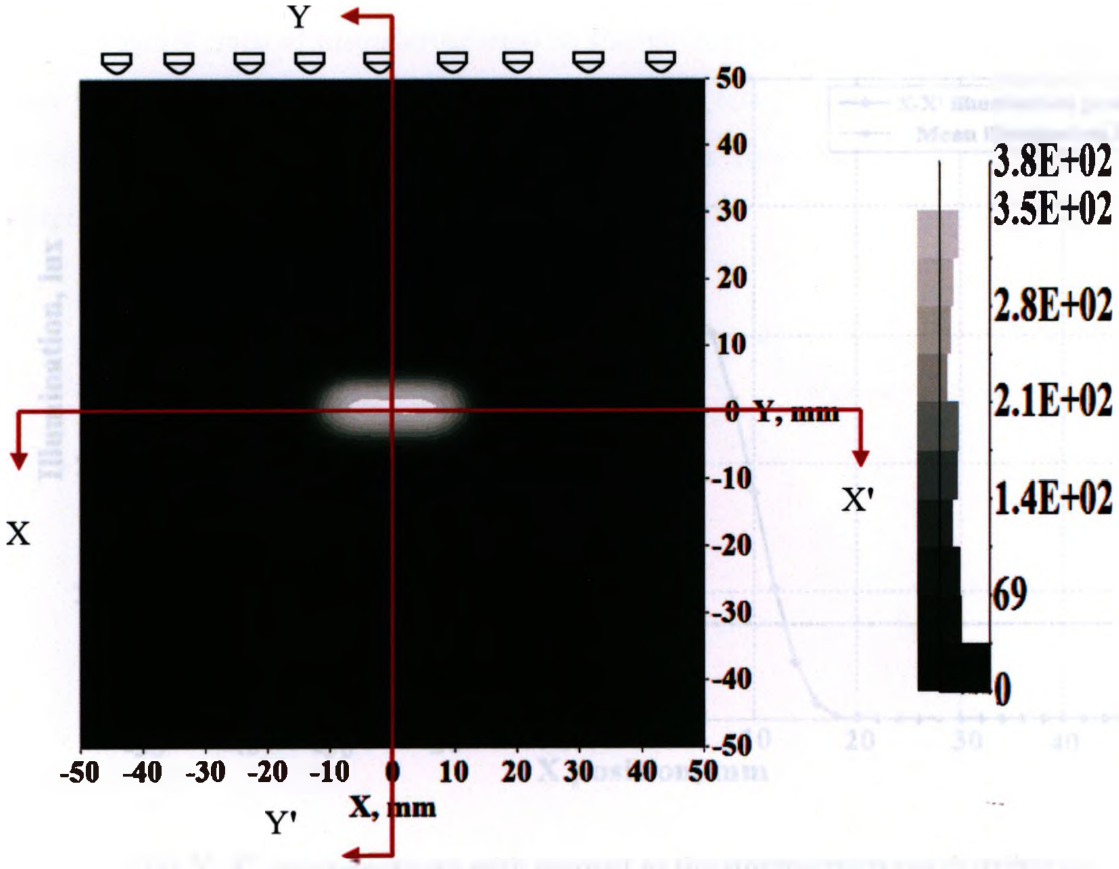

(a) Illumination on active (top) surface

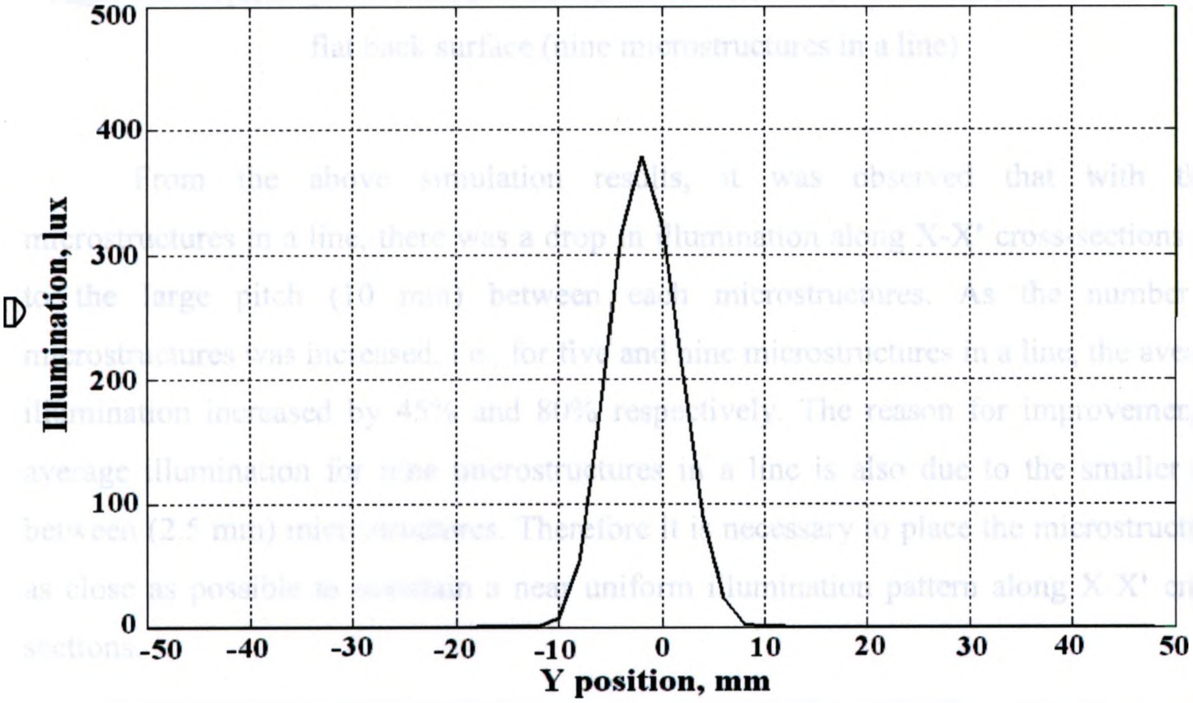

(b) Y-Y' cross-sections with respect to the microstructures distribution

Figure 3.9 (continued)

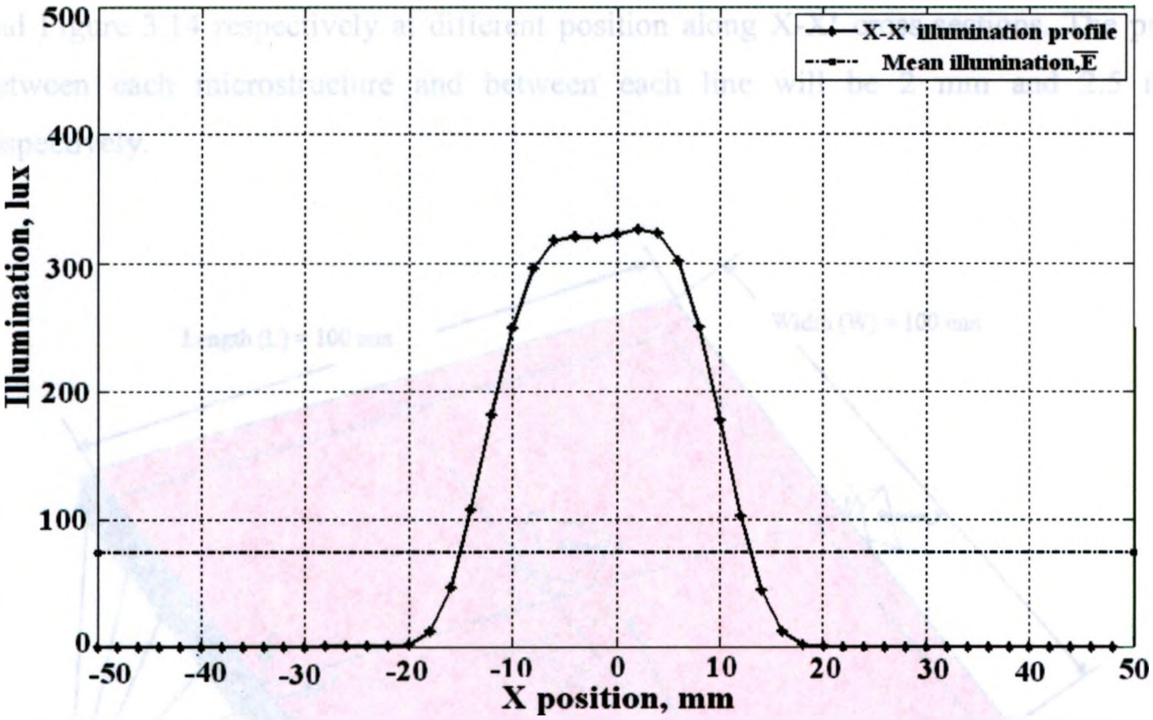

(c) X-X' cross-sections with respect to the microstructures distribution

Figure 3.9 Optical performance of one horizontal line of concave microstructures on a flat back surface (nine microstructures in a line)

From the above simulation results, it was observed that with three microstructures in a line, there was a drop in illumination along X-X' cross-sections due to the large pitch (10 mm) between each microstructures. As the number of microstructures was increased, i.e., for five and nine microstructures in a line, the average illumination increased by 45% and 80% respectively. The reason for improvement in average illumination for nine microstructures in a line is also due to the smaller gap between (2.5 mm) microstructures. Therefore it is necessary to place the microstructures as close as possible to maintain a near uniform illumination pattern along X-X' cross-sections.

For vertical orientation of microstructures as shown in Figure 3.10, there was a fixed number (26) of microstructures in a line and the number of lines will be increased

(1, 3, 5 and 9 lines of microstructures) as shown in Figure 3.11, Figure 3.12, Figure 3.13 and Figure 3.14 respectively at different position along X-X' cross-sections. The pitch between each microstructure and between each line will be 2 mm and 2.5 mm respectively.

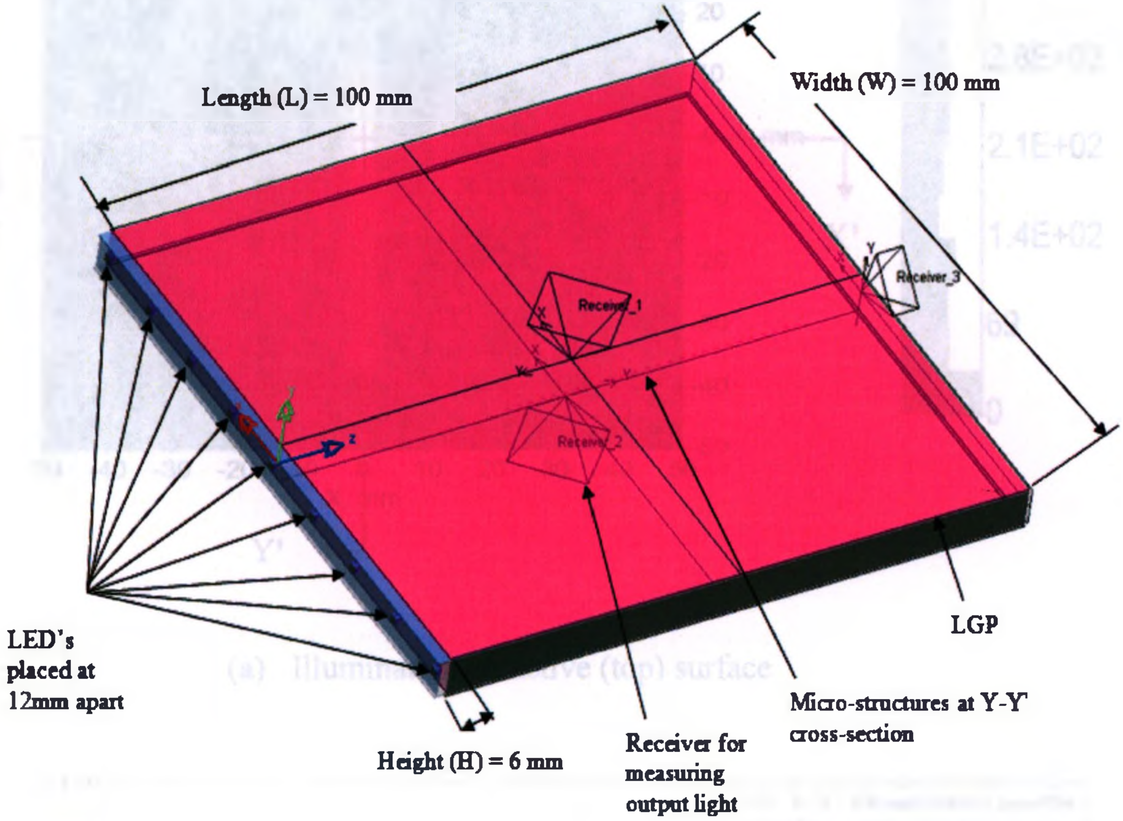
Length (L) = 100 mm
Width (W) = 100 mm
Receiver_1
Receiver_3
Receiver_2
LED's placed at 12mm apart
LGP
Height (H) = 6 mm
Receiver for measuring output light
Micro-structures at Y-Y' cross-section

Figure 3.10 Basic design for analyzing the effect of vertical lines of concave microstructures on a flat back surface. Location of line of microstructure is at Y-Y' cross-section.

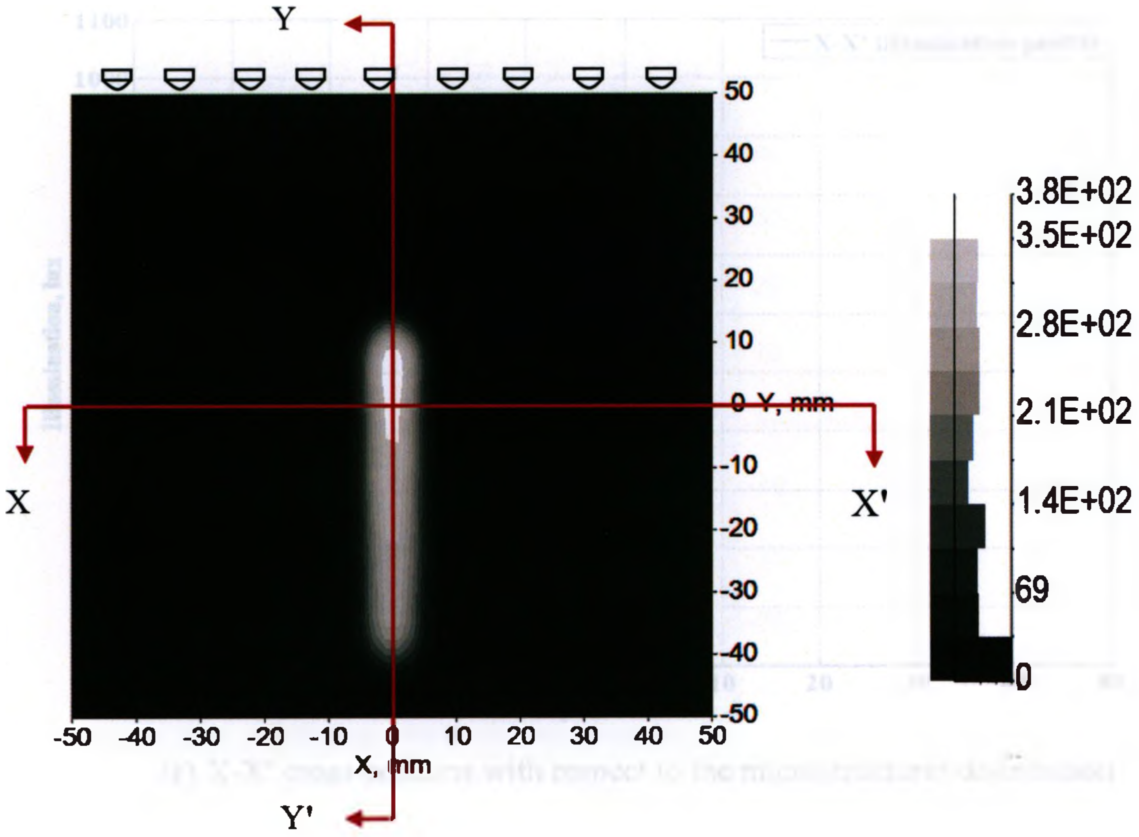

(a) Illumination on active (top) surface

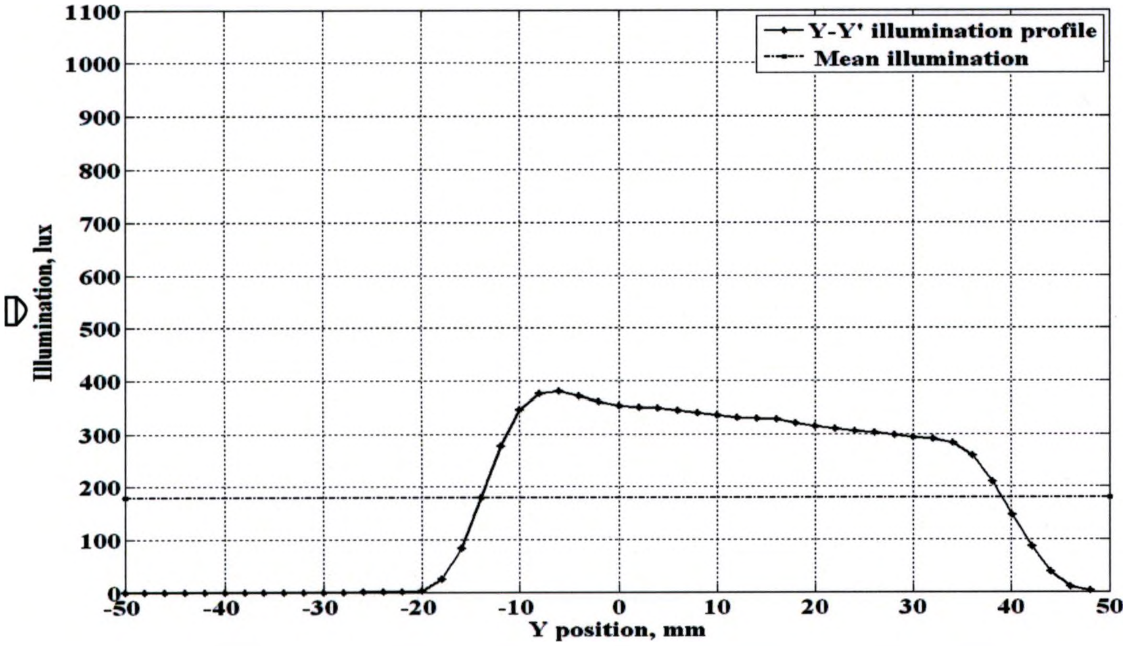

(b) Y-Y' cross-sections with respect to the microstructures distribution

Figure 3.11 (continued)

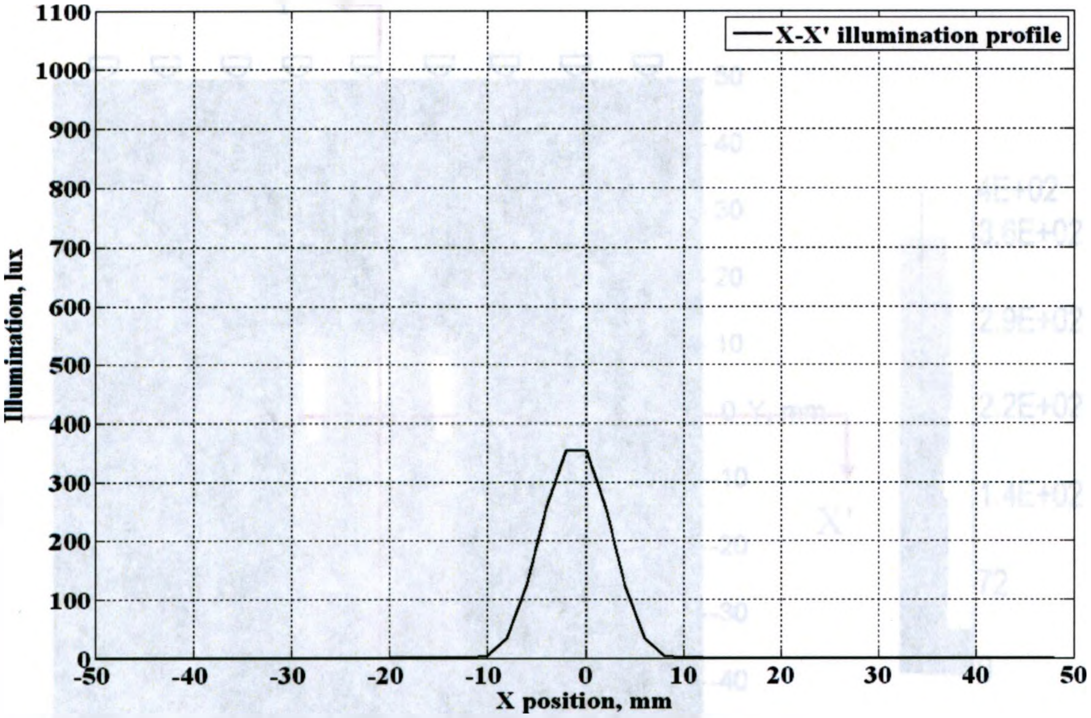

(c) X-X' cross-sections with respect to the microstructures distribution

Figure 3.11 Optical performance of one vertical line of concave microstructures on a flat back surface.

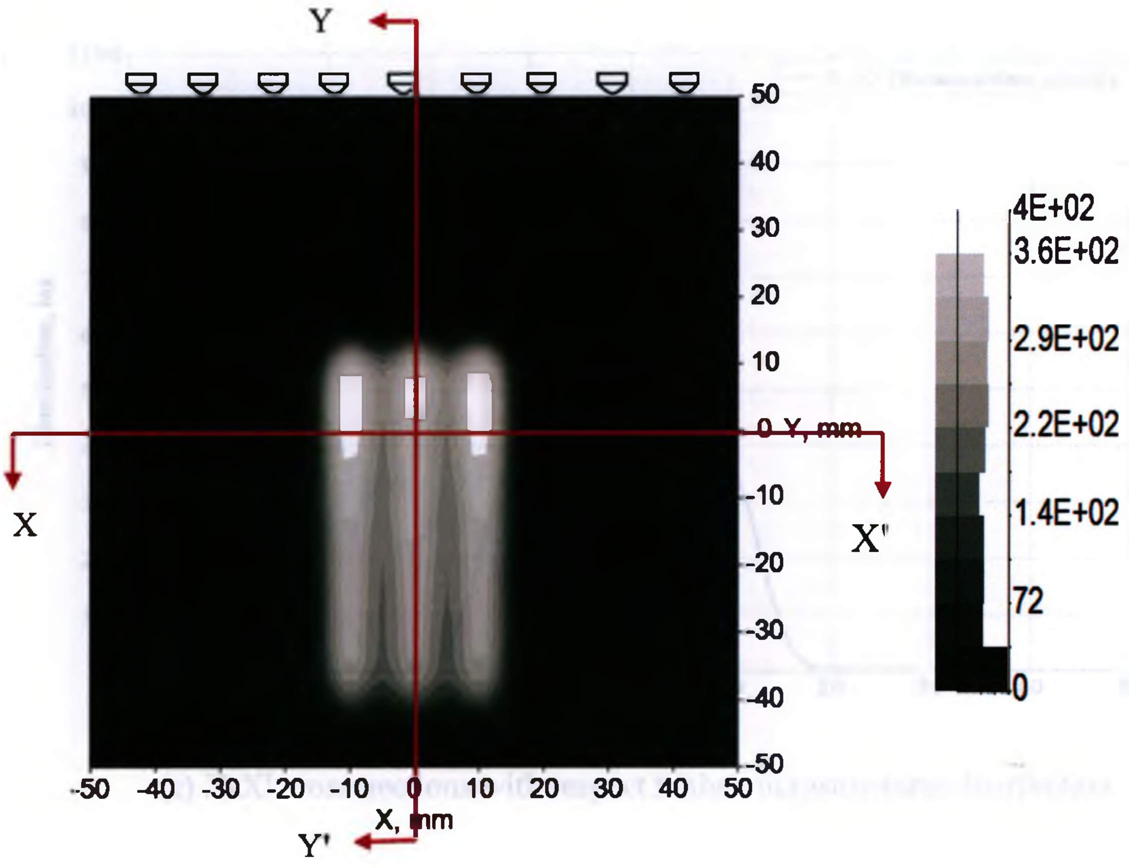

(a) Illumination on active (top) surface

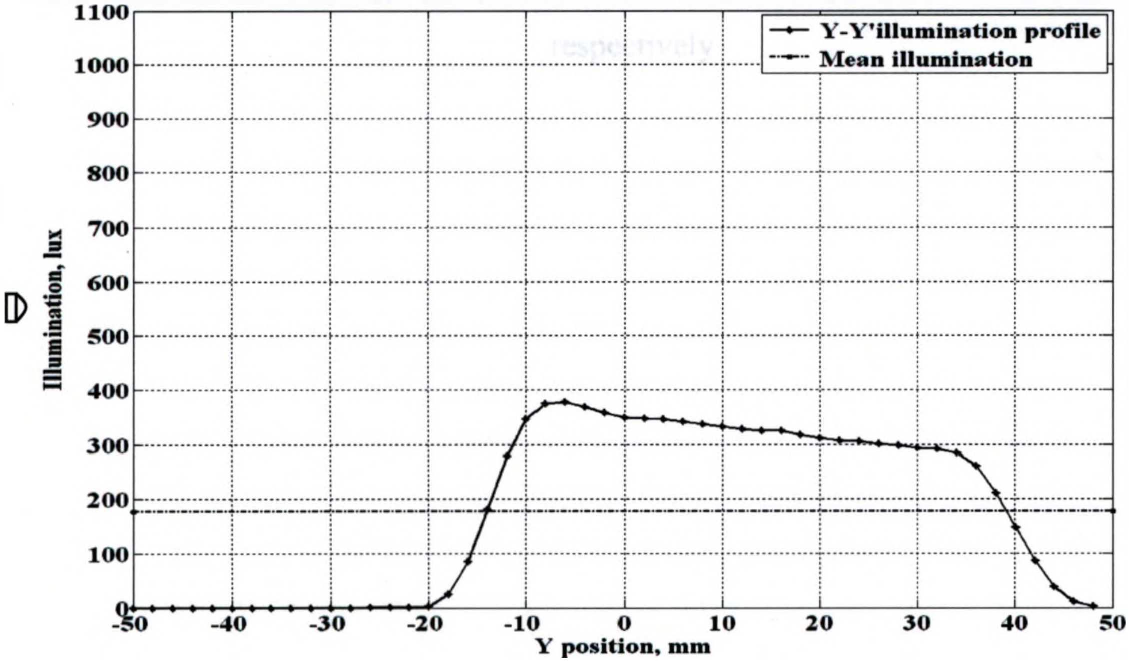

(b) Y-Y' cross-sections with respect to the microstructures distribution

Figure 3.12 (continued)

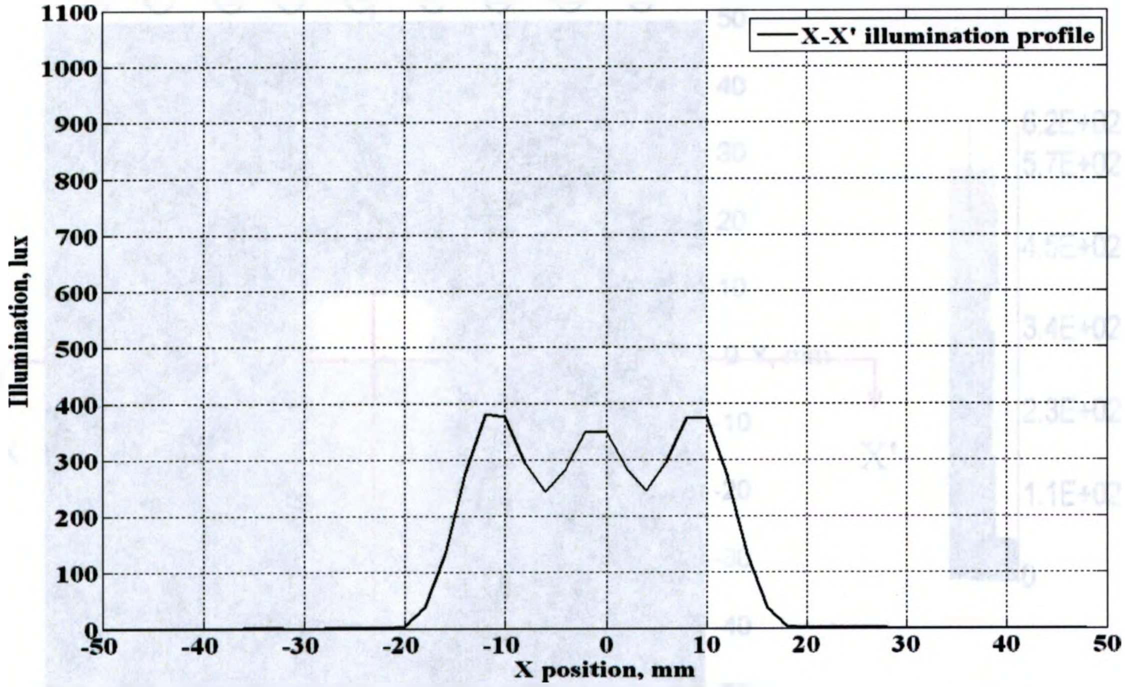

(c) X-X' cross-sections with respect to the microstructures distribution

Figure 3.12 Optical performance of three vertical lines of concave microstructures on a flat back surface. Gap between each microstructure and each line are 2 mm and 10 mm respectively.

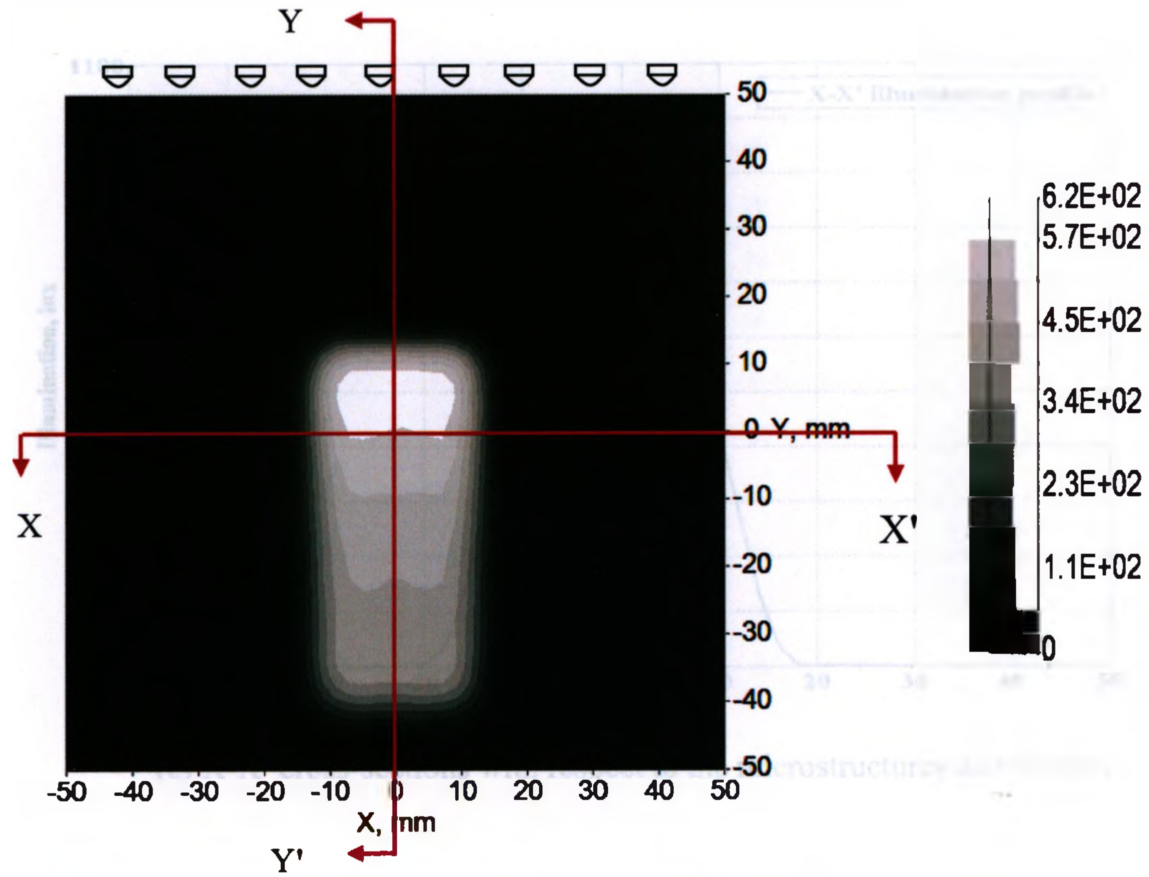

(a) Illumination on active (top) surface

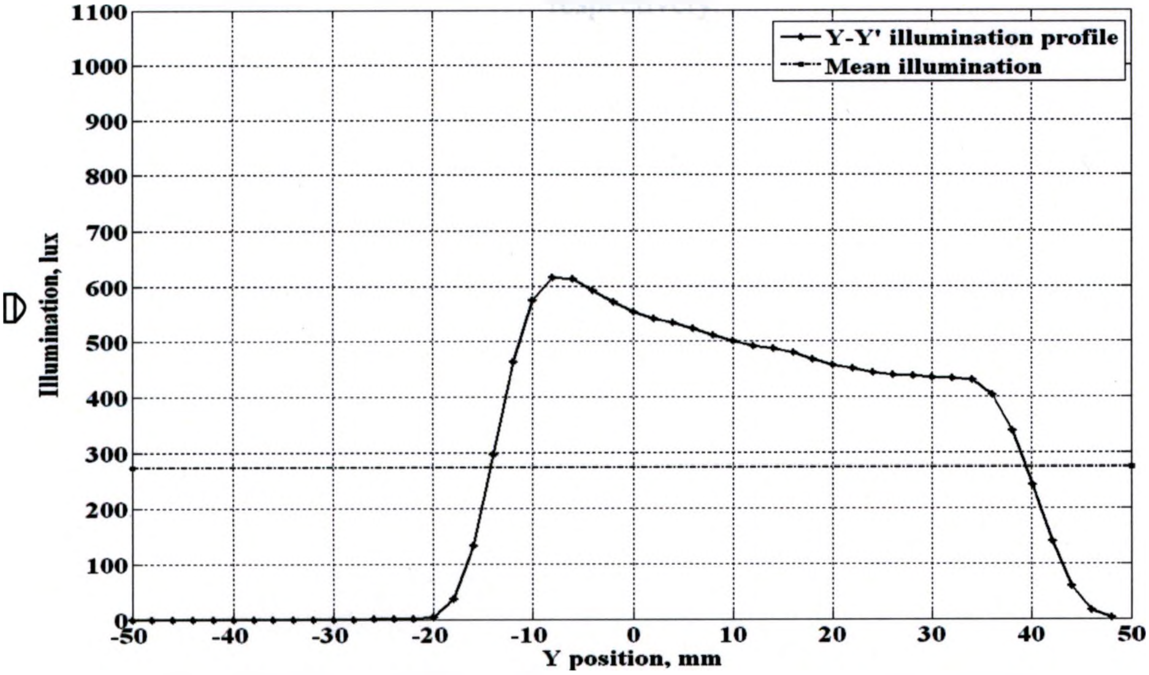

(b) Y-Y' cross-sections with respect to the microstructures distribution

Figure 3.13 (continued)

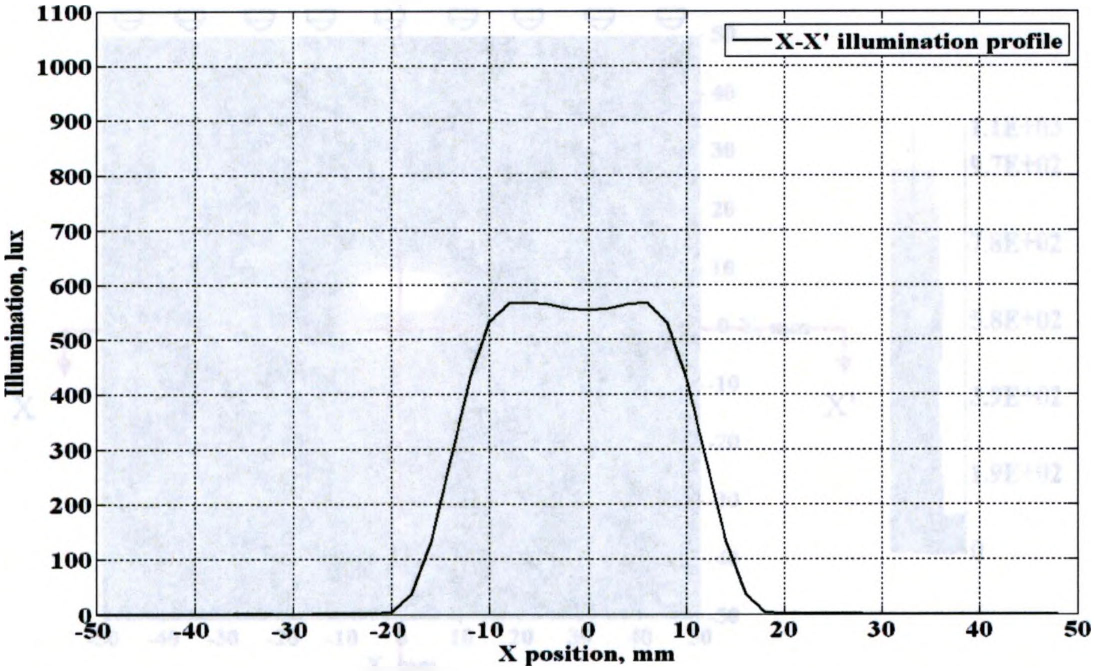

(c) X-X' cross-sections with respect to the microstructures distribution

Figure 3.13 Optical performance of five vertical lines of concave microstructures on a flat back surface. Gap between each microstructure and each line are 2 mm and 5 mm respectively.

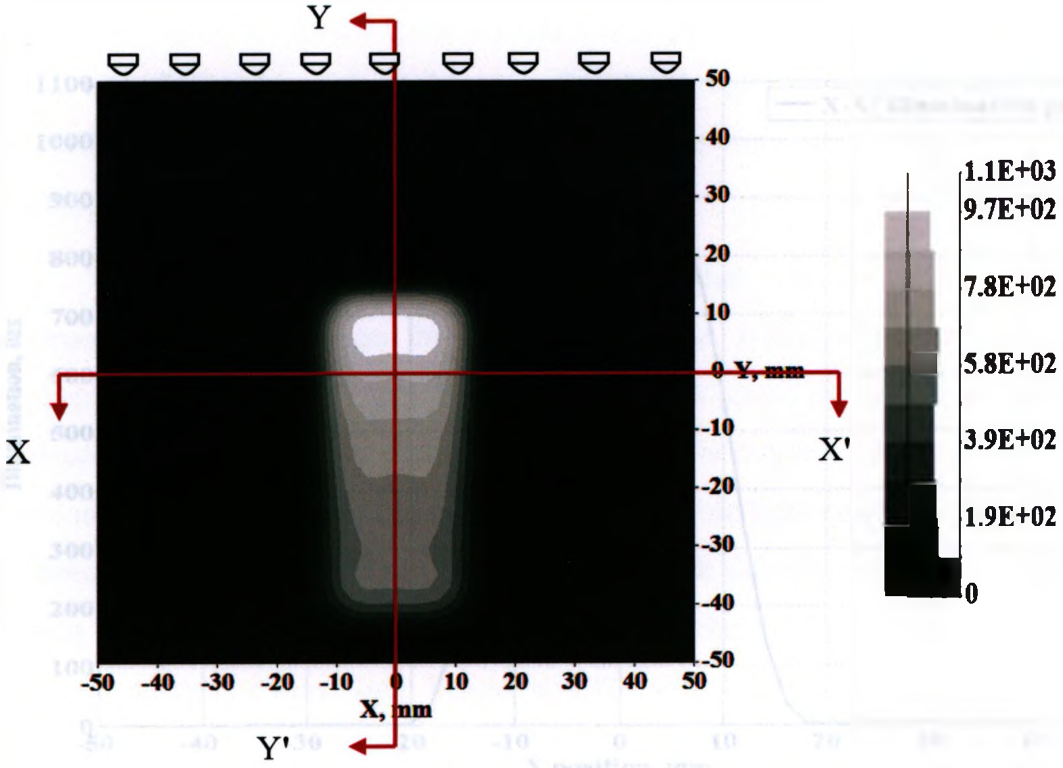

(a) Illumination on active (top) surface

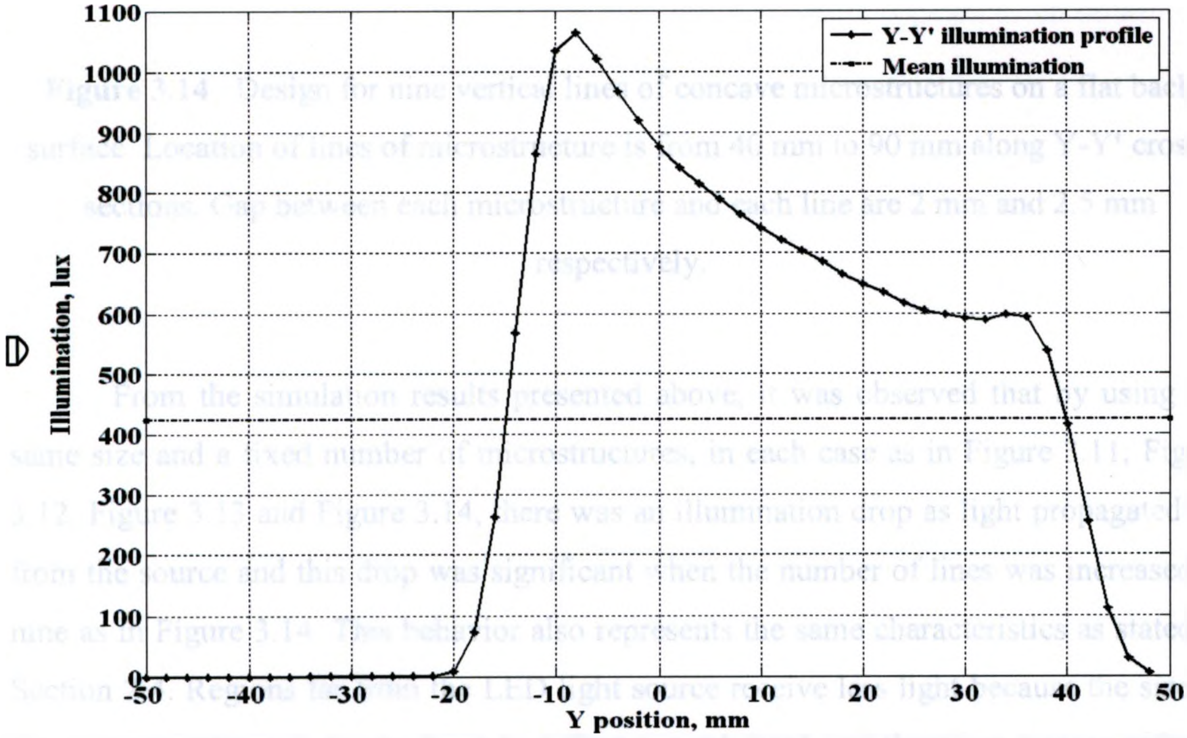

(b) Y-Y' cross-sections with respect to the microstructures distribution

Figure 3.14 (continued)

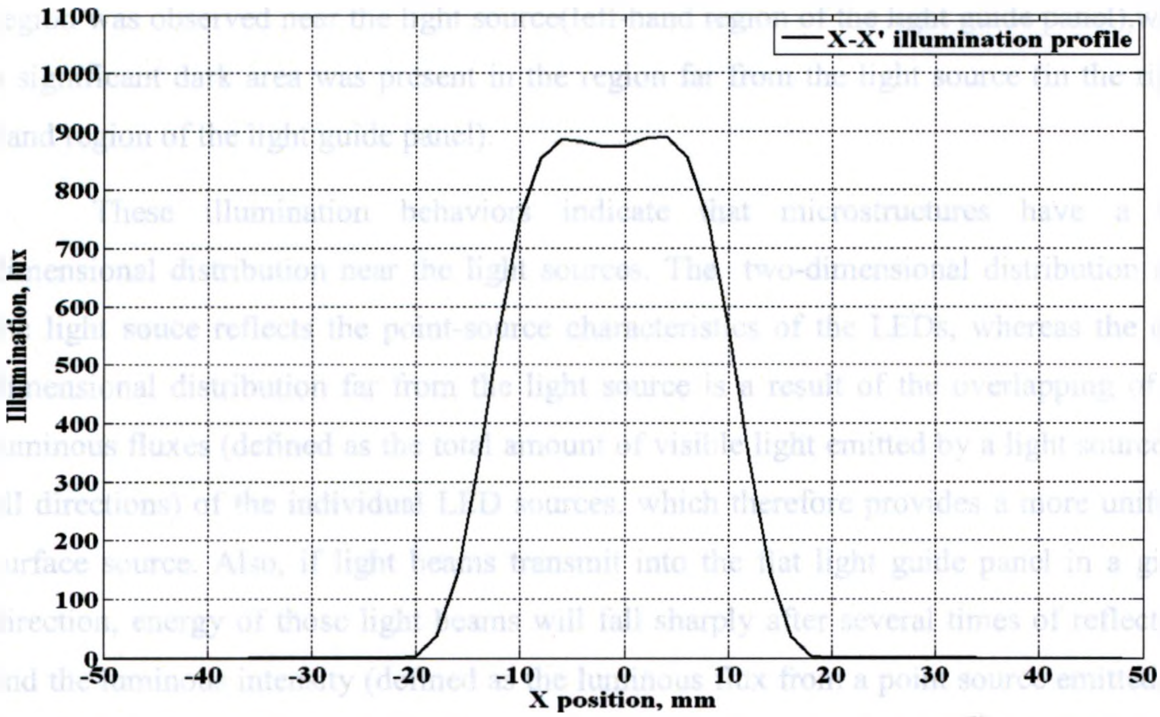

(c) X-X' cross-sections with respect to the microstructures distribution

Figure 3.14 Design for nine vertical lines of concave microstructures on a flat back surface. Location of lines of microstructure is from 40 mm to 90 mm along Y-Y' cross-sections. Gap between each microstructure and each line are 2 mm and 2.5 mm respectively.

From the simulation results presented above, it was observed that by using the same size and a fixed number of microstructures, in each case as in Figure 3.11, Figure 3.12, Figure 3.13 and Figure 3.14, there was an illumination drop as light propagated far from the source and this drop was significant when the number of lines was increased to nine as in Figure 3.14. This behavior also represents the same characteristics as stated in Section 2.4. Regions far from the LED light source receive less light because the size of the microstructures is not so large to reflect enough light and therefore require either a higher density or large size of microstructures to allow more light to pass through the light guide panel in order to achieve near homogeneous illuminance. From the contour plot, as in Figure 3.12(a), Figure 3.13(a) and Figure 3.14(a), it was seen that a bright region was observed near the light source(left-hand region of the light guide panel),while a significant dark area was present in the region far from the light source (in the right-hand region of the light guide panel).

These illumination behaviors indicate that microstructures have a two dimensional distribution near the light sources. The two-dimensional distribution near the light souce reflects the point-source characteristics of the LEDs, whereas the one-dimensional distribution far from the light source is a result of the overlapping of the luminous fluxes (defined as the total amount of visible light emitted by a light source, in all directions) of the individual LED sources, which therefore provides a more uniform surface source. Also, if light beams transmit into the flat light guide panel in a given direction, energy of those light beams will fall sharply after several times of reflection, and the luminous intensity (defined as the luminous flux from a point source emitted per unit solid angle in a given direction) in the end position of the light guide panel will be quite low compared with the light entrance surface of the panel. The solid angle of an object subtends at a point is a measure of how big that object appears to an observer at that point. Details about all photometric units are discussed in Appendix C.

From the analysis presented above (for the case of placing single and multiple microstructures in the LGP), it is also clear that a smaller gap between microstructures increases the illumination value. Two types of array (rectangular and hexagonal array) arrangement of microstructures was analyzed before going to further optimization. In an array of microstructures in the LGP, microstructures should be positioned as close as possible. This is quantified by the fill factor, which should be maximized in order to collect the maximum amount of light and minimize light loss. It is standard that for round type microstructures, hexagonal array arrangement has the higher fill factor (more than 90%) than that of rectangular array arrangement as shown in Figure 3.15 [Nussbaum et al., 1997].

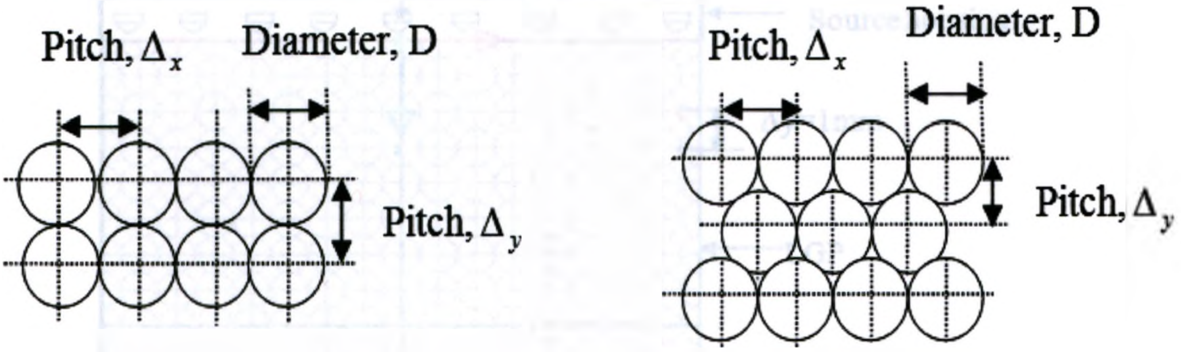

Figure 3.15 Fill factor calculation for rectangular and hexagonal array arrangement of microstructures [adapted from Nussbaum et al., 1997]

The fill factor describes the percentage of total area occupied by the microstructures to the total area of the LGP and is given by

$$\text{Fill factor} = \frac{r^2\pi}{\Delta_x\Delta_y} \tag{3.1}$$

where Δ_x and Δ_y are the pitch in X and Y directions respectively. The radius of the microstructure is r and the pitch between microstructures is $D - \Delta x$.

Given this condition, in both arrays, the pitch between each microstructure was maintained as 1 mm for a fixed size of microstructure (radius and depth both are 0.5 mm) and a fixed size of the LGP. The design and simulation results for each arrangement are presented in Figure 3.16 and Figure 3.17 respectively.

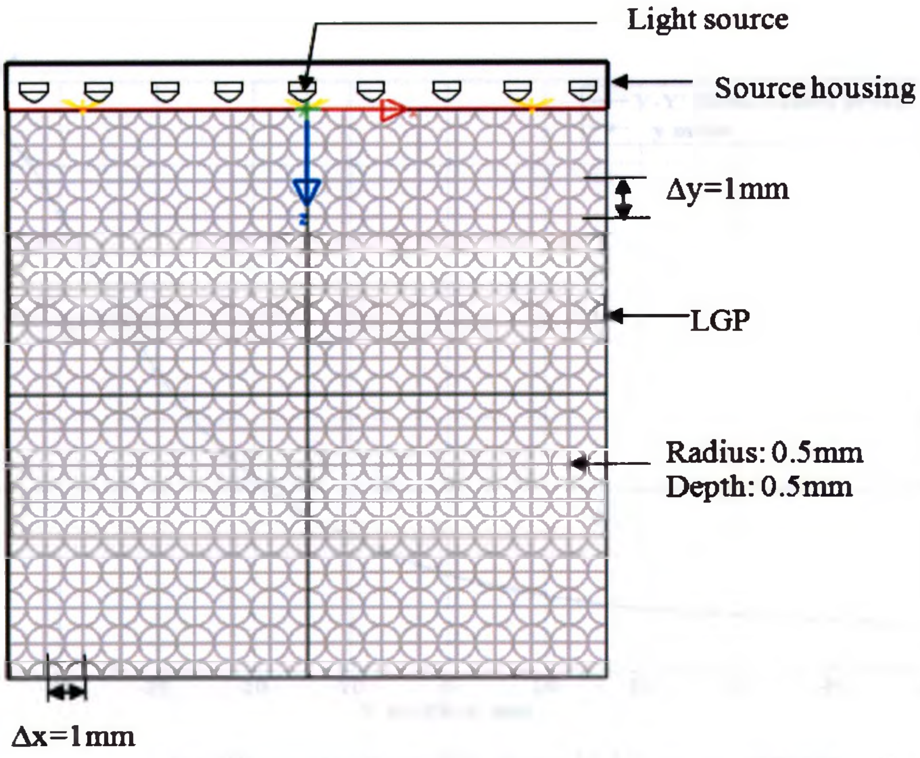
Light source
Source housing
Δy=1mm
LGP
Radius: 0.5mm
Depth: 0.5mm
Δx=1mm

(a) Design (Top view)

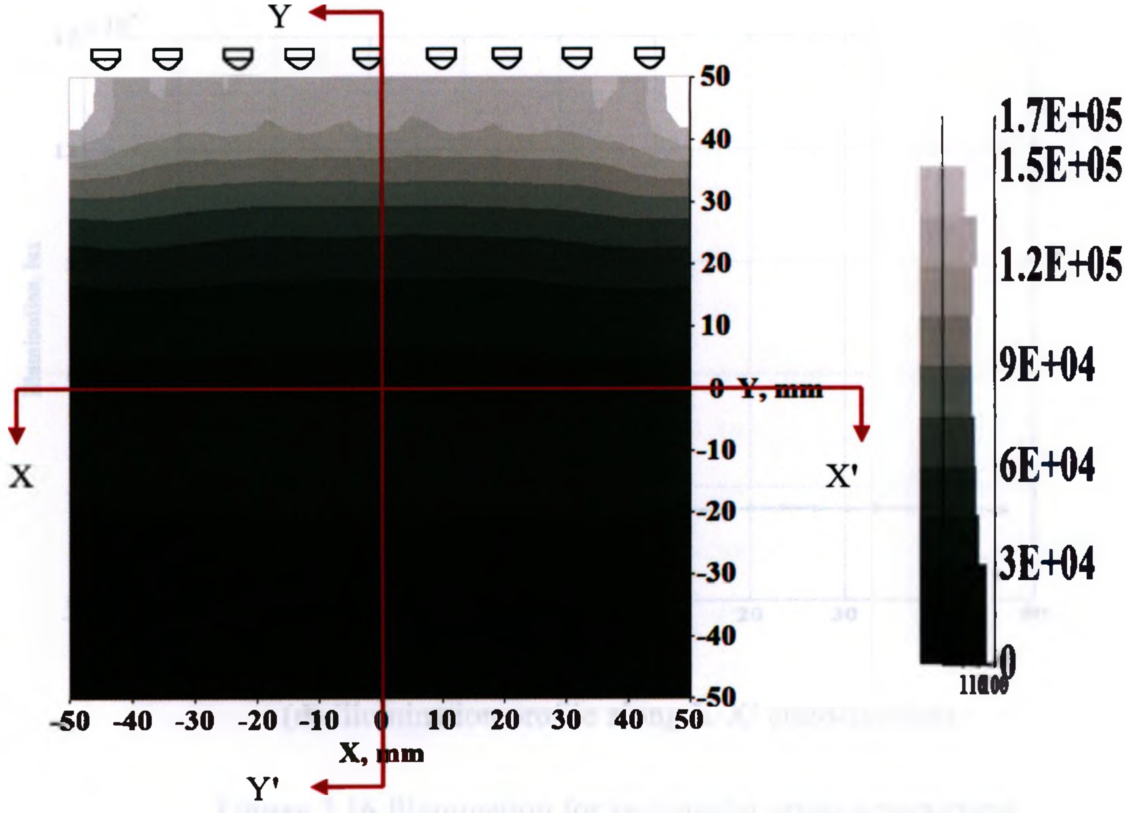

(b) Illumination on active (top) surface

Figure 3.16 (continued)

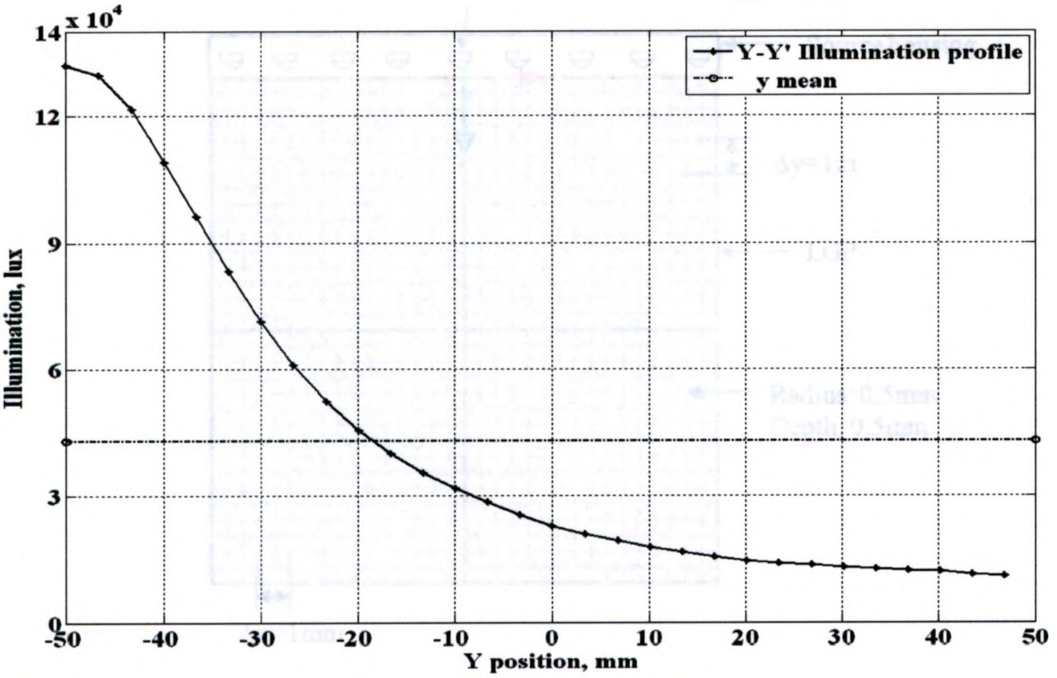

(c) Illumination profile along Y-Y' cross-sections

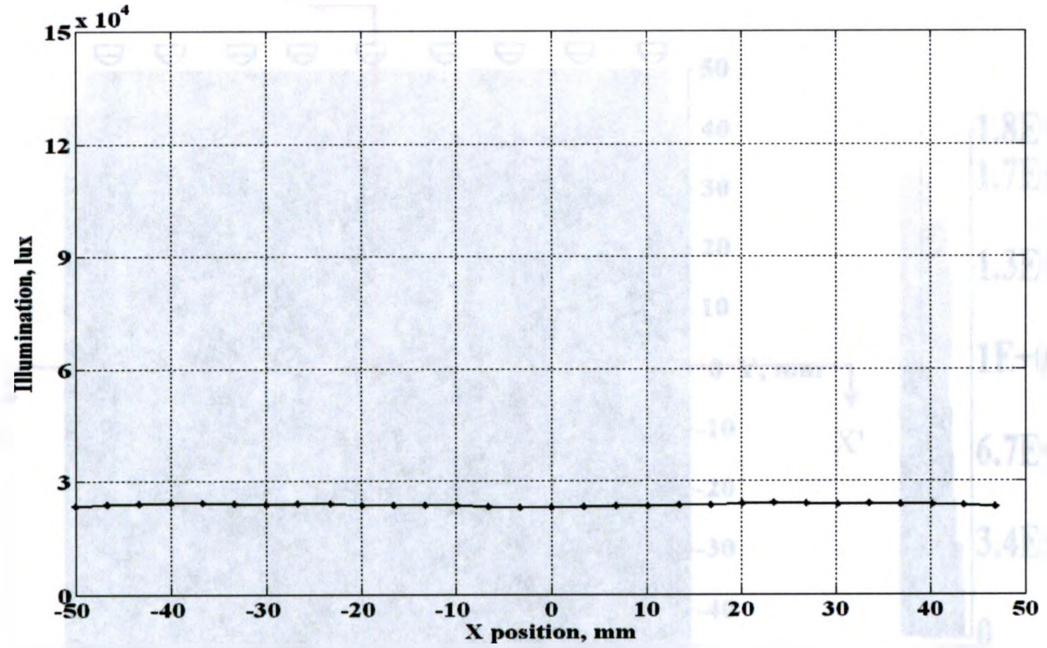

(d) Illumination profile along X-X' cross-sections

Figure 3.16 Illumination for rectangular array arrangement.

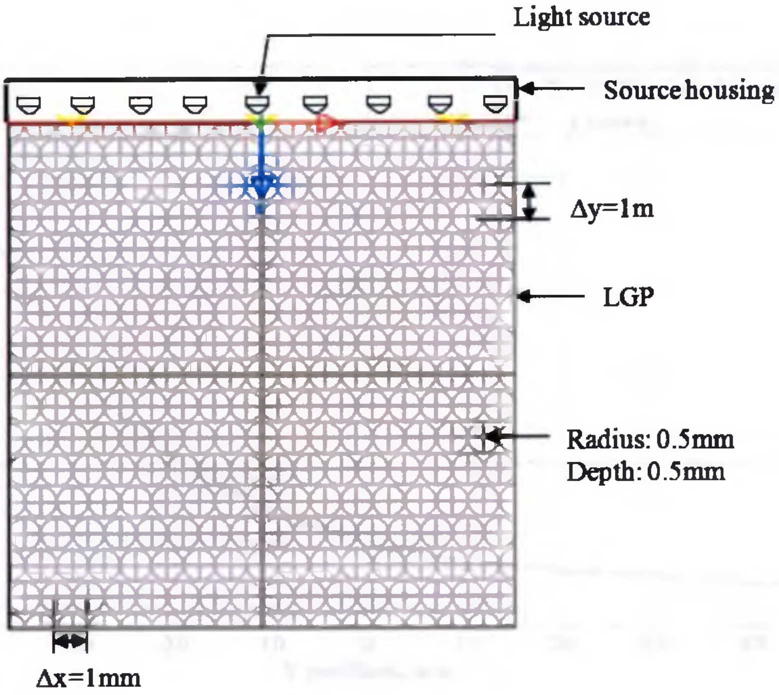
Light source
Source housing
Δy=1m
LGP
Radius: 0.5mm
Depth: 0.5mm
Δx=1mm

(a) Design (Top view)

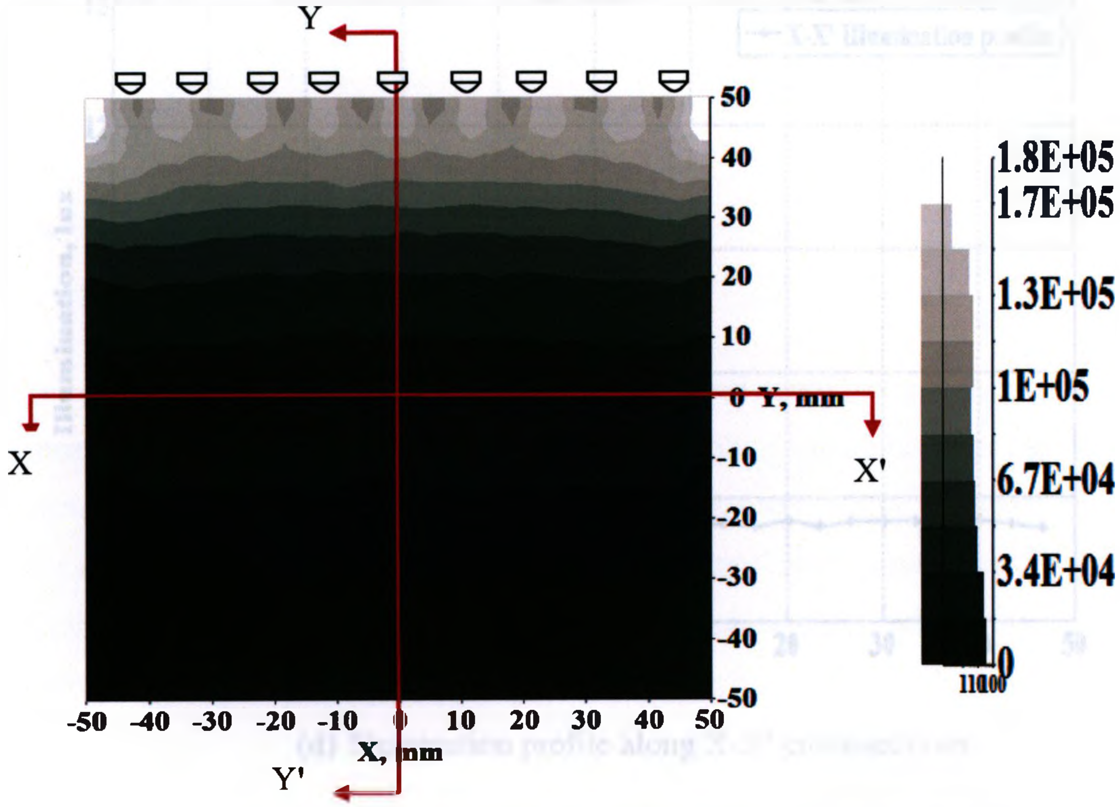

(b) Illumination on active (top) surface

Figure 3.17 (continued)

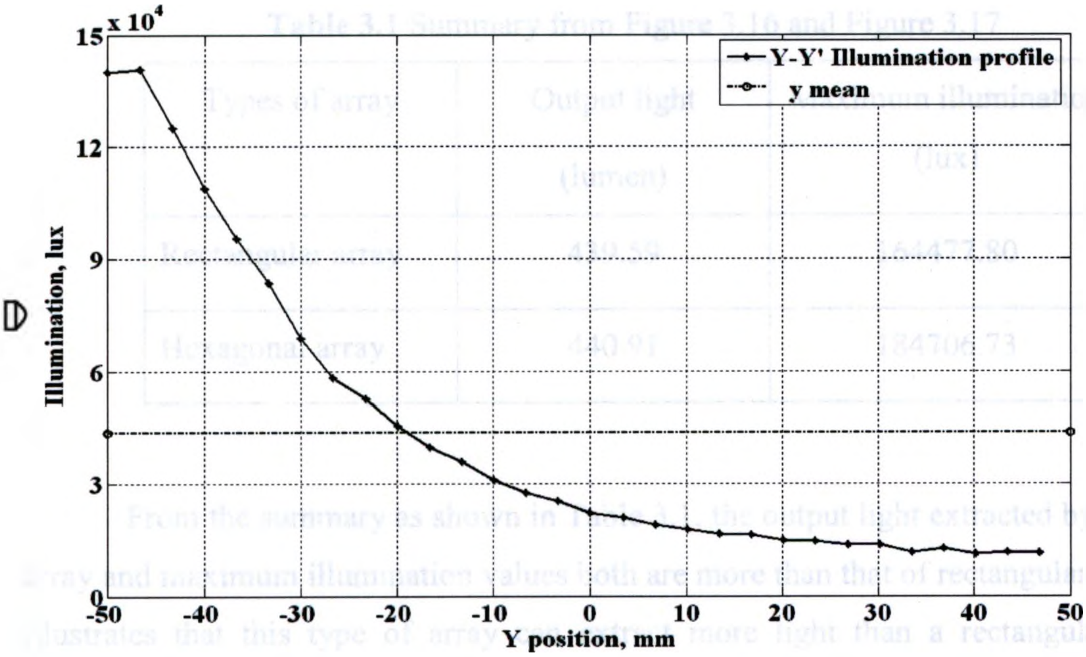

(c) Illumination profile along Y-Y' cross-sections

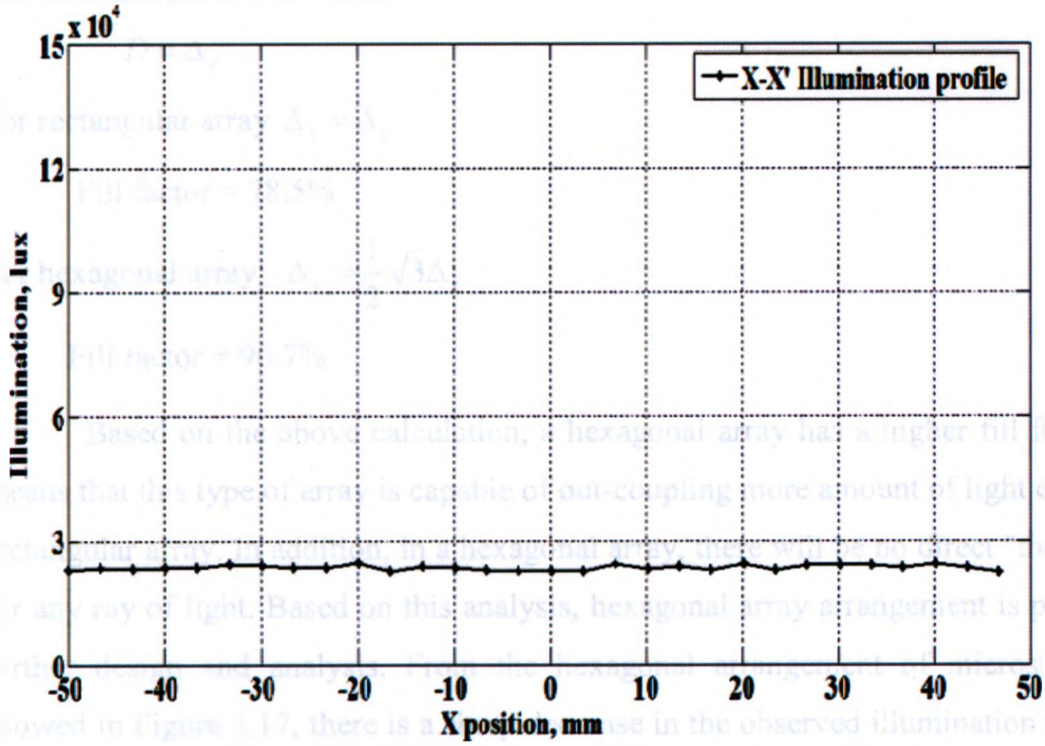

(d) Illumination profile along X-X' cross-sections

Figure 3.17 Illumination for hexagonal array arrangement.

Table 3.1 Summary from Figure 3.16 and Figure 3.17

Types of array	Output light (lumen)	Maximum illumination (lux)
Rectangular array	439.59	164477.80
Hexagonal array	440.91	184706.73

From the summary as shown in Table 3.1, the output light extracted by hexagonal array and maximum illumination values both are more than that of rectangular array. This illustrates that this type of array can extract more light than a rectangular array of microstructures. In the simulation results presented in Figure 3.16 and Figure 3.17, the diameter and pitch was 1 mm.

$D = \Delta_x$

For rectangular array $\Delta_x = \Delta_y$

Fill factor = 78.5%

For hexagonal array $\Delta_y = \frac{1}{2}\sqrt{3}\Delta_x$

Fill factor = 90.7%

Based on the above calculation, a hexagonal array has a higher fill factor which means that this type of array is capable of out-coupling more amount of light compared to rectangular array. In addition, in a hexagonal array, there will be no direct "through path" for any ray of light. Based on this analysis, hexagonal array arrangement is preferred for further design and analysis. From the hexagonal arrangement of microstructures as showed in Figure 3.17, there is a sharp decrease in the observed illumination after 30mm from the light source. In other words, the majority of light is emitted from the LGP after 30mm producing a non-uniform light distribution and largely ineffective illumination panel. The ratio of average illumination (E_{ave}) to maximum illumination (E_{max}) over the active surface is a measure of illumination uniformity, and is given by

$$U_E = \frac{E_{ave}}{E_{\max}} \times 100 \qquad (3.1)$$

The design goal for creating an illuminating surface is to increase this ratio (i.e., where this ratio approaches unity). The average illumination over the active surface was determined to be 44,090 lux with a maximum value of 184,706 lux near the LEDs. This results in a uniformity ratio of U_E = 0.24. These initial results clearly demonstrate the need for a better design strategy for embedding microstructures on a LGP surface.

There are several variables, i.e., microstructure geometry, distribution of microstructures, pitch between them, etc., which can be used as an optimization variable. For the proposed model, the output surface of the LGP will act as a surface illuminator, therefore the available parameters are: radius and depth of cylindrical shape microstructure, pitch for array arrangement. Considering the manufacturing point of view, the near optimal design should be able to reduce the number of steps in machining, should be simple enough to fabricate the prototype right away to compare with the simulated result and should reduce the machining time and cost. Varying the radius of microstructure need tool change during machining operation which may increase the cost and machining time, as well as varying the density or pitch for distribution of microstructures will also introduce complexity. Keeping all these things under consideration, for the proposed design the number of variable for optimization was reduced to one and the maximum depth of microstructure was the only dominant parameter, considered as variable. Such microstructures can be fabricated directly by a micromilling operation by defining the different maximum depth the tool will travel during machining in different area of the LGP. To validate the effect of maximum depth on illumination pattern, several simulations was conducted to find out the condition for maximum uniformity and average illumination for whole LGP.

3.3.2 Non-linear arrays

Non-linear arrays are those where either the pitch between microstructures or the size of microstructures or both are considered to vary. The next analysis involved using a similar patterned surface with optical microstructures that have a fixed radius (0.5mm) and distributed in a hexagonal arrangement (pitch of 1mm). However, the depth of microstructures are varied linearly along each row (i_1, i_2.......... i_n) on the hexagonal arrangement from an intial depth of 0.1mm near the light source to 5.5 mm at the most distant end. The maximum depth is constrained by the 6mm thickness of the LGP substrate as shown in Figure 3.18(a).

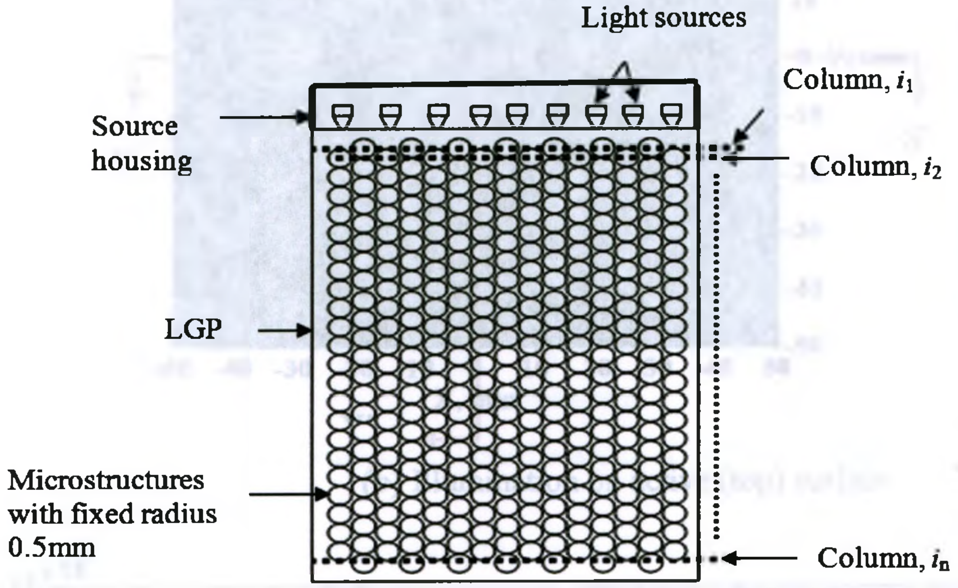
Light sources
Column, i_1
Source housing
Column, i_2
LGP
Microstructures with fixed radius 0.5mm
Column, i_n

(a) Design (Top view)

Figure 3.18 (continued)

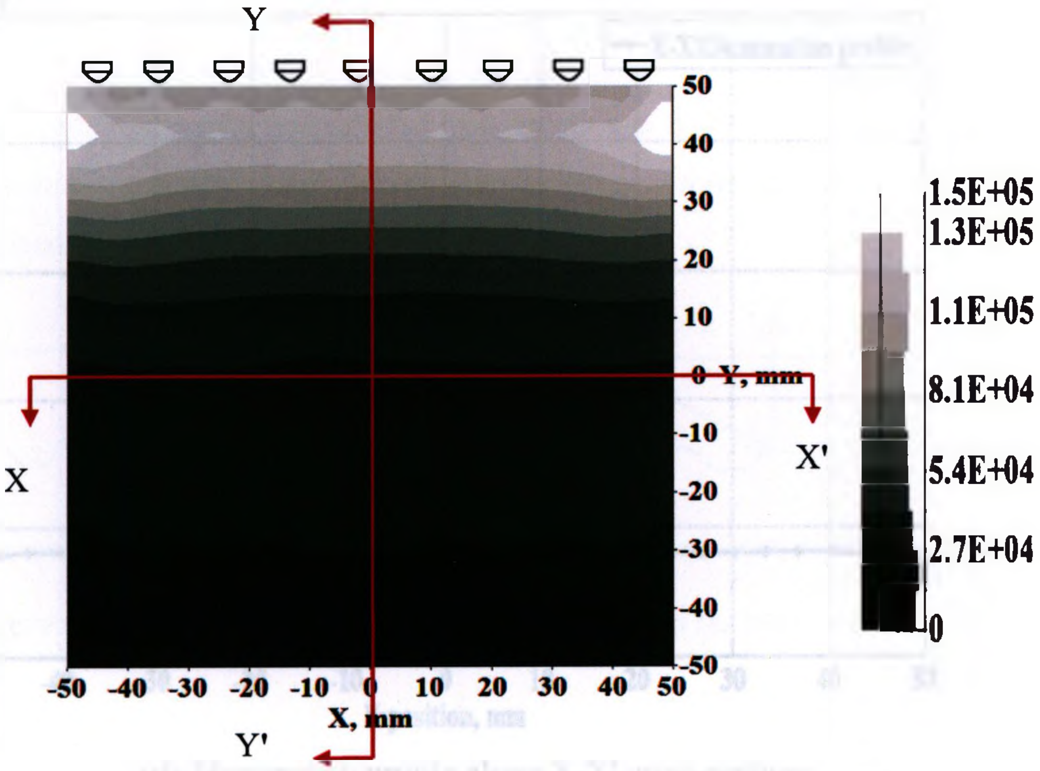

(b) Illumination on active (top) surface

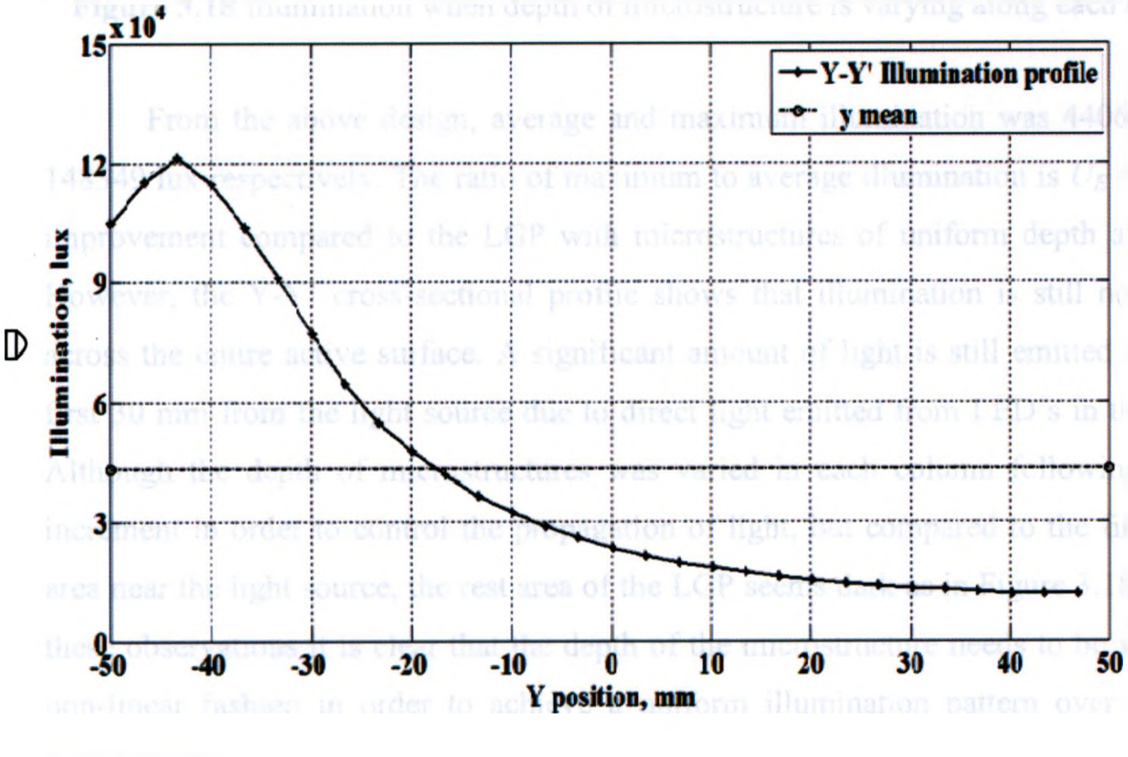

(c) Illumination profile along Y-Y' cross-sections

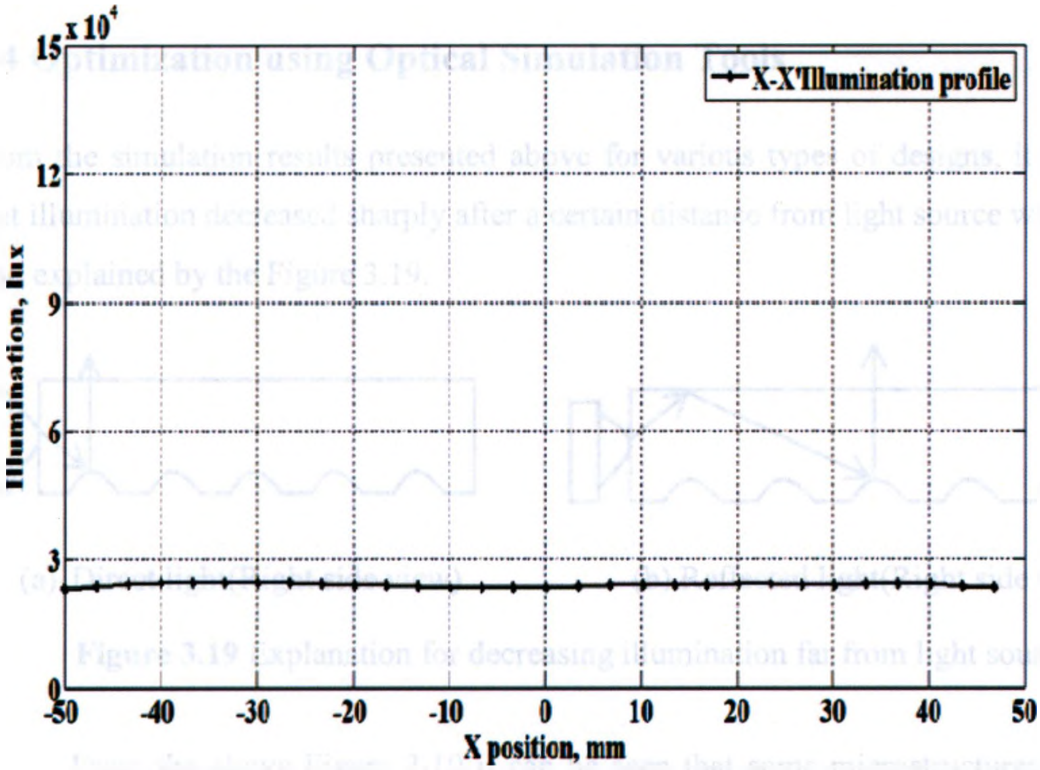

(d) Illumination profile along X-X' cross-sections

Figure 3.18 Illumination when depth of microstructure is varying along each column.

From the above design, average and maximum illumination was 44065 lux and 148349 lux respectively. The ratio of maximum to average illumination is $U_E = 0.29$, an improvement compared to the LGP with microstructures of uniform depth and radius. However, the Y-Y' cross-sectional profile shows that illumination is still not uniform across the entire active surface. A significant amount of light is still emitted within the first 30 mm from the light source due to direct light emitted from LED's in this region. Although the depth of microstructures was varied in each column following a linear increment in order to control the propagation of light, but compared to the first 30 mm area near the light source, the rest area of the LGP seems dark as in Figure 3.18(b). From these observations it is clear that the depth of the microstructure needs to be varied in a non-linear fashion in order to achieve a uniform illumination pattern over the entire active region.

3.4 Optimization using Optical Simulation Tools

From the simulation results presented above for various types of designs, it was found that illumination decreased sharply after a certain distance from light source which can be also explained by the Figure 3.19.

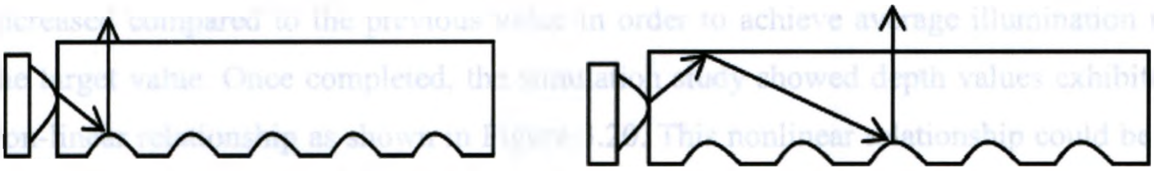

(a) Direct light(Right side view) (b) Reflected light(Right side view)

Figure 3.19 Explanation for decreasing illumination far from light source.

From the above Figure 3.19 it can be seen that some microstructures which are located near the light source receives light directly from light source as in Figure 3.19 (a) and some microstructures located far from the source continue receiving reflected light as in Figure 3.19 (b). As light rays reduced their energy over distance as discussed in Chapter 2, therefore when light ray with reduced energy hits the optical microstructures located far from the light source, the resulting illumination gets dimmer. Therefore, optimization of the distribution of optical microstructures in the bottom surfaces on the LGP is necessary.

The optimization technique proposed here uses only the depth of microstructures as a variable. The objective of this strategy was to select appropriate depths that produce an average luminance near 44,090 lux over the entire surface. The depth of microstructures in the first column, nearest the light source, was determined by performing several tests with different values of depth. Observations revealed that the target average illumination could be achieved with a depth of 0.095 mm. The depth of microstructures near the light sources was shallower in order to transmit more amount of light to the far end of the LGP. Increasing and decreasing the depth above and below 0.095 mm produced a much brighter and darker region at the beginning compared to other area of the LGP. Then this depth value was continued for next successive column and stopped at the column where the average illumination value tends to decreased than the average illumination. At this column, the depth was increased and continued until the average illumination value started to decrease. This iterative optimization continued for the rest area of the LGP. It was found that in the last 30mm area of the LGP, the average illumination was significantly lower than the target value since the light intensity reduced after the interaction with previous microstructures. Then the depth value was significantly increased compared to the previous value in order to achieve average illumination near the target value. Once completed, the simulation study showed depth values exhibited a non-linear relationship as shown in Figure 3.20. This nonlinear relationship could be use to increase the number of depth values or extrapolated for slightly larger LGPs.

Figure 3.21 shows the illumination pattern and cross-sectional profiles after the iterative process. Based on the simulation results, the minimum, average and maximum illumination was 37003 lux, 43741 lux and 50857 lux, respectively. The ratio of average to maximum illumination is 0.86 which is more compared to the ratio (0. 24) of a uniform array. Furthermore, the X-X' and Y-Y' illumination profiles indicate that a fairly uniform pattern of light is emitted from the surface.

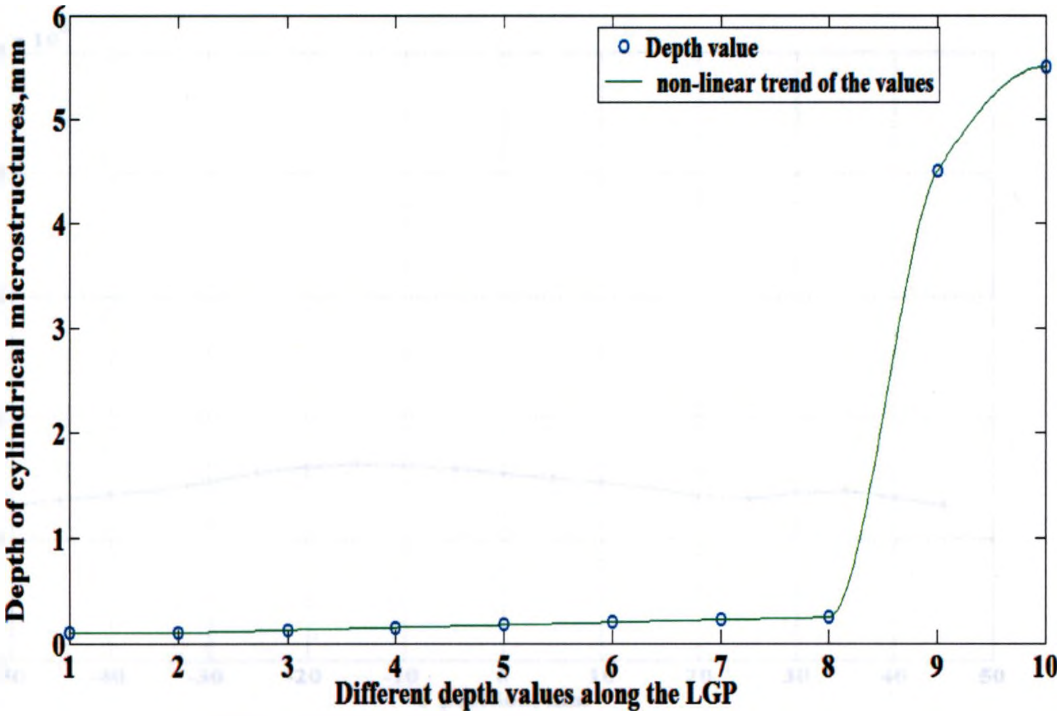

Figure 3.20 Distribution of microstructures for the proposed optimization approach.

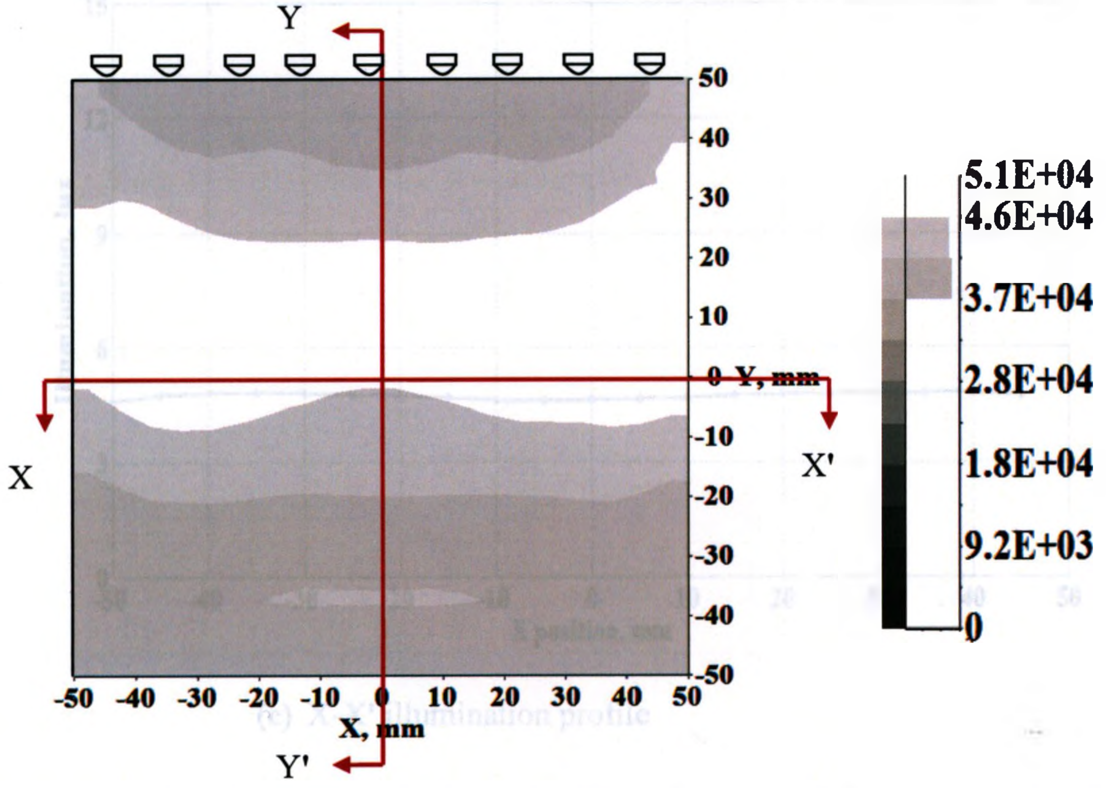

(a) Illumination on active (top surface)

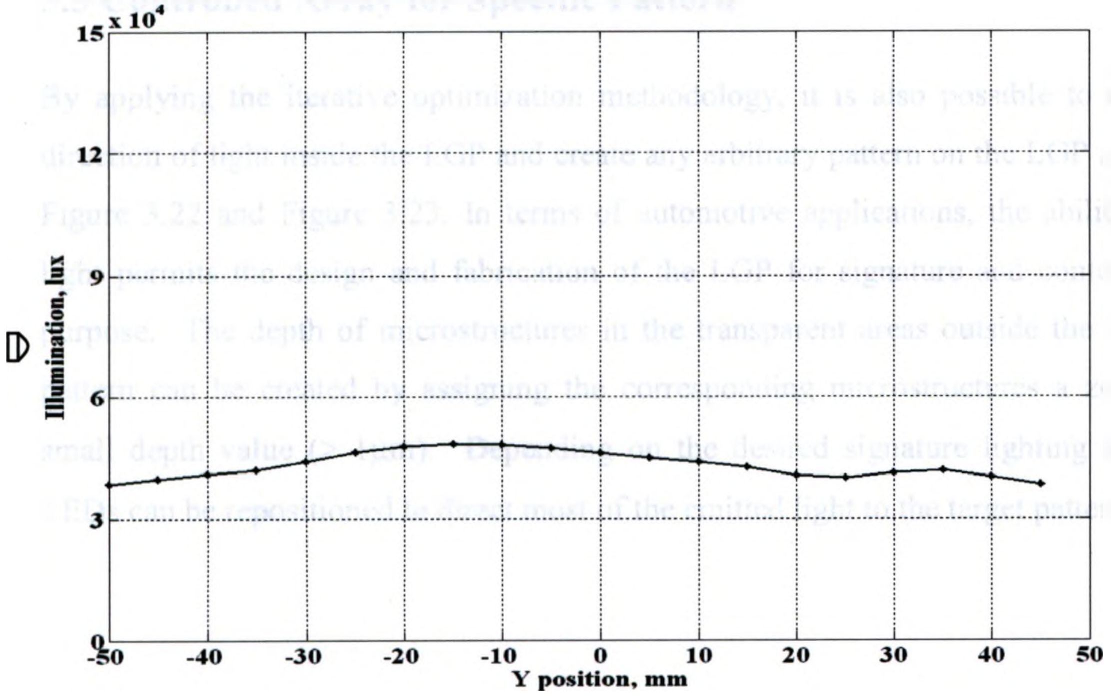

(b) Y-Y' illumination profile

Figure3.21 (continued)

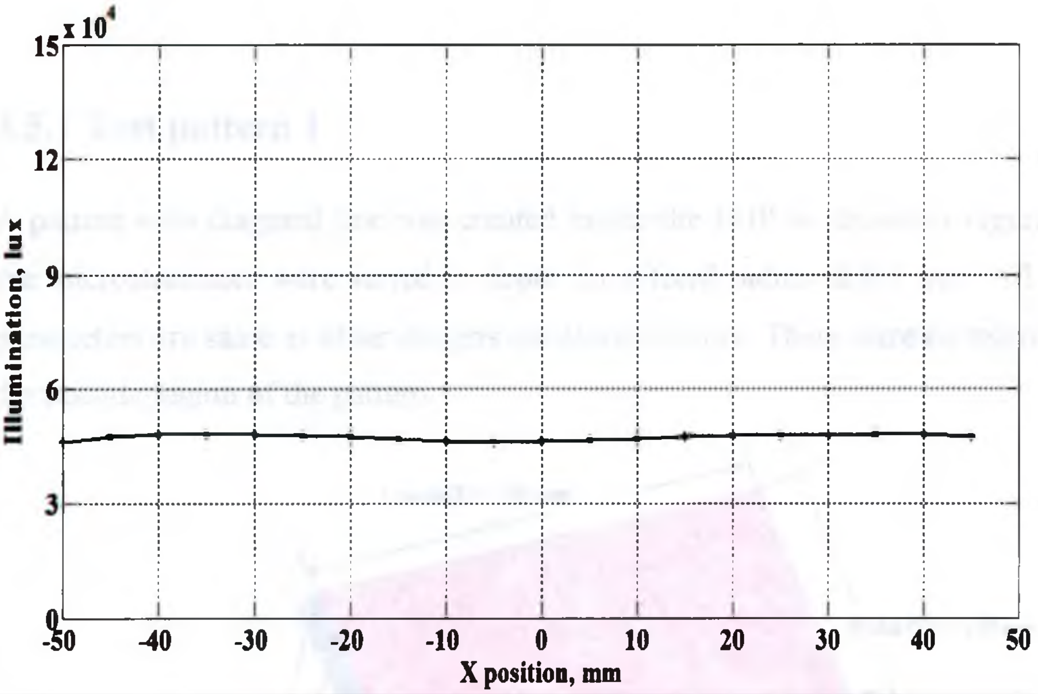

(c) X-X' illumination profile

Figure 3.21 Illumination for the optimized distribution of microstructures in the LGP.

3.5 Controlled Array for Specific Pattern

By applying the iterative optimization methodology, it is also possible to control the direction of light inside the LGP and create any arbitrary pattern on the LGP as shown in Figure 3.22 and Figure 3.23. In terms of automotive applications, the ability to direct light permits the design and fabrication of the LGP for signature and contour lighting purpose. The depth of microstructures in the transparent areas outside the illuminated pattern can be created by assigning the corresponding microstructures a zero or very small depth value (> 1μm). Depending on the desired signature lighting pattern, the LEDs can be repositioned to direct most of the emitted light to the target pattern.

3.5.1 Test pattern 1

A pattern with diagonal line was created inside the LGP as shown in Figure 3.22 where the microstructures were varied in depth for a fixed radius of 0.5 mm. All other design parameters are same as other designs mentioned before. There were no microstructures in the outside region of the pattern.

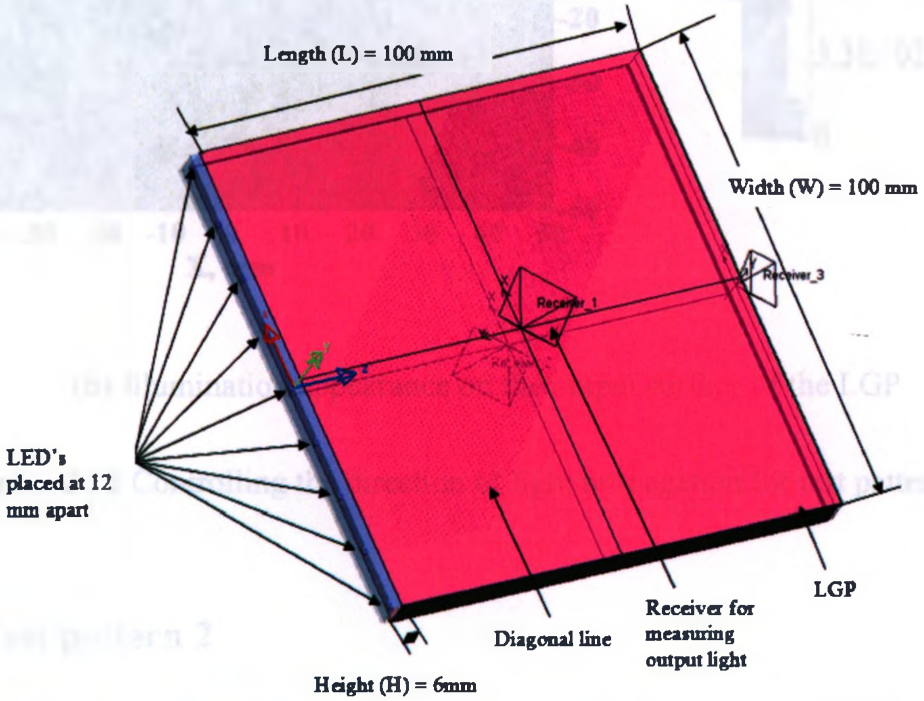
Length (L) = 100 mm
Width (W) = 100 mm
Receiver_1
Receiver_3
LED's placed at 12 mm apart
LGP
Receiver for measuring output light
Diagonal line
Height (H) = 6mm

(a) Design

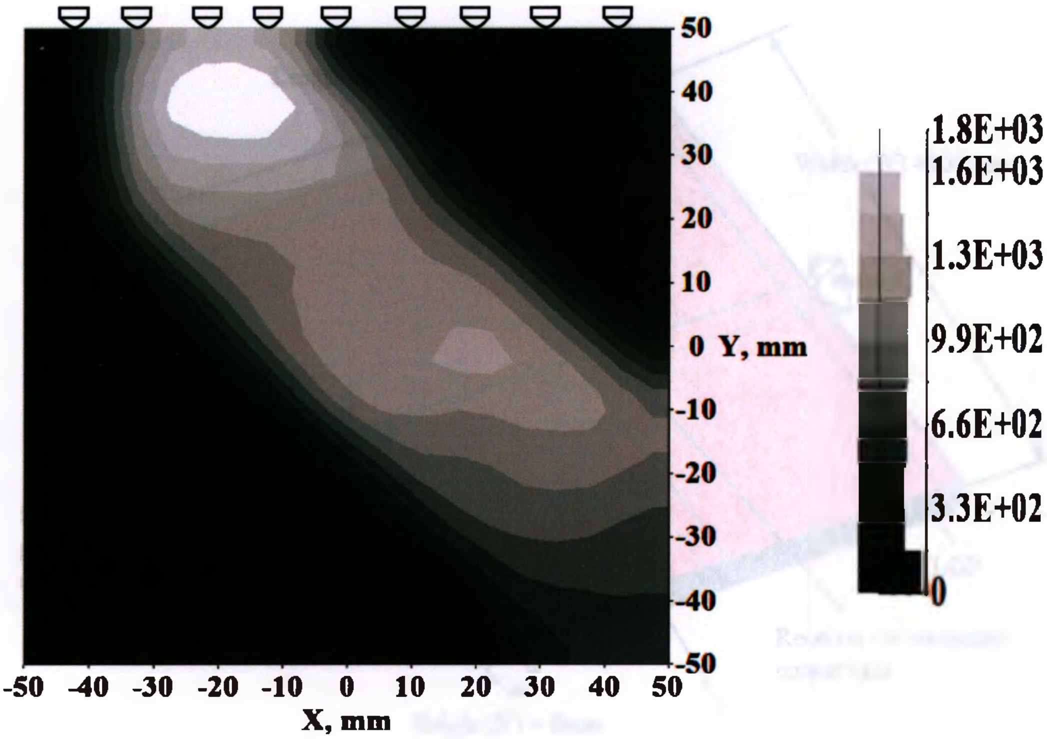

(b) Illumination appearance on the output surface of the LGP

Figure 3.22 Controlling the direction of light propagation for test pattern one.

3.5.2 Test pattern 2

A pattern with half diagonal line was created inside the LGP as shown in Figure 3.23 where the microstructures were varied in depth for a fixed radius of 0.5 mm. All other design parameters are same as other designs mentioned before. There were no microstructures in the outside region of the pattern.

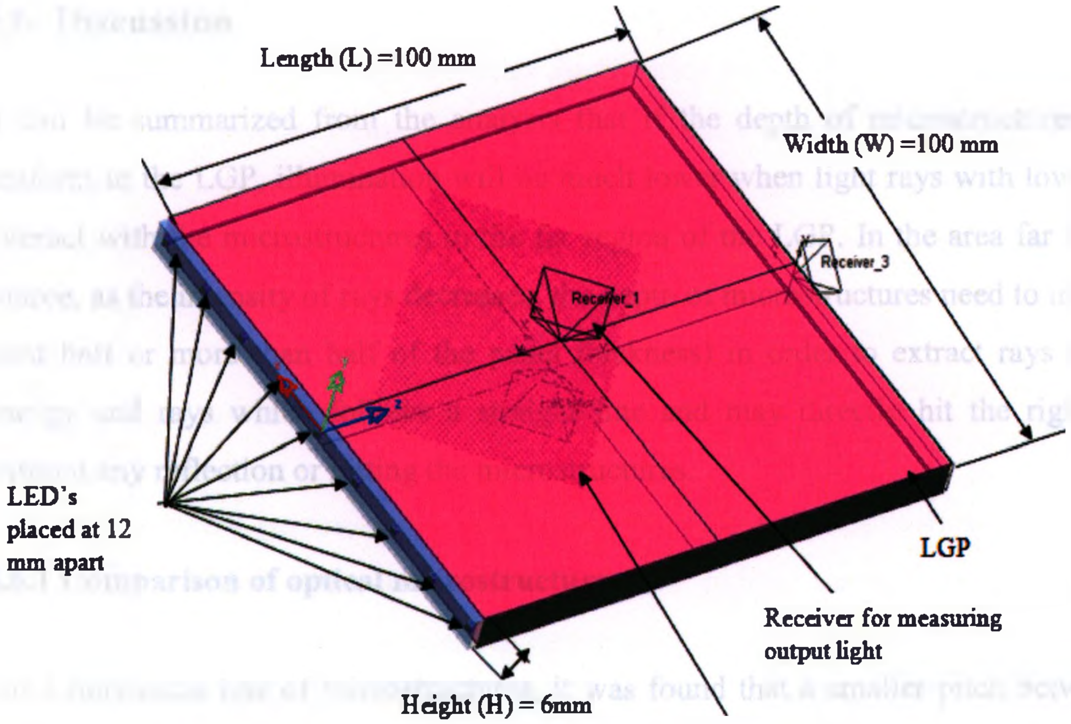
Length (L) =100 mm
Width (W) =100 mm
Receiver_3
Receiver_1
LED's placed at 12 mm apart
LGP
Receiver for measuring output light
Height (H) = 6mm
Half diagonal line

(a) Design

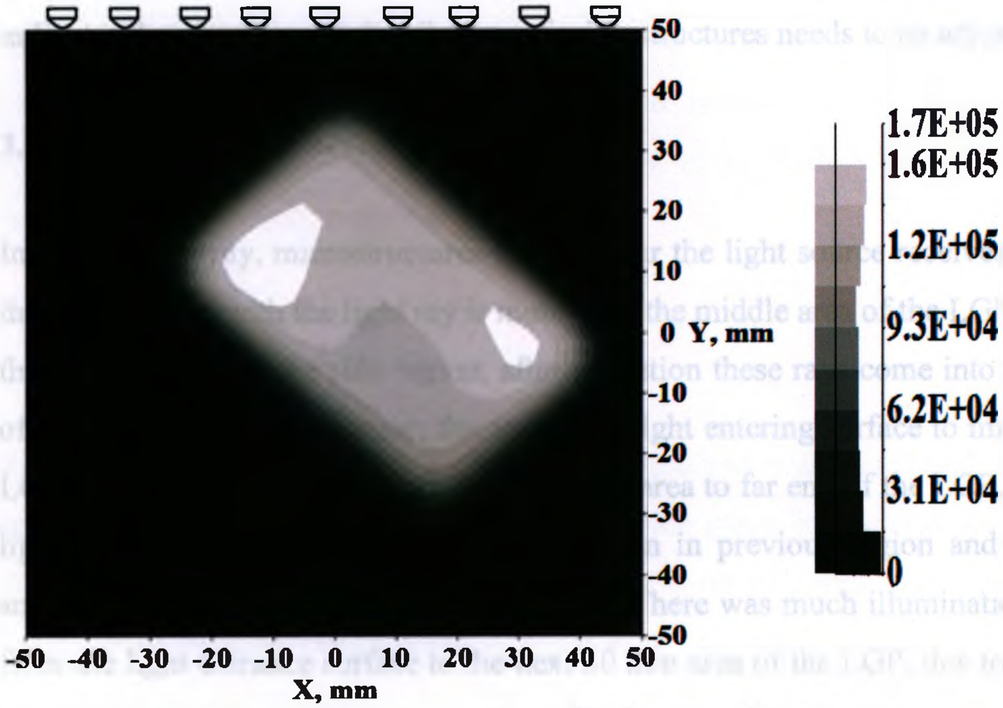

(b) Illumination appearance on the output surface of the LGP

Figure 3.23 Controlling the direction of light propagation for test pattern two.

3.6 Discussion

It can be summarized from the analysis that if the depth of microstructures remains uniform in the LGP, illumination will be much lower when light rays with lower energy interact with the microstructures in the far region of the LGP. In the area far from light source, as the intensity of rays decreases, the depth of microstructures need to increase (at least half or more than half of the panel thickness) in order to extract rays with little energy and rays which follows a straight line and may directly hit the right surface without any reflection or hitting the microstructures.

3.6.1 Comparison of optical microstructures

For a horizontal line of microstructures, it was found that a smaller pitch between each microstructures shows better performance along X-X' cross-section of the LGP. For vertical line of microstructures, in each case when the number of lines was increased, it was observed that illumination continues to decrease after a certain distance. This indicates that the size and distribution of microstructures needs to be adjusted.

3.6. 2 Comparison of array arrangements

In a uniform array, microstructures located near the light source receives more light and their interaction with the light ray is more until the middle area of the LGP, also light rays that are incident on the side region, after reflection these rays come into the middle area of the LGP. As a consequence, the area from light entering surface to middle area of the LGP becomes more illuminated. From middle area to far end of the LGP, the intensity of light ray becomes less due to their interaction in previous region and because of the smaller depth of microstructures in that area. There was much illumination in the region from the light entrance surface to the next 30 mm area of the LGP, due to the availability of more light intensity, more interaction of light rays with microstructures.

When depth of microstructures varied linearly along each column in the LGP, there was no significant improvement in illumination pattern. This indicates that a small incremental value in maximum depth of microstructures along each column is not capable to maintain a near homogeneous illumination pattern.

For the optimized case when the depth of microstructures was varied in a non-linear manner, the illumination uniformity was improved by 62%. The depth of microstructures was deeper in the area far from the light sources so that they can easily capture light rays and direct toward the top surface.

3.6. 3 Advantages of the proposed optimization method

Although "optimal performance" can be achieved for each application using a unique combination of the substrate material, variable radius, depth, density and pattern distribution, from a design and manufacturing perspective it would be far more beneficial to reduce the number of variable parameters to "one". From the simulation results, it is observed that depth of cylindrical microstructure has significant effect on illumination distribution and it is the dominant parameter that can control the size of the microstructure and pitch between microstructures. By only altering the depth of the individual microstructures during micromilling it is possible to achieve "near optimal" performance and to contour the illumination pattern on the active surface. Such microstructures will be easy to fabricate directly on the PMMA material by micromilling with good optical surface finish.

3. 7 Concluding Remarks

In this chapter, a cutting-edge optimization method was discussed to acquire near optimum illumination uniformity of a light guide panel by varying only the maximum depth of cylindrical microstructures at different areas of a light guide panel. To observe the effect of different design patterns on the homogeneous illumination, the "Light Tools" software was used to perform the simulation. Reflective and diffusive light sheeting for minimizing "moiré" fringe effects has not been included in the design and analysis in an effort to better examine the impact of the microstructure parameters and spatial density on optical performance. Regions of uniformly spaced microstructures produces a "mosaic" effect and can have some residual artifacts because of the underlying rectilinear microstructure placement. Mosaic effect is not also considered as a significant issue in the proposed design, because "moiré" and "mosaic" effects are unwanted in display systems but not a significant factor in diminishing the performance of illumination panels.

This research considers the design of the LGP instead of the whole backlight module because it is not for use in a LCD. The automotive lighting applications are different than edge-lit backlights for small and medium size liquid crystal displays (LCDs) for laptop computers, digital televisions and cell phones. A typical LCD backlight system consists of a light source, a flat light-guide plate (LGP) and several optical sheets such as light reflection sheets, diffusion sheets and prism sheets. For display technology, light reflection and diffusion sheets are used to uniformly disperse the light as it emanates from the active substrate surface. The reflective and diffusive light sheeting also reduce the "moiré" fringe effects making the information on the display panel easier to read. In the present research, the fringe patterns are not design issue because the automotive light guide panel is used for illumination purposes. However, reflective sheeting or coatings on the edges and back can be used to redirect light to the active surface. From a design perspective, the optical efficiency of the automotive light panel and reduction in light loss along the edges and non-active side of the plastic substrate can be controlled through selective design of the individual optical microstructures shape and the spatial distribution of elements on the light panel.

CHAPTER 4

MICROFABRICATION METHOD

4.1 Introduction

Microfabrication involves manufacturing processes for creating miniature structures in micrometer and nanometer sizes. Many of the techniques originally came from the microelectronics industry and from small tool machining for mechanical parts production. In Chapter 2, the state-of-the-art in creating optical microstructures in the LGP was presented. Available manufacturing methods for miniature components have been based on semi-conductor processing techniques, where silicon materials are photo-etched through chemical and dry processes, usually in large batch production. The reflow process being a popular method but limited to only semispherical micro-lens and the process needs high processing temperature and long processing time.

To create a mold of nickel or any other material by any of the processes such as LIGA (a photo-lithography method using a synchrotron), laser, ultrasonic, ion beam, micro electro discharge machining methods, diamond turning and milling and then replication into PMMA material by hot embossing or injection molding is the general idea to produce a prototype after the design. This is a time consuming process and expensive as well to compare the fabricated prototype with the simulation result right after the design step. Also in order to obtain concave shaped microstructures, the mold needs to be patterned with convex shape microstructures. In illumination design, common techniques to distribute the microstructures in the LGP is by varying the radius of microstructure and the pitch between them in order to create less density of microstructures near the light entering surface of the LGP and more density of microstructures in the region far from the light source since the size and density of the microstructures affect the illumination pattern. To create microstructures in the LGP using micromilling the design rules requires use of different diameter tools. During the fabrication process, it requires an extra time and special attention to change the tool frequently which is also related with higher cost of tooling. From a manufacturing perspective, the complexity of using different diameter tool during fabrication, the cost and time of total fabrication process can be reduced by using only one tool of fixed diameter.

In this chapter, a micromilling fabrication method for creating optical microstructures directly into PMMA material is presented. The fabrication process involves only varying the depth of cylindrical microstructures with a fixed radius ball end milling tool while maintaining the less density of microstructures near the light source and more density of microstructures far from the light source. The mechanical micromachining is capable of producing profile accuracy, surface finish, and sub-surface integrity and can create miniature devices and components with features that range from tens of micrometers to a few millimeters in size. To validate the fabrication method, several prototype of LGP made from PMMA material with cylindrical microstructures are fabricated. The prototypes were tested for surface roughness and illumination on the top surface was measured in an illumination test set up to compare with the simulation results.

4.2 Micromilling

Micromechanical machining is an alternative method of non-traditional machining for optical microstructure which can improve productivity and expand the choice of applicable materials. During micromilling material is removed from the work-piece by geometrically defined cutting edges in order to create precise three dimensional microstructures and the depth of cut can be maintained at the level of a micrometer or less. Ball end tool was used in this research in order to maintain the curvature.

Micromilling is capable of creating optical microstructures directly into PMMA material. The milling machine consists of a motor driven spindle, which mounts and revolves the milling cutter, and a reciprocating adjustable worktable to mounts and feeds the work-piece. Micromilling tool are chucked in a v-block diamond bearing to minimize radial errors (1 μm). Rotational speed, feed rates, depth per pass, cooling pressure etc. are typical process parameters in micromilling operations in order to achieve low surface roughness value and high machining quality [Gentili et al., 2005]. The speed of milling, FPM (Feed per minute) is the distance where the cutter circumference passes over the workpiece. The spindle RPM is necessary to give a desired peripheral speed depends on the size of the milling cutter.

The optimum speed in micromilling is determined by certain parameters that are related to the cutter speed, e.g., the type of material being cut, the size and type of the cutter used, width and depth of cut finish required, type of cutting fluid and method of application, power and available speed [U.S. Army, 1996]. Spindle speed in revolutions per minute is calculated by the equation below:

$$RPM = \frac{CS \times 4}{D} \tag{4.1}$$

where RPM is the spindle speed (in revolution per minute), CS stands for cutting speed of milling cutter (in SFPM) and D is the diameter of milling cutter (in inches)

The feed of the milling machine is expressed in inches per minute or millimeters per minute and is determined by the equation below:

$$Feed\ \text{rate}\ (inch/\min) = Chip\ load \times N \times RPM \tag{4.2}$$

where N represents the number of teeth per minute of the milling cutter.

Figure 4.1 shows the process of creating microstructures on the bottom surface of the LGP made from PMMA. Tungsten carbide (WC) was used as milling tool due to its availability with 5.5 mm length. Tungsten carbide has hardness and strength over a broad range of temperature [Chae et al., 2006].

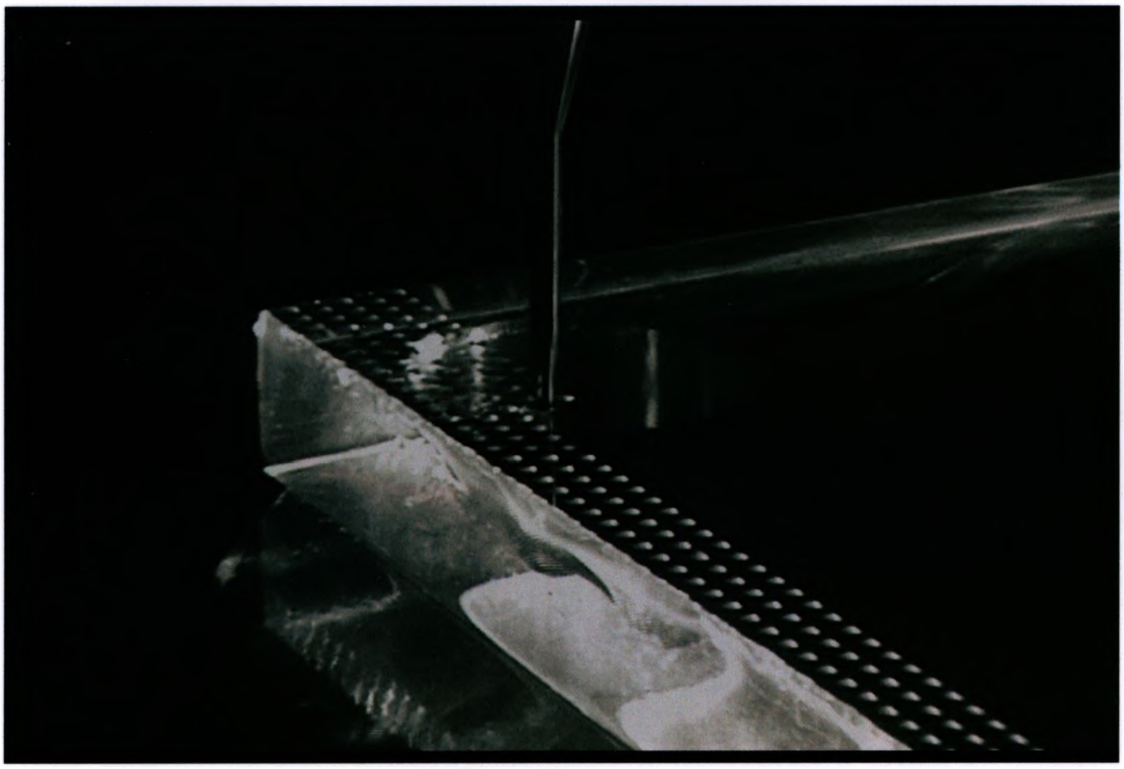

Figure 4.1 Fabrication of microstructures by micromilling.

4. 3 Experimental Verification and Results

Several PMMA samples with microstructures were fabricated to validate the proposed design and fabrication method. In this research, the purpose was to examine the illumination performance of the fabricated LGP according to the simulation results. The fabricated samples were tested for surface finish before undergoing illumination testing. In this research a WYKO NT1100 optical profiling system from Veeco Instruments Inc., NY, USA, was used to measure the surface roughness (average surface roughness, Ra) and visualize the quality of the 3D microstructures created in the PMMA. Surface roughness was measured by analyzing a sub-region near the centre inside a microstructure. Figure 4.2 shows the surface analysis of cylindrical microstructures.

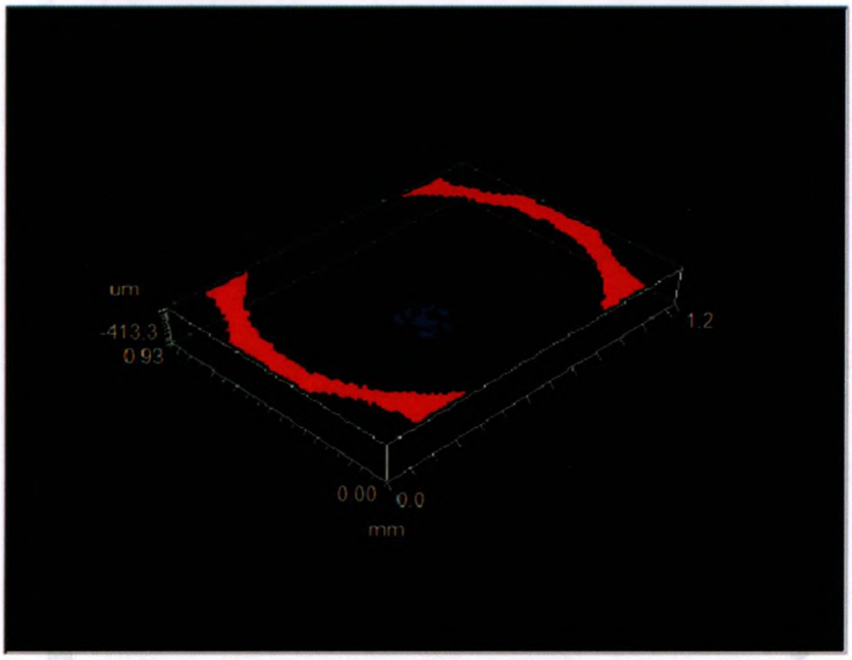
um
-413.3
0.93
1.2
0.00
0.0
mm

(a) 3D plot of microstructure

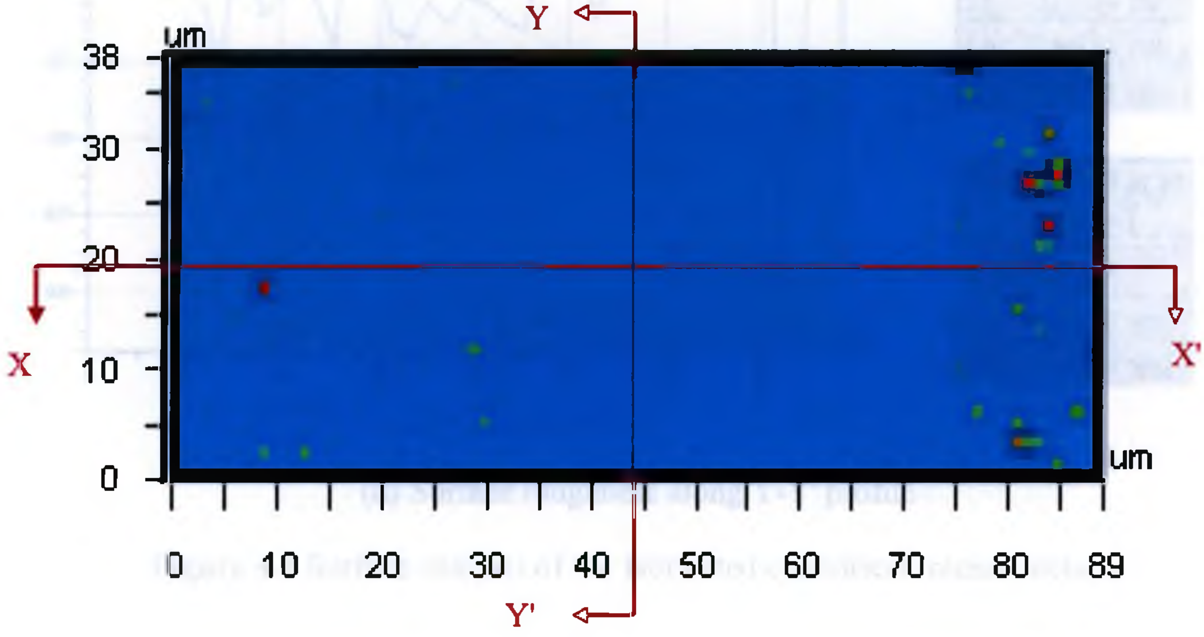

(b) Sub-region analysis of cylindrical microstructures

Figure 4.2 (continued)

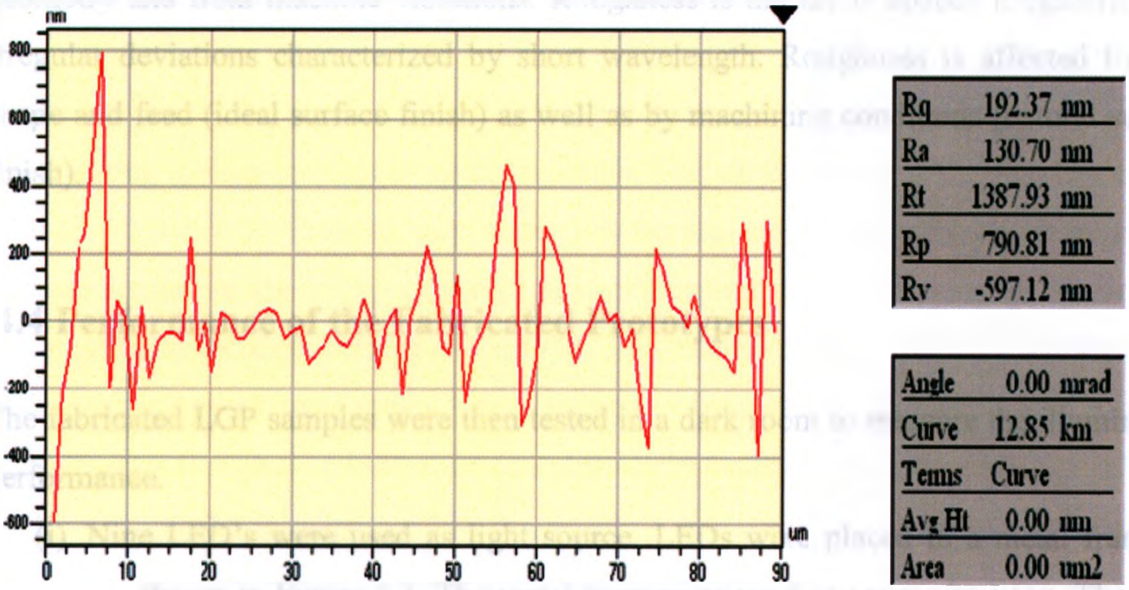

(c) Surface roughness along X-X' profile

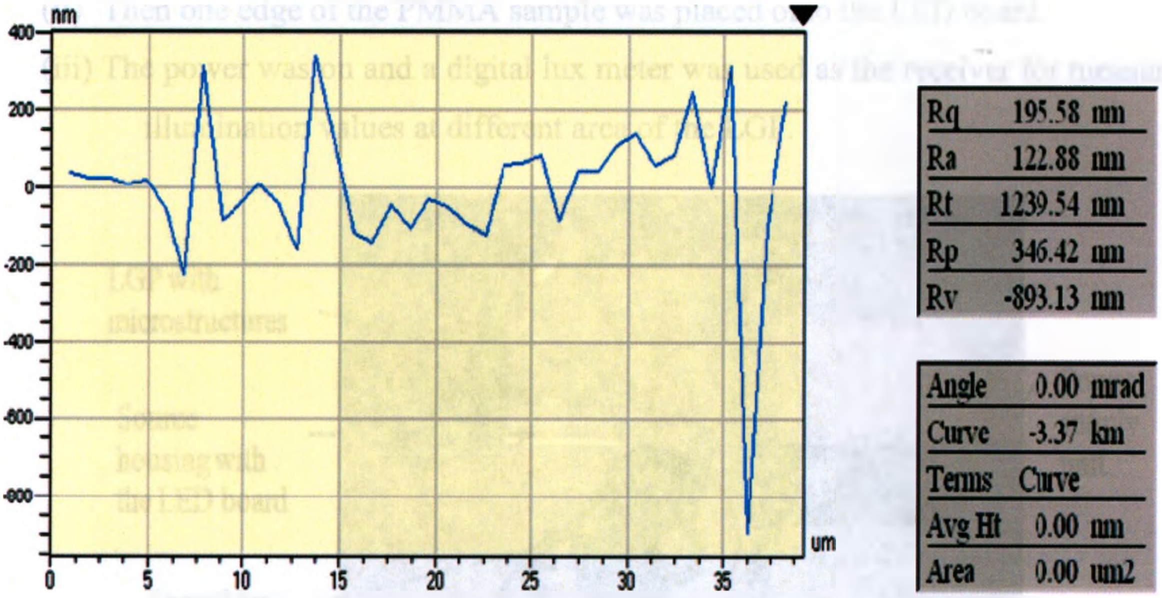

(d) Surface roughness along Y-Y' profile

Figure 4.2 Surface analysis of the fabricated cylindrical microstructure.

From Figure 4.2, the average surface roughness (Ra) was ~123nmRa which shows near optical quality surface finish. Surface profile is typically described by its waviness, and roughness. Waviness is the recurrent deviations from an ideal surface which may result from deflections in the machine tool and cutting tool, from errors in the tool geometry and from machine vibrations. Roughness is the finely spaced irregularities or irregular deviations characterized by short wavelength. Roughness is affected by tool shape and feed (ideal surface finish) as well as by machining conditions (natural surface finish).

4.4 Performance of the Fabricated Prototypes

The fabricated LGP samples were then tested in a dark room to measure the illumination performance.

(i) Nine LED's were used as light source. LEDs were placed in a metal frame as shown in Figure 4.3. The metal frame was used as source housing. The LED board was connected to a power supply unit.

(ii) Then one edge of the PMMA sample was placed onto the LED board.

(iii) The power was on and a digital lux meter was used as the receiver for measuring illumination values at different area of the LGP.

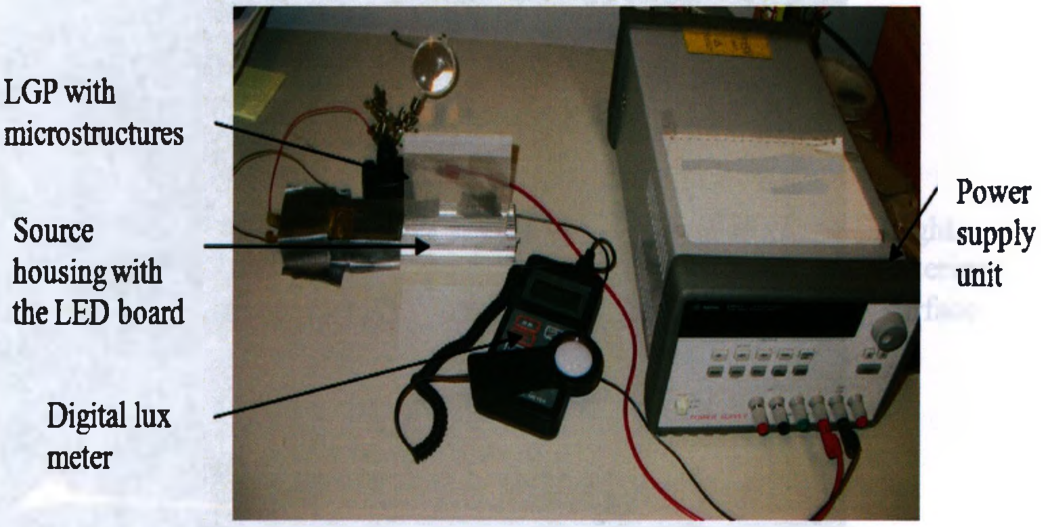

Figure 4.3 Illumination performance test set-up for LGP.

The detail analysis for each case is presented in below.

4.4.1 LGP without any microstructures

Figure 4.4 shows the propagation of light when there are no microstructures in the LGP. After testing in illumination set up, it was found that, all light are transmitting to the right surface of the LGP without any scattering during propagation. Since there are no microstructures in the LGP, light rays are propagating by total internal reflection and transmitting to the right surface of the LGP. This behavior makes sense according to the basic technology of light guiding in a panel as discussed in Chapter 2. The test also closely matches with the observation found from the simulations results in Figure 3.3.

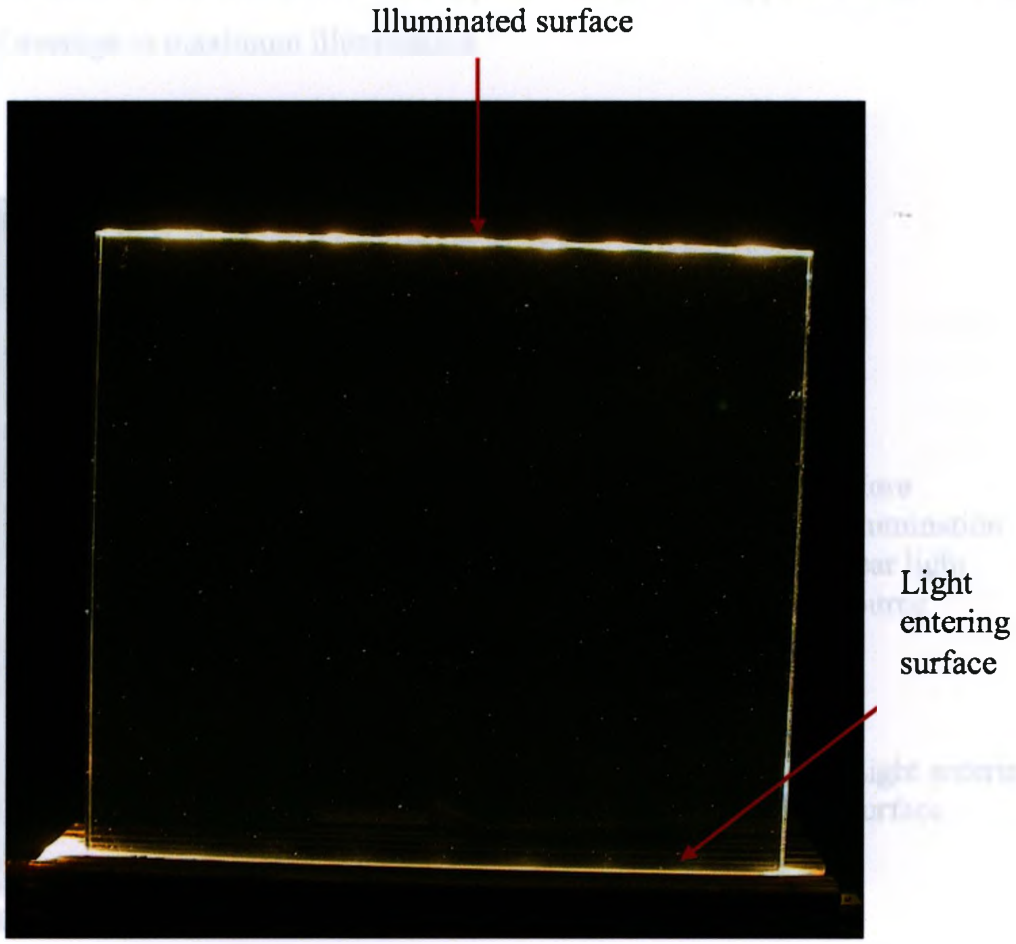

Figure 4.4 Illumination performance for a LGP without any microstructures.

4.4.2 LGP with linear array of microstructures

Figure 4.5 shows the illumination performance of a LGP with linear array of microstructures. The radius and depth of microstructures are 0.5 mm and pitch between each microstructure is 1 mm in a hexagonal array arrangement. The surface region near the light source was found to be much brighter than the far end of the LGP. This characteristic is relevant to the simulations results in Figure 3.17). The illumination values at different points of the LGP were measured by the digital lux meter, and the average and maximum illumination was determined to be 528lux and 1,747lux respectively. The illumination uniformity was found to be approximately 30% from the ratio of average to maximum illumination.

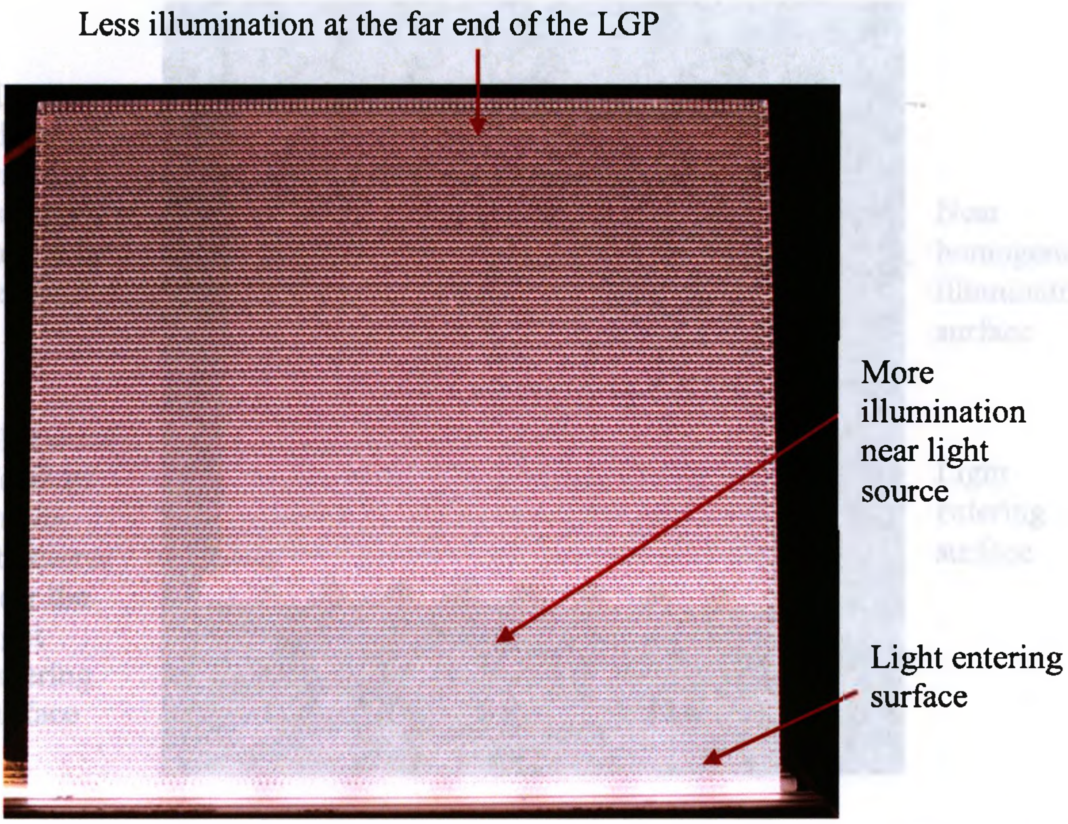
Less illumination at the far end of the LGP
More illumination near light source
Light entering surface

Figure 4.5 Illumination performance for a LGP with linear array of microstructures (fixed radius and depth of microstructure, uniform pitch between microstructures).

4.4.3 LGP with optimized array of microstructures

From Figure 4.6 it was found that depth has significant impact in controlling the distribution of light. By creating shallower depth of microstructures near the light source and deeper depth at the far end of the LGP, light can be guided in a specific direction for intended applications. Illumination values at different point of the LGP were taken by the digital lux meter in order to observe the illumination trend. The average and maximum illumination was 1496lux and 1672lux, respectively. The illumination uniformity was found to be approximately 89%.

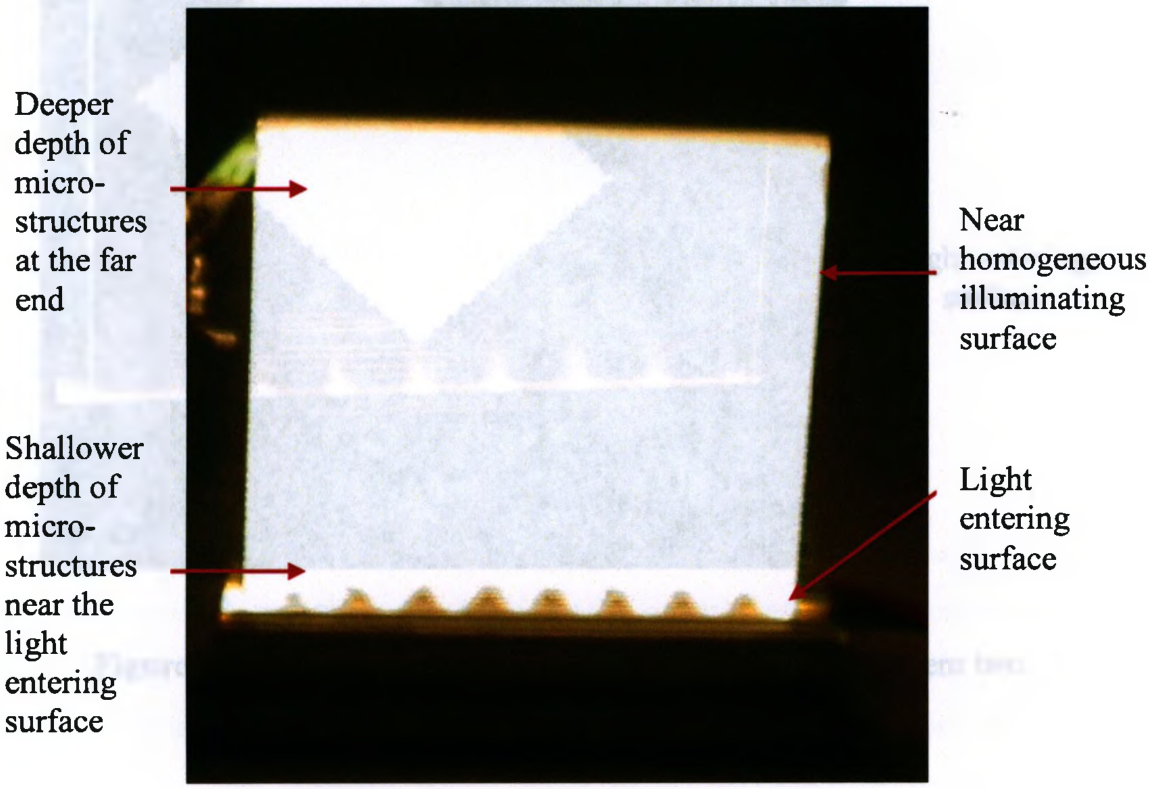
Deeper depth of micro-structures at the far end
Shallower depth of micro-structures near the light entering surface
Near homogeneous illuminating surface
Light entering surface

Figure 4.6 Illumination performance for a LGP with optimized array of microstructures (with varying depth of microstructure).

4.4.4 LGP with half diagonal pattern of microstructures

Figure 4.7 illustrates that by creating any arbitrary shape, i.e., half diagonal line with microstructures; it is possible to control the direction of light. The figure clearly shows the total area of the half diagonal line. This type of feature can be used for signature lighting. The photograph matches with the contour plot showed in Figure 3.23.

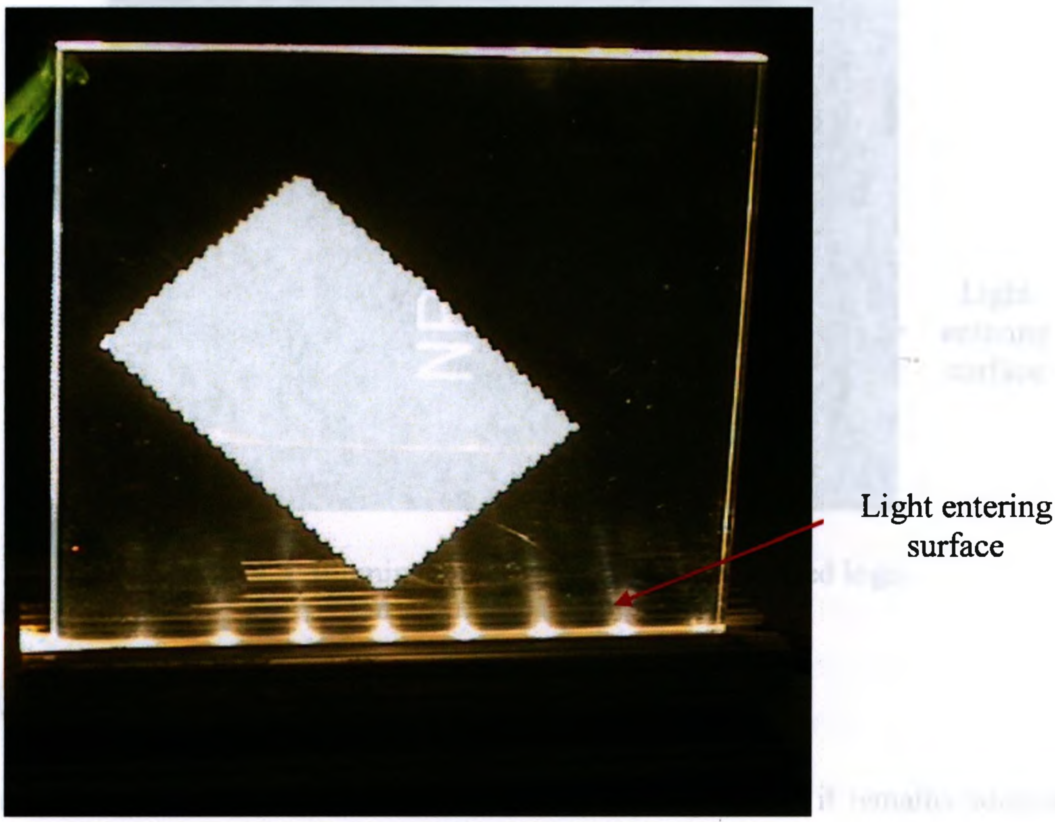

Figure 4.7 Illumination performance for a LGP with test pattern two.

4.4.5 LGP with patterned logo

"NRC-UWO" logo was fabricated as shown in Figure 4.8 and it was seen that by applying the proposed design methodology, it is possible to illuminate any logo inside the LGP that can be used for signature lighting.

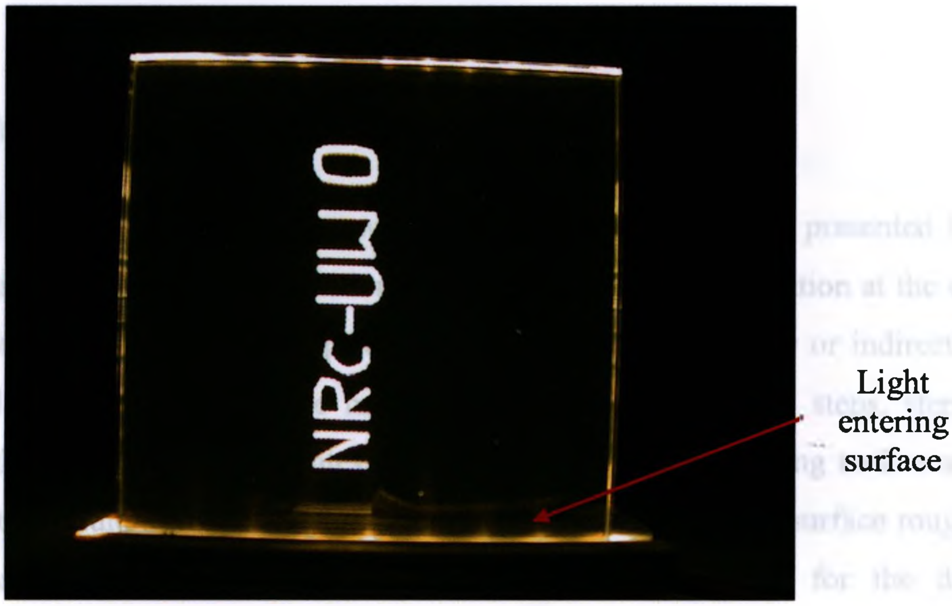

Figure 4.8 Illumination behavior of the fabricated logo.

4. 5 General Observations and Discussion

Although the quality of the surface finish is near optical grade, it remains adequate for illumination applications where the function of microstructures are to scatter the incident light in order to convert the point source into an surface source. It may be possible to improve the quality of surface finishes through different combinations parameters in micromilling but this requires further investigation and detailed study. Illumination uniformity was increased for the optimized array compared to the linear array with uniform radius and depth of microstructures. Although numerical values for illumination uniformity was more generated by the simulation tool compared to the experimental set up but the illumination trend matched in both cases.

The proposed fabrication method provides a quick and cost-effective solution to fabricate the functional prototype of LGP right after the design. To reduce the machining time and cost as much as possible, the proposed fabrication approach is suitable. The linear array of microstructures was fabricated in less than four hours. It took nearly several (seven) hours to fabricate the optimized array of microstructures. The half diagonal line was fabricated in less than 40 minutes.

4. 6 Concluding Remarks

A method of creating optical microstructures in PMMA material was presented in this chapter. In micromilling, special attention should be paid to burr formation at the end of each cut. In addition, other process parameters that can affect directly or indirectly the accuracy and surface quality of the machined thin features are side steps, step over movements, the depth of cut, feed rates per tooth, cutting speeds, cutting tool wear, and the use of cutting fluid/air/oil mist [Popov et al., 2006]. The resultant surface roughness after machining is an important factor that needs considerations for the desired applications. Although this research presented the fabrication method for direct prototyping of microstructures in the LGP, however this method may not be suitable for mass production as it requires several hours to fabricate an array of microstructures. However for mass production of LGP with optical microstructures, the fabricated LGP prototype will require some post processing steps as mentioned in Figure 4.8. The fabricated PMMA sample needs to be coated first by sputtering or evaporation. Then this coated PMMA sample will be used as a master (positive) in order to produce a tool insert (negative) by electroforming. The electroformed tool insert usually consisting of a thin activation layer and a thick and wear resistant layer of nickel or nickel alloys. After electroforming and machining of the back of the insert, the substrate or master is dissolved [Bissacco et al., 2005]. Then this master will go for replication by injection molding.

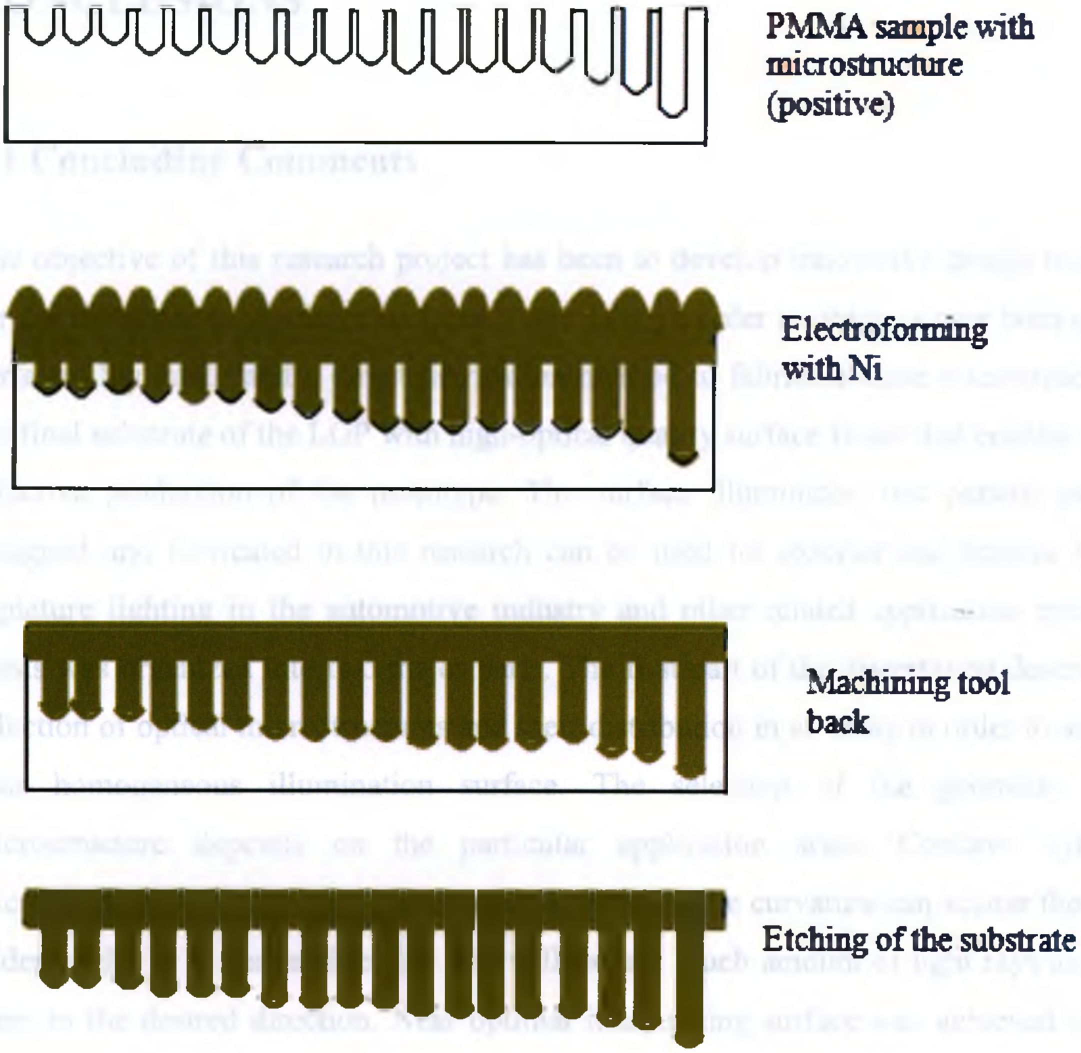
PMMA sample with microstructure (positive)
Electroforming with Ni
Machining tool back
Etching of the substrate

Figure 4.9 Technique for mass production of LGP with microstructures.

CHAPTER 5

CONCLUSIONS

5.1 Concluding Comments

The objective of this research project has been to develop innovative design techniques for the distribution of microstructures in the LGP in order to obtain a near homogeneous surface illuminator and a direct fabrication method to fabricate these microstructures in the final substrate of the LGP with high-optical quality surface finish that enables the cost effective production of the prototype. The surface illuminator, test pattern and logo, designed and fabricated in this research can be used for exterior and interior lighting, signature lighting in the automotive industry and other related application areas. This thesis was organized into two major parts. The first part of the dissertation described the selection of optical microstructures and their distribution in an array in order to achieve a near homogeneous illumination surface. The selection of the geometry of the microstructure depends on the particular application areas. Concave cylindrical microstructures with a round tip are suitable because the curvature can scatter the light at wider angles in different direction and will extract much amount of light rays and direct them in the desired direction. Near optimal illuminating surface was achieved by using only one parameter, i.e., depth of the cylindrical microstructure without using any reflective layer or coating under the bottom surface and without any layer above the top surface. Most of the distribution technique of microstructures in the LGP involves more than one parameter as a variable in order to convert point or linear sources to a uniform area of light source. Dealing with more variables to obtain the desired output usually requires more time and effort to find out the exact combination of dominant parameters that influence the output. Moreover in most of the cases several other layers, i.e., reflective layer, diffusion sheet, brightness enhancement film, etc. are added with the LGP that increase the thickness of the whole system and cost as well. However, for LGPs that will only be used as a surface illuminator, the proposed shape and distribution technique of microstructures are more suitable. Some fundamental analysis was conducted before distributing the microstructures over the full area of bottom surface in the LGP in order to gain additional insight and a fundamental understanding of how the distribution of microstructures can affect the illumination pattern in the LGP. The proposed design also illustrates a way of illuminating any specific pattern and logo in any area of the LGP that can be used for signature lighting.

The second part of this thesis describes the microfabrication method to observe the proof of functionality for the design. Micromilling was determined to be the most suitable microfabrication technique in the research to create concave microstructures directly in PMMA. The advantage of the proposed fabrication method is that concave microstructures can be fabricated directly into the final substrate of the LGP with good optical quality surface finish. By varying only the depth of the ball end milling tool during machining, it is possible to obtain a less dense area of microstructures near the light source and more density of microstructures at the far end of the LGP to obtain a homogeneous illuminating surface. The process does not require any mold or different diameter tool to produce a prototype. Therefore the prototypes can be made easily by this fabrication method with less expensive set up and less processing time with good optical quality surface finishes. The fabricated prototypes were tested with the illumination set up and the performance was closely matched with the simulation results.

5.2 Thesis Summary

This thesis illustrated a novel design technique to achieve near optimal illumination uniformity which will enable the rapid and inexpensive fabrication of LGP prototype. The illuminating surface of the LGP can be used as a surface illuminator in automotive lighting and other related application areas. The distribution of microstructures in LGPs need to be simple enough to achieve the desired output and will be easier to fabricate in a single processing step without the need of any mold. Generally after the design, it is also necessary to create a prototype to validate the design approach. Therefore, the fabrication method must be capable of creating the microstructures directly into the LGP substrate. Using PMMA as a material for LGP will be economical as they are available at low cost while maintaining the good performance. However, as plastic is sensitive to heat, care should be taken in handling these LGP's.

Chapter 2 discussed several important design and microfabrication techniques currently used in order to achieve homogeneous illumination over the whole area of the LGP. These techniques involve more design variables and layers in LGP to obtain illumination in the top surface of the LGP and expensive fabrication set up in order to produce a prototype right after the design. To reduce the number of design variables, Chapter 3 presented state-of-the-art design method for distribution of optical microstructures in the LGP to achieve a near homogeneous illuminating surface. Since light rays reduce their energy over distance during propagation inside a panel, the microstructures were much shallower in front of the light sources in the LGP in order to reduce the interaction of light rays with microstructures in this area. This will allow the light to pass to the rest of the area of the LGP with a sufficient amount of energy. The microstructures were much deeper at the far end of the LGP to extract the light rays with reduced energy and to prevent their propagation to the right end of the LGP. With the proposed design approach, it is possible to create and illuminate any arbitrary pattern and logo inside the LGP for signature lighting and other related applications. The proposed design of the LGP does not consider any reflective layer or any surface treatment under the bottom surface. From the simulation result it was found that there was an average illumination of 2031 lux on the bottom surface where microstructures were located. This indicates that with the proposed distribution technique of microstructures it is possible to prevent the leakage of light under the bottom surface which in turn eliminates the cost associated with the use of any additional layer or surface treatment.

In order to create prototypes according to the design, Chapter 4 describes a new approach to fabricate these microstructures in the LGP made from PMMA material. Vacuum suction technique was employed to mount the work-piece instead of clamping it. As the material was plastic and the minimum depth of the microstructures was up to 95 μm, the proposed mounting technique of work-piece will be suitable to create such smaller size microstructures and removal of the work-piece after fabrication without any damage. The maximum depth of microstructures was 5.5 mm which was up to panel thickness, i.e., 6 mm. After fabrication the removal of the work-piece from the workstation may introduce damage if it is mounted by clamping method. The surface finish of optical microstructures was near optical quality, around 123nmRa. LGPs prototype were fabricated in order to validate the surface illuminator with a near homogeneous illumination surface, a pattern and logo for signature lighting applications. The illumination performance of the LGP's was also closely matched with the simulation results.

5. 3 Recommendations and Future Work

Distribution of optical microstructures by only varying the depth appears to be a promising technique for rapid fabrication of the LGP prototype. It was found that micromilling is capable of producing optical quality microstructure directly into the PMMA material. Therefore, further investigation should be conducted to prepare the fabricated LGP as a tooling insert for mass production, apply the design and fabrication approach to bend LGP and to improve the surface finishes of the fabricated optical microstructures.

The fabricated LGP was tested using an illumination set up that consists of LED as the light source and a digital lux meter as receiver above the top surface to observe the illumination uniformity in the LGP. Further research should be conducted to test the LGP's according to the standards of automotive lighting mentioned in Appendix B to validate the performance for the proposed application area. In addition, future research work should also include the mass production of LGP with microstructures by preparing the fabricated prototype as a tool insert according to the steps mentioned in Figure 4.8.Then replication technology will be used for mass production. Also the research presented in this study only demonstrated the medium size LGP, but this can be extended to large size LGP. The experimental findings showed that there is a strong correlation between the depth of cylindrical microstructures and illumination pattern.

BIBLIOGRAPHY

Ahmad, J.Y. S. (2009). *Machining of Polymer Composites*. Springer-Verlag GmbH.

Banks, D. (2006). *Microengineering, MEMS, and Interfacing: A Practical Guide*. CRC Press Taylor & Francis Group.

Brinksmeier, E., Riemer, O., Stern, R. (2001). Machining of precision parts and microstructures, Proceedings of the 10th ICPE Conference, Okohama, Japan, 3–11.

Bao, W.Y., Tansel, I. N.(2000). Modeling micro-end-milling operations. Part I: Analytical cutting force model. International Journal of Machine Tools and Manufacture, 40(15): 2155-2173.

Bao,W.Y., Tansel, I. N. (2000). Modeling micro-end-milling operations. Part II: Tool run-out. International Journal of Machine Tools and Manufacture, 40: 2175-2192.

Bao,W.Y., Tansel, I. N (2000). Modeling micro-end-milling operations. Part III: Influence of tool wear. International Journal of Machine Tools and Manufacture, 40: 2193-2211.

Bissacco, G., Hansen, H.N., Tang, P.T., Fugl, J.(2005). Precision manufacturing methods of inserts for injection molding of microfluidic systems. Proceedings of the ASPE Spring Topical meeting, 57-63.

Cassarly,W. J. (2007). Backlight pattern optimization. Proc. of SPIE 6834, 683407.

Cassarly,W. J., Irving, B. (2004). Noise tolerant illumination optimization applied to display devices. SPIE 5638, 67-80.

Chien,C.H., Chen, Z. P. (2008). Fabrication of light guide plate on PDMS-based using MEMS Technique for application of LED-backlight. Key Engineering Materials. 7: 364-366.

Chang, C.Y., Yang, S.Y., Chu, M.H. (2007). Rapid fabrication of ultraviolet-cured polymer microlens arrays by soft roller stamping process. Microelectron. Eng. 84: 355-361.

Chien, C.-H., Chen, Z.-P. (2006). Fabrication of a novel integrated light guiding plate by microelectromechanical systems technique for backlight system. J. Microlith., Microfab., Microsyst. 5 (4): 043011.

Chang, J. G., Su, M. H., Lee, C. T., Hwan, C. C. (2005). Generating random and non overlapping dot pattern for liquid-crystal display backlight light guides using molecular-dynamics method. J. Appl. Phys. 98, 114910.

Choi,J., Hahn,K., Seo, H., Kim, S.(2004). Design, analysis, and optimization of LCD backlight unit using ray tracing simulation. Proc. ICCSA (3): 837-846.

Chang, J.- G., Lee C.-T.(2007). Random-dot pattern design of a light guide in an edge-lit backlight:Integration of optical design and dot generation scheme by the molecular-dynamics method. J. Opt. Soc. Am. A 24 (3): 839-849.

Chae, J., Park*, S. S., Freiheit, T. (2006). Investigation of micro-cutting operations. International Journal of Machine Tools & Manufacture 46: 313–332.

Chou, M.-C., Pan, C. T., Shen, S.C., Chen, M.-F., Lin, K.L., Wu, S.-T (2005). A novel method to fabricate gapless hexagonal micro-lens array. Sensors and Actuators A 118: 298–306.

Dhanorkar, A., Liu, X., Özel, T. (2007). Micromilling process planning and modeling for micromold manufacturing. Proceedings of ASME International Conference on Manufacturing Science and Engineering, 31070: 759-769.

Dutton, H. J. R. (1998). *Understanding Optical Communications*. Prentice Hall Series in Networking. http://www.redbooks.ibm.com/pubs/pdfs/redbooks/sg245230.pdf, IBM Redbooks.

Dimov, S., Pham, D. T., Ivanov, A., Popov, K., Fansen, K. (2004). Micromilling strategies: Optimization issues. Proc. Instn Mech Engrs, 218 (B): 731-736.

Dow, T., Miller, E., Garrard, K. (2004).Tool force and deflection compensation for small milling tools. Precision Engineering, 28: 31-45.

ECE R48. Installation of lighting and light-signaling devices on motor vehicle. FMVSS No.108: Lamps and Reflective devices.

Feng, D., Yan, Y., Yang, X., Jin, G., Fan, S. (2005). Novel integrated light-guide plates for liquid crystal display backlight. J. Opt. A, Pure Appl. Opt. 7(3): 111–117.

Fu, Y., Bryan, N. K. A. (2002). Focused ion beam direct fabrication of microoptical elements: features compared with laser beam and electron beam direct writing. http://hdl.handle.net/1721.1/3904.

Gentili, E., Tabaglio, L., Aggogeri, F. (2005). Review on Micromachining Techniques. Proceedings of the 7th International Conference on Advance Manufacturing Systems and Technology (AMST). 486: 387-396.

Hocheng , H.,Wen, T.-T., Yang, S.-Y. (2008). Replication of microlens arrays by gas-assisted hot embossing. Materials and Manufacturing Processes, 23: 261 – 268.

Herzig, H. P. (1997). *Micro-Optics: Elements, Systems and Application*. Taylor & Francis, London.

Hunsperger, R. G. (2009). *Integrated Optics: Theory and Technology*.6th Edition, Springer.

Iga, K., Kokburn,Y., Oikawa, M. (1984). *Fundamentals of Microoptics*. Academic Press Inc., Tokyo, 94-96.

Ide, T., Mizuta, H., Numata, H., Taira,Y., Suzuki, M., Noguchi, M., Katsu, Y. (2003). Dot pattern generation technique using molecular dynamics, J. Opt. Soc. Am. A 20: 248–255.

Joo, B.-Y., Shin, D.-H. (2010). Design guidance of backlight optic for improvement of the brightness in the conventional edge-lit LCD backlight. Displays 31, 87–92.

Jeong, J. H., Lee, G., Yoon, S. -J.,Choi, D.-H. (2008). Design Optimization for Optical Pattern to Improve Illuminance and Uniformity of Light Guide Panel in LCD Back Light Unit. 5th China-Japan-Korea Joint Symposium on Optimization of Structural and Mechanical Systems, Jeju Island, Korea.

Kim, J. S., Kim, D. S., Kang, J. J., Kim,J.D., Hwang, C. J. (2010). Replication and Comparison of Concave and Convex Microlens Arrays of Light Guide Plate for Liquid Crystal Display in Injection Molding. Polymer Engineering and Science, 1696-1704.

Kuo1, S.-M., Lin, C.-H. (2010). Fabrication of aspherical SU-8 microlens array utilizing novel stamping process and electrostatic pulling method. Optics Express, 18(18): 19114-19119.

Kuo, S. -M., Lin, C.-H. (2008). The fabrication of non-spherical microlens arrays utilizing a novel SU-8 stamping method. J. Micromech. Microeng.18, 125012.

Li, C.-J., Fang, Y.-C., Chu, W.-T., Cheng, M.-C. (2008). Optimization of Light Guide Plate with Microstructures for Extra Light Modern Backlight Module. Jpn. J. Appl. Phys. 47(8): 6683–6687.

Lin, T.-W., Chen, C.-F., Yang, J.-J., Liao, Y.-S. (2008). A dual-directional light-control film with a high-sag and high-asymmetrical-shape microlens array fabricated by a UV imprinting process. J. Micromech. Microeng. 18(9), 095029.

Lee, W.-J., Lim, J. W., Hwang, S. H., Rho, B.S. (2008). Imprint Master Fabricated by Ultra Precision Machining for Optical Waveguide. IEEE Proceedings of Opto-Electronics and Communications Conference and the Australian Conference on Optical, 1–2.

Lu, Y., Chen, S. (2008). Direct write of microlens array using digital projection photopolymerization. Appl.Phys. Lett. 92,041109.

"Light Tools" User manual. (2010). Version7.0. Optical Research Associates, Synopsis Inc.

Malacara, D. (2001). *Handbook of Optical Engineering*. CRC press.

Monreal, M., Rodriguez, C. A. (2003). Influence of tool path strategy on the cycle time of high-speed milling. Computer- Aided Des.35: 395–401.

Nussbaum, Ph., V¨olkel, R., Herzig, H. P., Eisner, M., Haselbeck, S. (1997). Design, fabrication and testing of microlens arrays for sensors and Microsystems. Pure Appl. Opt. 6: 617–636.

Ottevaere, H., Cox, R., Herzig, H. P., Miyashita, T., Naessens, K., Taghizadeh, M., V¨olkel, R., Woo, H. J., Thienpont, H. (2006). Comparing glass and plastic refractive microlenses fabricated with different technologies. J. Opt. A, Pure Appl. Opt. 8(7): 407–S429.

Pan, C. T., Su, C. H. (2007). Fabrication of gapless triangular micro-lens array. Sensors and Actuators A 134: 631–640.

Popov, K., Dimov, S., Pham, D. T., Ivanov, A. (2006). Micromilling strategies for machining thin features. Proceedings of the IMECH E Part C Journal of Mechanical Engineering Science, 220 (11): 1677-1684.

Qin,Y. (2010). Micro-Manufacturing Engineering and Technology. Elsevier Science and Technology.

Rea, M. S. (2000). *The IESNA Lighting Handbook: reference & application.*9th edition. Illuminating Engineering society of North America.

Stager,B., Gale,M.T.,Rossi,M.(2005). Replicated micro-optics for automotive applications. Proceedings of SPIE 5663, 238-245.

Serway, R. A., Jewett, J. W. (2004). *Physics for Scientists and Engineers*. 6th Edition, Thomson Brooks/Cole.

Sinzinger, S., Jahns, J. (2003). *Microoptics*. 2nd edition, WILEY-VCH GmbH & Co. KGaA, Weinheim, Germany.

SAE Ground Vehicle Lighting Standards. (2009). SAE HS-34.

Trager, F. (2007). *Handbook of Laser and Optics*. Springer.

U.S. Army. (1996). *Fundamentals of Machine Tools.*TC 9-524, Washington, DC.

Utsumi, Y., Kishimoto, T., Hattori, T., Minamitani, M. (2008). Proposal of Next-Generation Three-Dimensional X-Ray Lithography and Its Application to Fabrication of a High-Luminescence Optical Waveguide for a Liquid Crystal Backlight Unit. Electrical Engineering in Japan, 165: 52-59.

Wördenweber, B., Wallaschek, J., Boyce, P., Hoffman Donald D. (2007). *Automotive Lighting and Human Vision.* Springer-Verlag Berlin Heidelberg, New York.

Zhang, P., Londe, G., Sung, J., Johnson, E., Lee, M., Cho,H. J. (2007). Microlens fabrication using an etched glass master. Microsyst Technol 13: 339–342.

APPENDIX A

MODELING AND SIMULATING LGP's USING LIGHT TOOLS

The act of simulating something generally involves representing certain key characteristics of a selected physical system. Simulation can be used to show the eventual real effects of alternative conditions and courses of action. Key issues in simulation include acquisition of valid source information about the relevant selection of key characteristics and behaviors, the use of simplifying approximations and assumptions within the simulation and fidelity and validity of the simulation outcomes. Illumination design software must be able to model the geometric and optical properties of different types of light sources and transforming elements and it must also be able to evaluate the paths of light using optical ray tracing throughout the model to calculate the final light distribution.

A.1 Light Tools Simulator

In this research "Light Tools" was used as simulation software due to its specialization for illumination design. "Light Tools" is able to create LGP with accessories such as surface and volume-emitting light source, receiver for measuring output light, 2D and 3D microstructures on any surface of LGP with optical attributes and optical adherence. Generally modeling of microstructure arrays as a CAD model in particular can result in extremely large model sizes whereas "Light Tools" provides the capability to define arrays of 3D microstructures that trace rays and render accurately but are not explicitly constructed as part of the geometric model, thereby resulting in much smaller model sizes. Illumination in an edge-light LGP involves ray splitting and scattering from the surfaces of the light guide. Also in light guide a ray can bounce around inside of the light guide multiple times prior to exiting the light guide. The tools have option to specify the surface properties, i.e., refraction, TIR, reflection, diffraction, scattering separately for each surface of any 3D model. For optical objects, these properties can be specified separately for different zones on the surfaces. The probabilistic ray split control in "Light Tools" provides the control for an efficient ray trace by tracing only one outgoing ray for each ray incident on the split surface.

"Light Tools" do the illumination calculations by non-sequential Monte Carlo ray tracing. This calculation includes global analysis by simulating the propagation of incident light flux throughout the model and also local analysis by sampling the source luminance as seen from points on the receiver, yields in accurate simulation of light effects for the whole system. During simulation the tool considers the optical effects at every surface, even the interaction of light with component edges and mechanical structures. All these options in "Light Tools" ensure that the edge-lit LGP system will perform in a way as the real system do.

For edge-lit lighting, luminance and illumination uniformity on the top of the light guide, calculation of illumination in terms of various units, i.e., radiometric and photometric need to consider during analysis. The tool has 2D and 3D plots to see the illumination or intensity distribution at any number of arbitrarily chosen surfaces.

A.2 Testing and Verification of Light Tools

A prototype was fabricated for (100 mm x 100 mm x 6 mm) with cylindrical shape micro-structures on its bottom surface. Then the sample was placed in a black box with proper set-up. To validate the results the illumination performance of linear arrays from simulation result and fabricated prototype are shown in Figure A.1.

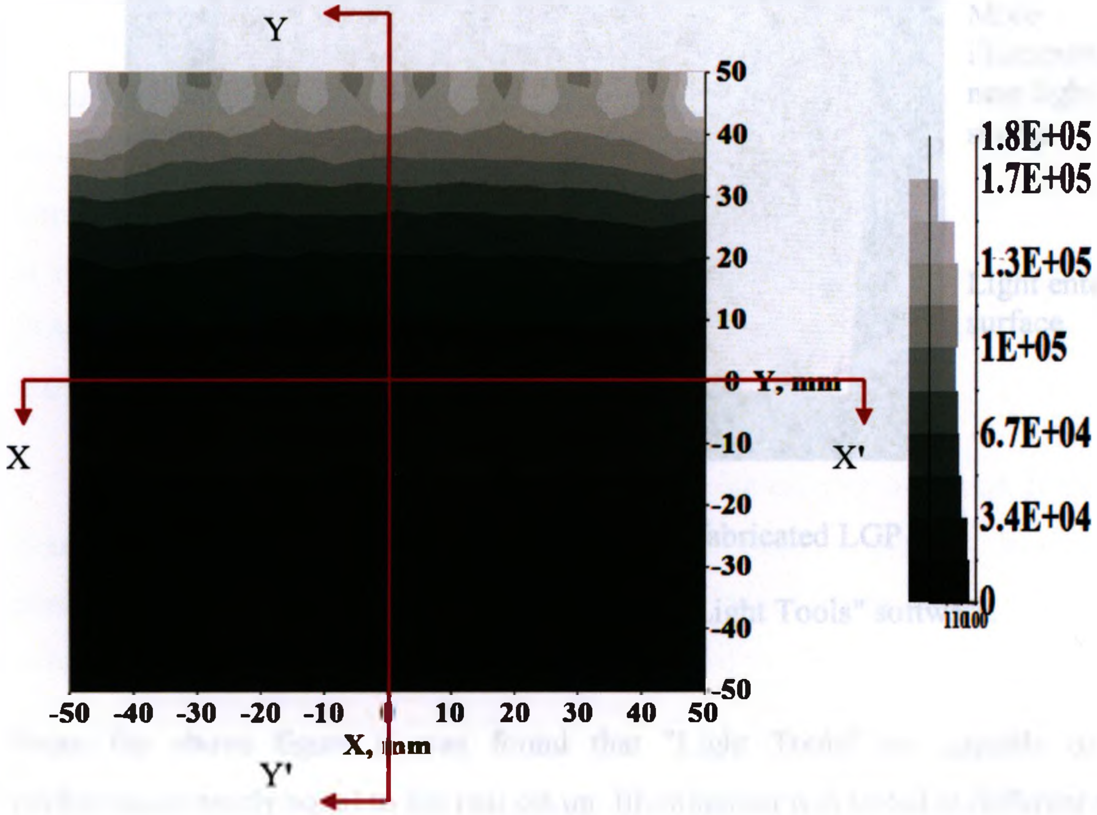

(a) Illumination on top surface from simulation result

Figure A.1 (continued)

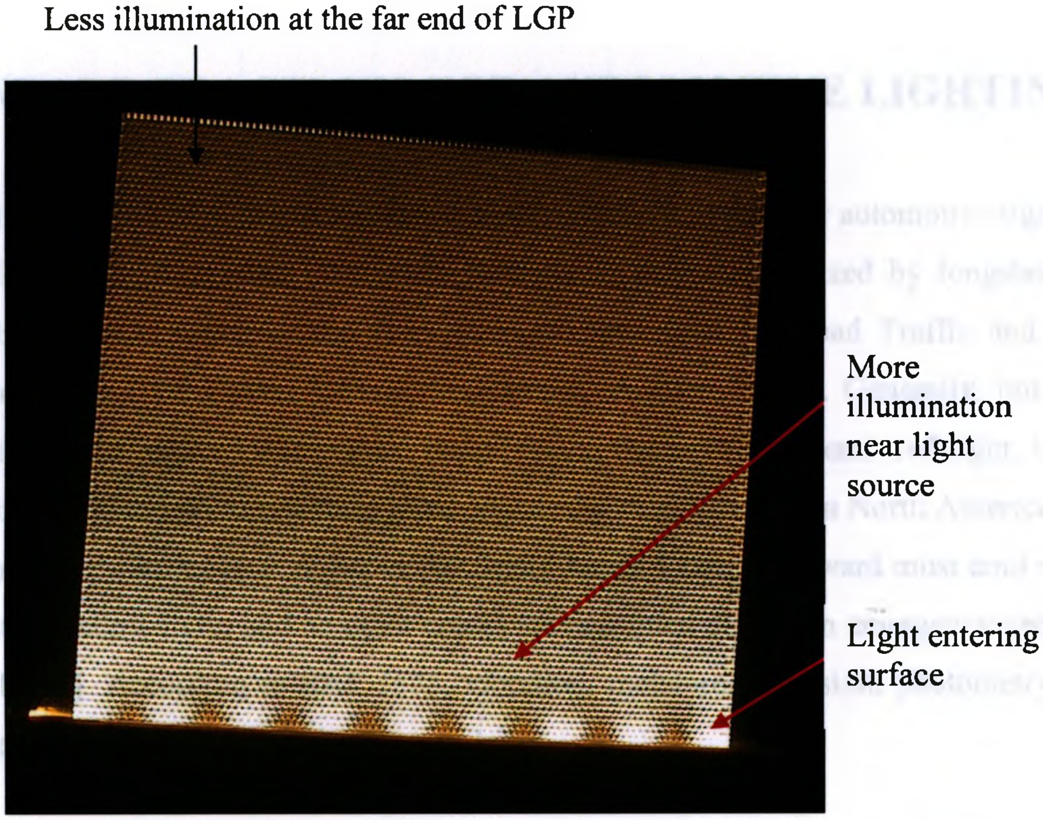
Less illumination at the far end of LGP
More illumination near light source
Light entering surface

(b) Illumination on the top surface of the fabricated LGP

Figure A. 1 Verification of the "Light Tools" software.

From the above figure it was found that "Light Tools" are capable of showing performance nearly equal to the real set up. Illumination was tested at different point by a luminance meter to measure the illumination uniformity. The average and maximum illumination was determined to be 528 lux and 1,747 lux respectively. The illumination uniformity was found to be approximately 30% for the LGP with a uniform array of microstructures. It was found that trend of illumination uniformity calculated from real set-up closely matches with that from the simulation results.

APPENDIX B

STANDARD PRACTICES FOR AUTOMOTIVE LIGHTING

Generally SAE and ECE regulation are available standard system for automotive lighting. The colour of light emitted by vehicle lights is largely standardized by longstanding convention, first codified in the 1949 Vienna Convention on Road Traffic and later specified in the 1968 United Nations Convention on Road Traffic. Generally, but with some global and regional exceptions, lamps facing rearward must emit red light, lamps facing sideward and all turn signals must emit amber light (though in North America rear turn signals may emit either amber or red light), lamps facing frontward must emit white or selective yellow light, and no other colors are permitted except on emergency vehicles [SAE HS-34]. According to SAE J575, vibration, moisture, corrosion, photometry and warpage test are required in order to test a lamp.

For front turn signal, minimum intensity at optical axis is 200 cd. If the turn bulb filament is less than 100 mm (4 in.) from the edge of the low beam headlamp, photometric requirements are 250% of normal. A minimum intensity of 4 cd at optical axis is and maximum intensity of 125 cd is required for front park signal. Tail lamp and stop lamp requires a minimum intensity of 2.0 cd and 80 cd respectively.

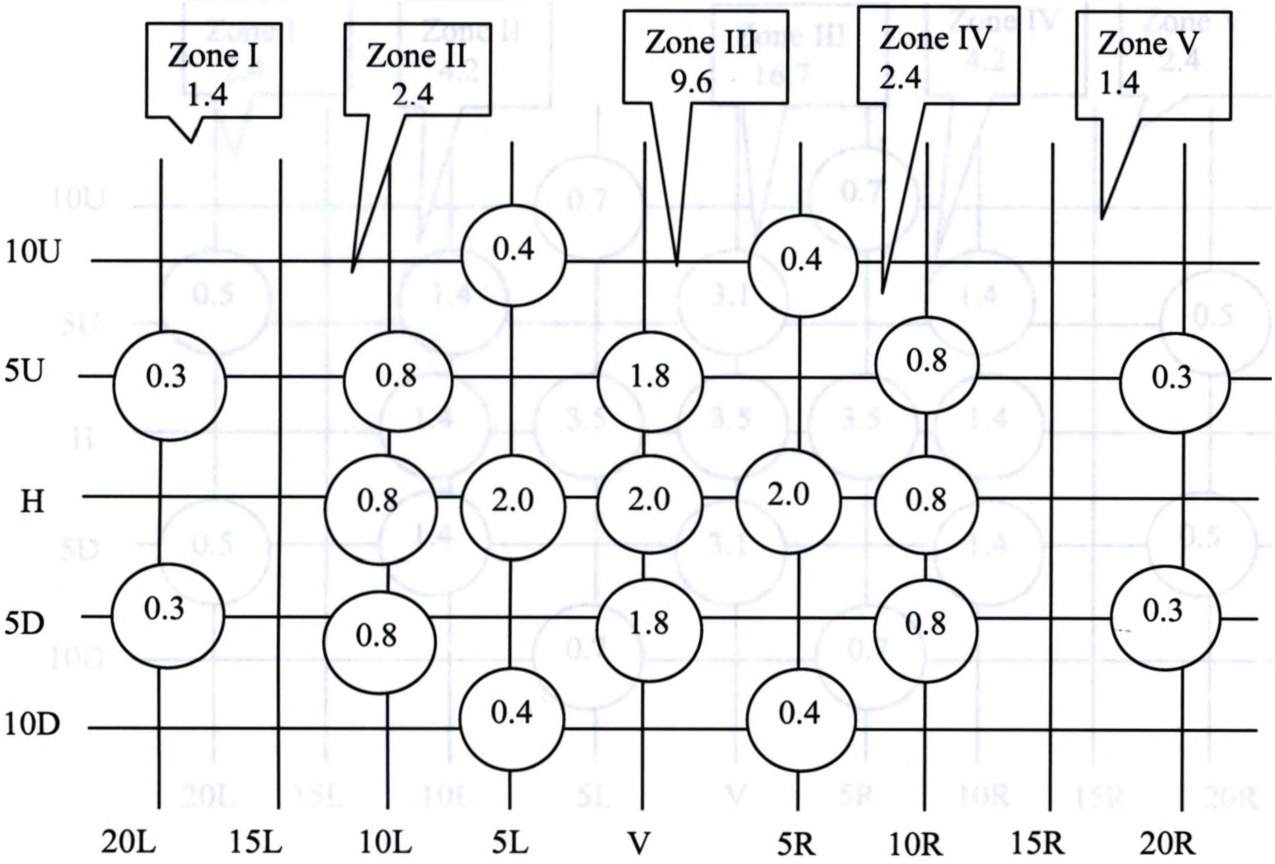
Zone I
1.4
Zone II
2.4
Zone III
9.6
Zone IV
2.4
Zone V
1.4
10U
5U
H
5D
10D
0.4
0.4
0.3
0.8
1.8
0.8
0.3
0.8
2.0
2.0
2.0
0.8
0.3
0.8
1.8
0.8
0.3
0.4
0.4
20L
15L
10L
5L
V
5R
10R
15R
20R

(a) Photometric requirements for Tail lamp. Minimum luminous intensity (cd) Size 1 (less than 225 cm^2)

Figure B.1 (continued)

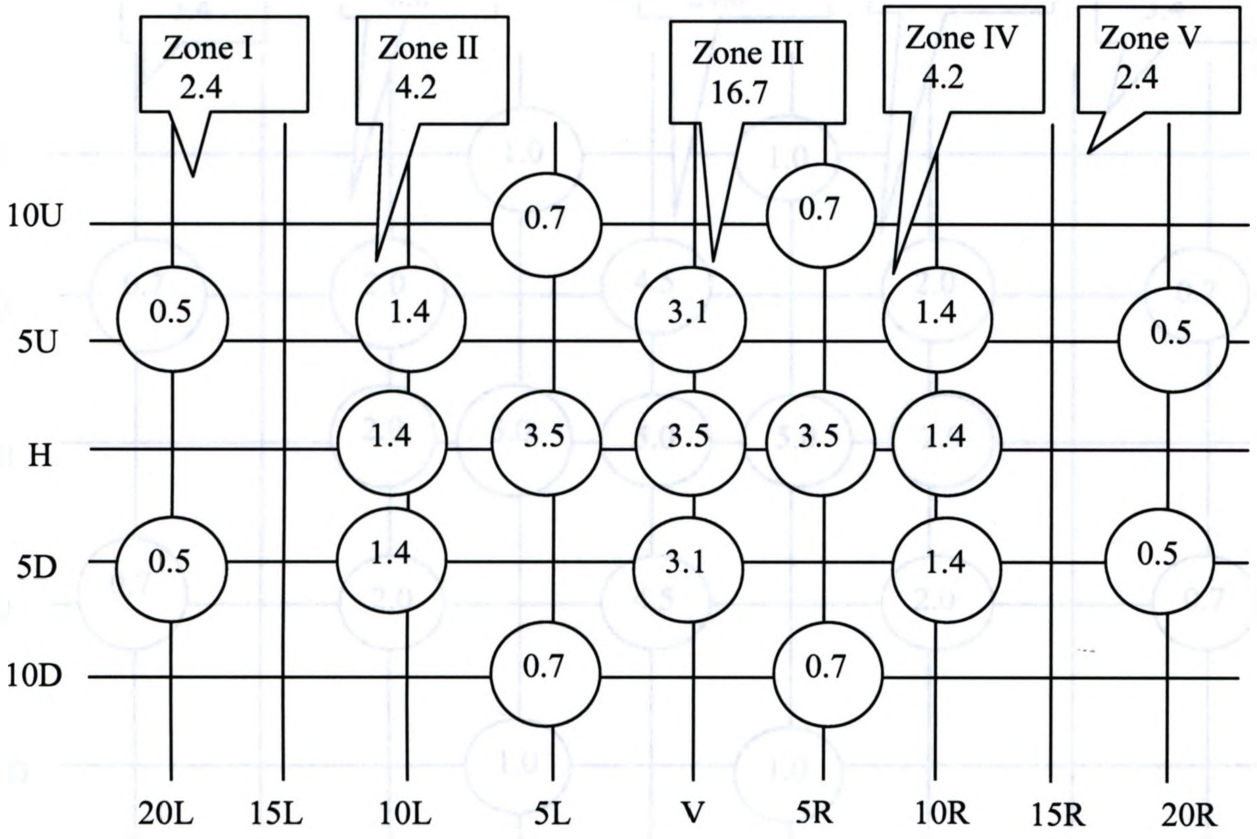
Zone I
2.4
Zone II
4.2
Zone III
16.7
Zone IV
4.2
Zone V
2.4
10U
5U
H
5D
10D
20L
15L
10L
5L
V
5R
10R
15R
20R
0.7
0.7
0.5
1.4
3.1
1.4
0.5
1.4
3.5
3.5
3.5
1.4
0.5
1.4
3.1
1.4
0.5
0.7
0.7

(b) Photometric requirements for Tail lamp. Minimum luminous intensity (cd)
Size 2 (225 – 450 cm^2)

Figure B.1 (continued)

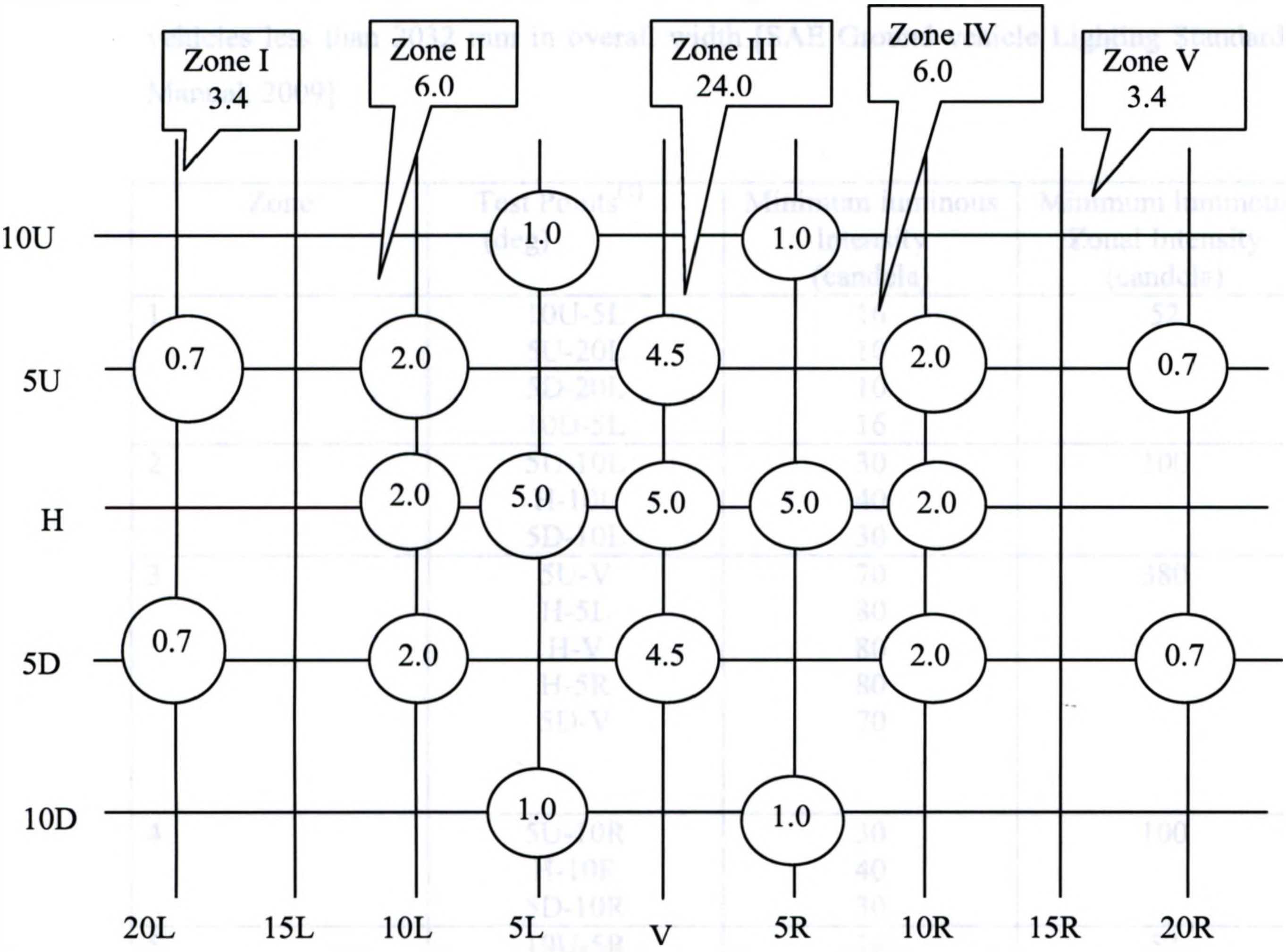
Zone I
3.4
Zone II
6.0
Zone III
24.0
Zone IV
6.0
Zone V
3.4
10U
5U
H
5D
10D
1.0
1.0
0.7
2.0
4.5
2.0
0.7
2.0
5.0
5.0
5.0
2.0
0.7
2.0
4.5
2.0
0.7
1.0
1.0
20L
15L
10L
5L
V
5R
10R
15R
20R

(c) Photometric requirements for Tail lamp. Minimum luminous intensity (cd) Size 3 (greater than 450 cm^2)

Figure B.1 Photometric requirements for Tail lamp with LED light sources according to SAE J1889 for use on vehicles less than 2032 mm in overall width [SAE Ground vehicle Lighting Standards Manual, 2009]

According to above three photometric patterns, maximum luminous intensity is 18 cd within the photometric pattern. As per SAE J1889, each tail lamp must provide a luminous intensity not less than 0.05 cd throughout the photometric pattern

Table B.1 Photometric requirements for Fog tail lamp as per SAE J575 for use on vehicles less than 2032 mm in overall width [SAE Ground vehicle Lighting Standards Manual, 2009]

Zone	Test Points(1) (deg)	Minimum luminous Intensity (candela)	Minimum luminous Zonal Intensity (candela)
1	10U-5L	16	52
	5U-20L	10	
	5D-20L	10	
	10D-5L	16	
2	5U-10L	30	100
	H-10L	40	
	5D-10L	30	
3	5U-V	70	380
	H-5L	80	
	H-V	80	
	H-5R	80	
	5D-V	70	
4	5U-10R	30	100
	H-10R	40	
	5D-10R	30	
5	10U-5R	16	52
	5U-20R	10	
	5D-20R	10	
	10D-5R	16	
Maximum Luminous Intensity (Candela(2))			300

1. To pass zonal the measured values of each test point shall not be less than 60% of the minimum point value in the Table B.1.

2. The listed maximum at any test point shall not be exceeded over any area larger than that generated by a 0.5 degree radius with the solid angle defined by the test points in the Table B.1.

3. The COP photometric performance requirements of ECE Reg 38 are an acceptable alternative to Table B.1, tested in accordance with ECE Reg. 38.

Table B.2 Photometric requirements for rear cornering lamps as per SAE J575 for use on vehicles less than 2032 mm in overall width [SAE Ground vehicle Lighting Standards Manual, 2009]

Test Position (Degrees)	Luminous Intensity Candela (cd)
2-1/2 D – 30 L	40 min
2-1/2 D – 45 L	80 min
2-1/2 D – 60 L	40 min
Horizontal and Above	500 max

Table B.3 Photometric Requirements for auxiliary upper beam lamp according to the requirements of SAE J575 for use on vehicles less than 2032 mm in overall width [SAE Ground vehicle Lighting Standards Manual, 2009]

Test Point, Degrees	**Candela, cd**
2U-3R and 3L	2000 min
1U-3R and 3L	5000 min
H-V	25000 min and 75000 max
H-3R and 3L	10000 min
1D-6R and 6L	3700 min
2D-6R and 6L	2000 min
4D-V	5000 max

Table B.4 Photometric Requirements for auxiliary upper beam lamp according to the requirements of SAE J2139 for use on vehicles 2032 mm or more in overall width [SAE Ground vehicle Lighting Standards Manual, 2009]

Zone	Test point (Degrees)	Minimum Luminous Intensity (cd)(3)	Zone Total Luminous Intensity (cd)(4)
I	10U 5L	0.4	1.4
	5U 20L	0.3	
	5D 20L	0.3	
	10D 5L	0.4	
II	5U 10L	0.8	2.4
	H 10L	0.8	
	5D 10L	0.8	
III	5U V	1.8	9.6
	H 5L	2.0	
	H V	2.0	
	H 5R	2.0	
	5D V	1.8	
IV	5U 10R	0.8	2.4
	H 10R	0.8	
	5D 10R	0.8	
V	10U 5R	0.4	1.4
	5U 20R	0.3	

	5D 20R 10D 5R	0.3 0.4	
Minimum Luminous Intensity (cd)$^{(5)}$			18

1. When a tail lamp is combined with the stop lamp or turn signal lamp, the stop lamp or turn signal lamp intensity shall not be less than three times the luminous intensity of the tail lamp at any test point, except that at H-V, H-5^{0}L, H-5^{0}R, and 5^{0}U-V, the stop lamp or turn signal lamp intensity shall not be less than five times the luminous intensity of the tail lamp. When a tail lamp is combined with the stop lamp or turn signal lamp, and the maximum luminous intensity of the tail lamp is located below the horizontal and is within an area generated by a 1.0 degree radius around the test point, the ratio for the test point may be computed using the lowest value of the tail lamp intensity within the generated area.

2. An arrangement of lamp may be used to meet the photometric requirements of the above table provided the distance between adjacent light sources does not exceed 560 mm for two lamp arrangements or does not exceed 410 mm for multiple lamp arrangements. If the distance between light sources exceeds those distances details previously then, each lamp shall individually comply with the photometric requirements of above Table B.4.

3. The measured value at each individual test point shall not be less than 60% of the required minimum value shown for that individual test point location.

4. The sum of the luminous intensity measurements at each test point within a zone shall not be less than the Zone Total Luminous Intensity shown.

5. The listed maximum shall not be exceeded over any area larger than that generated by a 0.5 degree radius within the solid angle defined by the test point.

APPENDIX C

PHOTOMETRIC UNITS

Photometry is the science of measuring visible light in units, weighted according to the sensitivity of the human eye. It is a quantitative science based on a statistical model of the human visual response to light, that is, our perception of light under carefully controlled conditions. The sensitivity of the human eye to light varies with wavelength. A light source with a radiance of one watt/m^2-steradian of green light, for example, appears much brighter than the same source with a radiance of one watt/m^2-steradian of red or blue light. In photometry, watts of radiant energy is not measured, rather, the subjective impression produced by stimulating the human eye-brain visual system is measured with radiant energy. Many different measure units are used for photometric measurements.

Luminous Flux (Luminous Power)

The luminous flux Φ is the total amount of visible light emitted by a light source, in all directions. Luminous flux is analogous to the total amount of electromagnetic radiation emitted by the light source, except that it is "weighted" by the luminous efficiency curve. For example, electromagnetic radiation with a wavelength near 555 nm is given more importance than radiation with a wavelength near 400 nm. This weighted average is luminous flux. In SI units, luminous flux is measured in units of lumens (lm), defined as 1/683 watts of radiant power at a frequency of 540 x 10^{12} Hertz. The CIE defines the lumen in terms of the luminous flux of monochromatic radiation at 555 nm, where the human eye is most sensitive at this wavelength the luminous efficiency is 683 lm/W. Luminous flux is often used as an objective measure of the useful power emitted by a light source and is not used to compare brightness, since this is a subjective perception which varies according to the distance from the light source. If a uniform point light source of 1 cd luminous intensity is positioned at the center of a sphere of 1 m radius, then every area of 1 m^2 on the inside of that sphere will receive a luminous flux of 1 lumen (lm).

$$\phi = \frac{dQ}{dt} \tag{C.1}$$

This relation also holds when using other units like 1 ft radius and 1 ft^2 area.

Luminous Intensity

Radiant intensity (I) or luminous intensity (I) is the radiant flux (luminous flux) from a point source emitted per unit solid angle in a given direction, as defined by

$$I = \frac{d\phi}{d\Omega} \tag{C.2}$$

where $d\phi$ is the radiant flux (luminous flux) leaving the source and propagating in an element of solid angle $d\Omega$ containing the given direction.

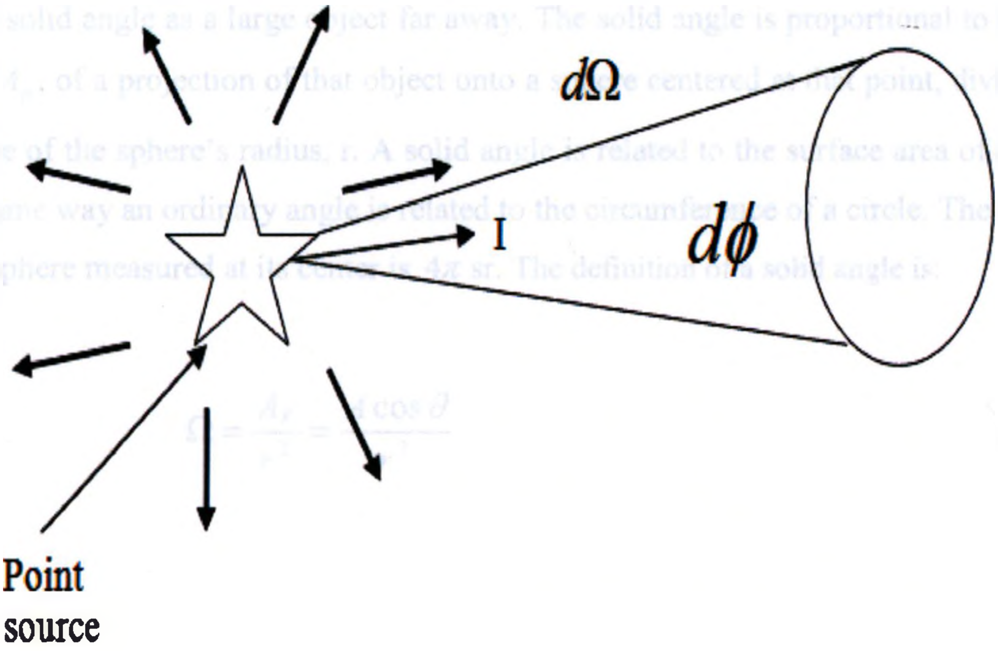

Figure C.1 Luminous Intensity

The unit for luminous intensity is 1 cd (which is the same as 1 lumen/steradian) and is essentially the starting point for the photometric units. The unit 1 cd corresponded originally to an extremely well-defined candle light, and even if its definition has been changed to a more general one, 1 cd still gives a good description of a candle. Therefore a 60 W light bulb with a luminous efficacy of 12 lumen /W has the luminous intensity of 57 cd. If it is placed in a reflector, directing the light into a cone with a half top angle of 10^0, one gets 7600 cd. A point source of one candlepower is one which emits one lumen into a solid angle of one steradian. A source of one candle intensity which radiates uniformly in all directions emits 4π lumens. From the definition of the lumen, it is apparent that a 1-cm^2 blackbody at 2042 K has an intensity of 60 candles.

Solid Angle

The solid angle Ω that an object subtends at a point is a measure of how big that object appears to an observer at that point. For instance, a small object nearby could subtend the same solid angle as a large object far away. The solid angle is proportional to the surface area, A_p, of a projection of that object onto a sphere centered at that point, divided by the square of the sphere's radius, r. A solid angle is related to the surface area of a sphere in the same way an ordinary angle is related to the circumference of a circle. The solid angle of a sphere measured at its center is 4π sr. The definition of a solid angle is:

$$\Omega = \frac{A_p}{r^2} = \frac{A\cos\theta}{r^2} \quad \text{(C.3)}$$

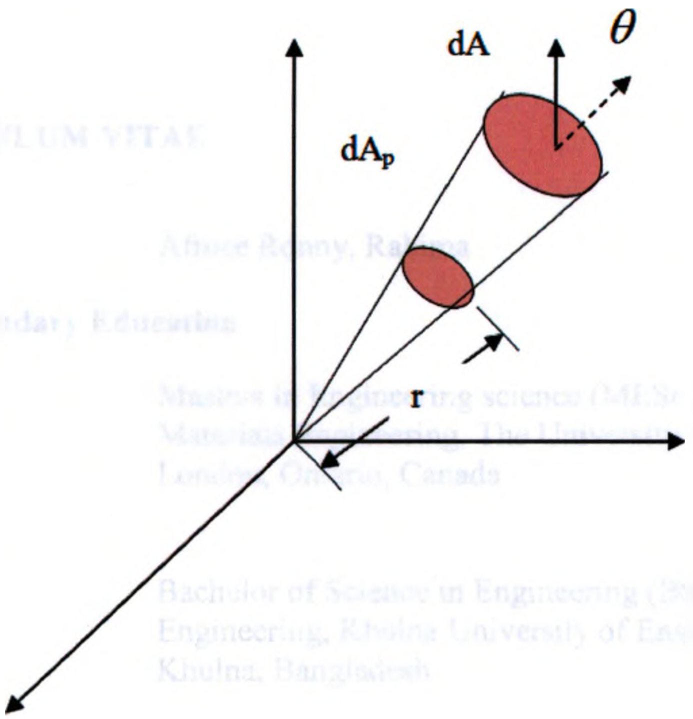
dA
θ
dA_p
r

Figure C.2 Solid angle